

CYPRUS UNIVERSITY OF TECHNOLOGY
FACULTY OF ENGINEERING AND TECHNOLOGY



Doctoral Dissertation

INTEGRATED USE OF FIELD SPECTROSCOPY
AND SATELLITE REMOTE SENSING FOR
MONITORING WATER QUALITY IN CASE-2
(INLAND AND COASTAL) WATER BODIES

Christiana Papoutsas

Lemesos 2015

CYPRUS UNIVERSITY OF TECHNOLOGY
FACULTY OF ENGINEERING AND TECHNOLOGY
DEPARTMENT OF CIVIL ENGINEERING AND GEOMATICS

INTEGRATED USE OF FIELD SPECTROSCOPY
AND SATELLITE REMOTE SENSING FOR
MONITORING WATER QUALITY IN CASE-2
(INLAND AND COASTAL) WATER BODIES

by
Christiana Papoutsas

Lemesos 2015

FORM APPROVAL

PhD Thesis

**Integrated use of field spectroscopy and satellite
remote sensing for monitoring water quality in
Case-2 (inland and coastal) water bodies**

Presented by

Christiana Papoutsa

Member of the Committee - Internal Examiner / PhD Supervisor:

Prof. Diofantos G. Hadjimitsis.....

Cyprus University of Technology

Chairman of the Committee - External Examiner:

Prof. Athanasios Loukas.....

University of Thessaly

Member of the Committee - Internal Examiner:

Prof. Phaedon C. Kyriakidis.....

Cyprus University of Technology

Cyprus University of Technology

October, 2015

SUPERVISING COMMITTEE


PhD Thesis

**Integrated use of field spectroscopy and satellite
remote sensing for monitoring water quality in
Case-2 (inland and coastal) water bodies**

Presented by

Christiana Papoutsa

Member of the Committee / PhD Supervisor:

Prof. Diofantos G. Hadjimitsis.....

Professor - Department of Civil Engineering and Geomatics,
Cyprus University of Technology

Member of the Committee:

Dr Leonidas Toulis.....

Senior Researcher - Industrial and Fodder Crops Institute,
Hellenic Agricultural Organization DEMETER (NAGREF)

Member of the Committee:

Dr Adrianos Retalis.....

Senior Researcher - Institute for Environmental Research and Sustainable
Development, National Observatory of Athens

Cyprus University of Technology

October, 2015

Copyright © Christiana Papoutsas, 2015

All rights reserved.

This Thesis is dedicated to my mother Anna
The one true constant in my life
For her unconditional love and support

ACKNOWLEDGEMENTS

Working on this thesis has been a wonderful and often overwhelming experience. The support and help of several people throughout my PhD years has been proven invaluable and this work would not have been possible without them.

First and foremost I would like to thank my PhD supervisor Prof. Diofantos Hadjimitsis for initiating and encouraging my research which allowed me to grow as a person and a research scientist, but also for his unfailing support during these past five years. The joy and enthusiasm of Diofantos was contagious and motivational, especially during the few difficult times in the PhD pursuit.

I am also thankful to my supervising committee members, Dr. Adrianos Retalis and Dr. Leonidas Toullos for investing their time in reviewing this work and for providing constructive comments. Their vital advice and suggestions helped make the PhD experience productive and stimulating.

I am especially grateful to Assoc. Prof. Evangelos Akylas, an exceptional scientist and one of the smartest people I know for a lot of insightful discussions regarding research and for encouraging me to have critical and independent thinking while analysing the experimental results.

The large scale field campaigns that allowed the collection of the data used in this work would not have been possible without all the people that help with the financial and technical aspects of the field campaigns. I gratefully acknowledge the European Regional Development Fund and the Republic of Cyprus who through the Research Promotion Foundation funded my work in the first 3 years in the Framework of the "SATCOAST" Project PENEK/0609/60. I thank the Cyprus Water Development Department for supporting the field campaigns in Asprokremmos Reservoir and especially Mr. Leonidas Laouris for his assistance and patience during the campaigns. Also the Department of Fisheries and Marine Research of Cyprus, and the Maritime Institute of Eastern Mediterranean for supporting the coastal

campaigns, the Department of Civil Engineering, University of Thessaly and especially Dr. Marios Spiliotopoulos and the Management Body of the Eco-Development area of Karla, Mavrovouni, Kefalovriso and Velestino for their support during the field campaigns in lake Karla. Finally, I am especially grateful to the Department of Civil Engineering and Geomatics, Cyprus University of Technology (Remote Sensing Lab) for providing the equipment used in this research and ESA for providing the satellite images.

Special thanks are due to my family. Words cannot express how grateful I am to them for their love and patience during these years, supporting me in all my pursuits and believing in me, even when I didn't believe in myself.

I would also like to thank my colleagues and friends from the remote sensing lab for being a second family to me and making the long hours at the office a bit more pleasant.

Last but definitely not least, I would like to thank all my friends for their endless support and valued friendship which managed to turn stressful situations to a mere laugh. Special thanks are due to all those who participated in the field campaigns and helped collect data for this PhD thesis.

RELATIVE PUBLICATIONS

Chapter in Book

PAPOUTSA, C., and HADJIMITSIS, D. G., "Remote Sensing for Water Quality Surveillance in Inland Waters: The Case Study of Asprokremmos Dam in Cyprus". Chapter in Book, (2012).

Journals:

PAPOUTSA, C., RETALIS, A., TOULIOS, L., and HADJIMITSIS, D. G., "Defining the Landsat TM/ETM+ and CHRIS/PROBA spectral regions in which turbidity can be retrieved in inland waterbodies using field spectroscopy", *International Journal of Remote Sensing*, Vol. 35(5), pp. 1674-1692 (2014); doi: 10.1080/01431161.2014.882029.

PAPOUTSA, C., AKYLAS, E., and HADJIMITSIS, D. G., "The Spectral Signature Analysis of Inland and Coastal Water Bodies Acquired from Field Spectroradiometric Measurements", *Central European Journal of Geosciences*, Vol. 6(1), pp.67-78 (2014); doi: 10.2478/s13533-012-0161-4

PAPOUTSA, C., and HADJIMITSIS, D. G., "Field Spectroscopy over Asprokremmos Dam in Cyprus Intended for Water Quality Monitoring", *Journal Key Engineering Materials*, Vol.500, pp. 813-819 (2012); doi:10.4028/www.scientific.net/KEM.500.813

PAPOUTSA, C., KOUNOUEDES, A., MILIS, M., TOULIOS, L., RETALIS, A., KYROU, K., and HADJIMITSIS, D., "Monitoring Turbidity in Asprokremmos Dam in Cyprus using Earth Observation and Smart Buoy Platform", *Journal of European Water*, Issue 38, pp. 25-32 (2012); http://www.ewra.net/ew/issue_38.htm

AGAPIOU A., D. G. HADJIMITSIS, C. **PAPOUTSA**, D. D. ALEXAKIS and G. PAPADAVID. "The Importance of Accounting for Atmospheric Effects in the Application of NDVI and Interpretation of Satellite Imagery Supporting Archaeological Research: The Case Studies of Palaepaphos and Nea Paphos Sites in Cyprus", *Journal of Remote Sensing*, Vol. 3(12), pp. 2605-2629 (2011); doi:10.3390/rs3122605; <http://www.mdpi.com/2072-4292/3/12/2605/>

Newsroom:

HADJIMITSIS D. G., HADJIMITSIS M. G., **PAPOUTSA CHR.**, AGAPIOU A. and THEMISTOCLEOUS, K., "Monitoring coastal water quality using ground-based and space technology", in *SPIE Newsroom*, August 17, 2010; doi:10.1117/2.1201007.002977

Conferences:

PAPOUTSA, C., RETALIS, A., and HADJIMITSIS, D. G., "Water Quality Monitoring over Asprokremmos Reservoir in Cyprus using MERIS satellite images", 8th GEO European Projects Workshop (GEPW-8), June 12-13, **2014**, Athens, Greece (poster).

PAPOUTSA, C., RETALIS, A., SCOULLOS, M., LOIZIDOU, M., ARGYROU, M., and HADJIMITSIS, D. G., "Coastal water quality monitoring over Cyprus based on ground truth field spectroradiometric data and remotely sensed observations", COMECAP 2014, ISBN: 978-960-524-430-9, Vol.3, pp. 49 (poster).

PAPOUTSA, C., RETALIS, A., TOULIOS, L., and HADJIMITSIS, D. G., "Monitoring Water Quality Parameters for Case II Waters in Cyprus using Satellite Data", in *Proceedings of the Second International Conference on Remote Sensing and Geoinformation of Environment - RSCy2014*, April 7-10, **2014**, Paphos, Cyprus.

AGAPIOU, A., ALEXAKIS, D. D., SARRIS, A., THEMISTOCLEOUS, K., PAPOUTSA, C., and HADJIMITSIS, D. G., "Satellite-derived land use changes along the Xin'an river watershed for supporting water quality investigation for potential fishing grounds in Qiandao Lake, China", in *Proceedings of the Second International Conference on Remote Sensing and Geoinformation of Environment - RSCy2014*, April 7-10, **2014**, Paphos, Cyprus.

PAPOUTSA, C., AKYLAS, E., and HADJIMITSIS, D. G., "The Spectral Signature Analysis of Inland and Coastal Water Bodies Acquired from Field Spectroradiometric Measurements", in *Proceedings of the First International Conference on Remote Sensing and Geoinformation of Environment - RSCy2013*, April 8-10, **2013**, Paphos, Cyprus.

PAPOUTSA, C., A. RETALIS, M. SCOULLOS, M. LOIZIDOU, M. ARGYROU and D. G. HADJIMITSIS, "Image Based Analysis for Assessing Coastal Water Quality Temporal and Spatial Variations in Limassol Harbor Area in Cyprus", in *Proceedings of the First International Conference on Remote Sensing and Geoinformation of Environment - RSCy2013*, April 8-10, **2013**, Paphos, Cyprus.

PAPOUTSA, C., D. G. HADJIMITSIS, L. TOULIOS, A. RETALIS and M. SCOULLOS, "Remote Sensing of Coastal Areas in Cyprus Using In-Situ Spectroradiometric Data and Water Quality Data: The "SAT-COAST" Project", in *Advances in Geosciences, Proceedings of 32nd EARSeL Symposium 2012*, May 21-24, **2012**, Mykonos Island, Greece.

AGAPIOU, A., D. G. HADJIMITSIS, A. NISANTZI, D. D. ALEXAKIS, K. THEMISTOCLEOUS, G. PAPADAVID and C. PAPOUTSA, "Variability of Field Spectroradiometric Measurements Using Nearly Lambertian Surfaces", in *Advances*

in Geosciences, Proceedings of 32nd EARSeL Symposium 2012, May 21-24, **2012**, Mykonos Island, Greece.

PAPOUTSA, C., T. KOUNOUEDES, M. MILIS, L. TOULIOS, A. RETALIS, K. KYROU and D.G. HADJIMITSIS, "Monitoring Turbidity in Asprokremmos Dam in Cyprus Using Earth Observation and Smart Buoy Platform", in *Proceedings of the VI International Symposium - EWRA 2011, Water Engineering and Management in a Changing Environment*, June 29 - July 2, **2011**, Catania, Italy.

PAPOUTSA, C., D. G. HADJIMITSIS and D. ALEXAKIS, "Characterizing the Spectral Signatures and Optical Properties of Dams in Cyprus using Field Spectroradiometric Measurements", in *Proceedings of SPIE 8174, in Remote Sensing for Agriculture, Ecosystems, and Hydrology XIII, 817419*, October 7, **2011**, Prague, Czech Republic; doi:10.1117/12.898353.

PAPOUTSA, C., D. G. HADJIMITSIS and D. ALEXAKIS, "Coastal Water Quality Near to Desalination Project in Cyprus using Earth Observation", in *Proceedings of SPIE 8181, in Earth Resources and Environmental Remote Sensing/GIS Applications II, 81810T*, October 26, **2011**, Prague, Czech Republic; doi:10.1117/12.898361

PAPOUTSA, C., D. G. HADJIMITSIS, A. RETALIS, and L. TOULIOS, "Statistical Analysis of Field Spectroradiometric Measurements Intended for Water Quality Monitoring in Asprokremmos Dam in Cyprus", in *Proceedings of 31st EARSeL Symposium and 34th General Assembly 2011*, May 30 - June 2, **2011**, Prague, Czech Republic.

PAPOUTSA CHR., and HADJIMITSIS, D. G., "Field Spectroscopy Measurements over Asprokremmos Dam in Cyprus Intended for Water Quality Monitoring", in *Proceedings of the International Conference on Remote Sensing, ICRS 2010*, October 5-6, **2010**, Hangzhou, China.

PAPOUTSA C., HADJIMITSIS D. G., THEMISTOKLEOUS K., PERDIKOU S., RETALIS A., and TOULIOS L., "Smart monitoring of water quality in Asprokremmos Dam in Paphos, Cyprus using satellite remote sensing and wireless sensor platform", in *Proceedings of SPIE 7831, in Earth Resources and Environmental Remote Sensing/GIS Applications, 78310Q*, September 20, **2010**, Toulouse, France; doi:10.1117/12.864824

PAPOUTSA CHR., and HADJIMITSIS D. G., "Assessment of Water Quality in Large Dams in Cyprus through Satellite Image Data", in *Proceedings of the 13th Pan-Hellenic Conference of the Greek Physical Union*, March 17 - 21, **2010**, Patra, Greece.

PAPOUTSA CHR., and HADJIMITSIS D. G., "A System for Monitoring and Observing the Surface Waters in Cyprus through Satellite Remote Sensing", in

Proceedings of the 13th Pan-Hellenic Conference of the Greek Physical Union, March 17 - 21, 2010, Patra, Greece.

PAPOUTSA CHR., and **HADJIMITSIS D.G.,** "Development of a New Innovative Method for Monitoring Coastal Water Quality near to Desalination Plants in Cyprus using Space Technology", in *Proceedings of Euroscience Mediterranean Event 2009 (ESME 2009), October 15 - 19, 2009, Athens, Greece.*

ABSTRACT

Maintaining water quality in inland and coastal water bodies in good condition is of the highest priority tasks in the implementation of the EU Water Framework Directive, and a key component in water resources management. This is of great importance for Cyprus, too, since a large number of reservoir water bodies have been developed to address drought, thus calling for systematic monitoring of water quality. Conventional methods for assessing water quality rely on sampling campaigns which are costly and time consuming. Aiming to fill the gap of the conventional field methods this PhD thesis is focused on providing novel methods for monitoring large surface Case-2 (inland and coastal) water bodies in the Mediterranean region using satellite images which can provide data on a systematic basis and offer synoptic coverage. To reach this goal, ground truth data measurements (spectroradiometric, turbidity and Secchi Disk Depth) were conducted simultaneously to satellite overpasses. Afterwards, statistical analysis and modelling techniques were employed to analyse and correlate the available data.

The first goal is to identify a suitable spectral region from which turbidity can be retrieved based on the field spectroradiometric measurements obtained during an extensive 3-years field campaign over Asprokremmos Reservoir, the main study area. Secondly, the aim is to provide the suitable bands for monitoring turbidity using different satellite sensors such as Landsat, Envisat MERIS and Chris-Proba. To test the derived algorithm eight available Landsat-5 TM and Landsat-7 ETM+ satellite images which were acquired at the same time as the field campaigns were processed; and the correlation between the satellite-derived data to the ground-based measurements was found statistically significant.

The third objective is to develop an algorithm which can be used for estimating the Trophic State Index over large surface Case-2 water bodies in the Mediterranean region on a systematic basis using remotely sensed data. All the data acquired during the field campaigns over different water bodies inland and coastal were

processed in order to examine and retrieve the 'best-fit' algorithm. This algorithm is of great importance since it can be applied for a wide range of water bodies with different trophic state values based on the band ratio values of the available Landsat satellite data. As a fourth objective the diffuse attenuation coefficient for Asprokremmos Reservoir was calculated and used in order to study its optical properties. Diffuse attenuation coefficient over the Reservoir was calculated for different bandwidths. The objective was to identify the optimal bandwidth which shows the best correlation with the TSI and SDD readings. For the calculation of the Diffuse Attenuation Coefficient values, field spectroradiometric data collected at different water depths below the water surface during the field campaigns in Asprokremmos were used.

Finally, this thesis provides a reference spectral library covering a wide range of Case-2 water bodies including oligotrophic and eutrophic inland water bodies, a shallow salt-lake and several coastal areas. This can assist the characterization of any water body based on its spectral characteristics being retrieved from the available satellite data.

All the above applications can become a very valuable tool for water quality monitoring of large reservoirs in Cyprus. This tool can be used on a systematic basis by the stakeholders, such as the Cyprus Water Development Department in the near future. All the field data can be further used to develop new algorithms based on the spectral resolution of any other satellite providing the opportunity to select satellites with different temporal and spatial resolution depending on the purpose of the application and the availability of satellite images.

Keywords: water quality; field spectroscopy; remote sensing; inland; coastal

TABLE OF CONTENTS

1	Introduction	22
1.1	Water Resources Management: A Global View	22
1.2	The Case of Cyprus	26
1.3	Remote Sensing as a Supporting Monitoring Tool.....	32
1.4	Problem Statement	33
1.5	Overall Structure of the Thesis	36
2	Literature Review: Water Quality Management and Monitoring of Surface Water Bodies using Field Spectroscopy and Remote Sensing Techniques.....	38
2.1	Remote Sensing for Monitoring Case-2 Water Bodies	38
2.2	Field Spectroscopy.....	42
2.3	The Underwater Light-field	45
2.4	Optical Properties.....	49
2.4.1	Pure Water	51
2.4.2	Phytoplankton.....	52
2.4.3	SPM.....	53
2.4.4	CDOM	55
2.5	Analysis of Reflectance Data.....	56
3	Resources and Methodology	59
3.1	Main Study Area.....	59
3.1.1	Meteorological and Hydrological Data of Study Area	60
3.1.2	Catchment Area & Geology of Study Area.....	61
3.1.3	Sampling Campaigns & Sampling Station Network.....	63

3.2	Other Study Areas	65
3.2.1	Lake Karla (Thessaly, Greece).....	65
3.2.2	Larnaca main Salt Lake (Alyki)	68
3.2.3	Coastal Areas in Cyprus (Limassol & Paphos District Areas).....	71
3.3	Resources	74
3.3.1	Boat & GPS.....	74
3.3.2	Field Spectroradiometer	75
3.3.3	Digital Turbidity Meter & Secchi Disk	79
3.3.4	Smart Buoy Monitoring System	81
3.4	Methodology	82
4	Development of Water Quality Predictive Models for Asprokremmos Reservoir	85
4.1	Field Campaigns	85
4.1.1	Sampling	87
4.1.2	Field Spectroradiometric Measurements	87
4.2	Statistical Analysis.....	89
4.2.1	Regression Analysis using <i>In Situ</i> Reflectance Data.....	89
4.2.2	Definition of Optimum Satellite Bands based on Regression Analysis of GER1500 Data versus SDD and Turbidity.....	92
4.3	Satellite Images Analysis	97
4.3.1	Pre-processing of Satellite Images.....	98
4.3.2	Comparing Results of Different Areas over Asprokremmos Reservoir	100
5	Development of the Trophic State Index (TSI) Predictive Algorithm for Case-2	
	Water Bodies	104
5.1	Theoretical Background.....	104

5.2	Study Areas	108
5.3	Results	109
6	Diffuse Attenuation Coefficient (k_d) over Asprokremmos Reservoir	119
6.1	Theoretical Background - Attenuation Coefficient.....	119
6.2	Analysis of Attenuation Coefficient.....	123
7	Examining the Spectral Characteristics of Different Water Bodies using Field Spectroscopy.....	129
7.1	Theoretical Background - Water Spectrum Characteristics	129
7.2	Analysis of Spectral Signatures over Different Water Bodies.....	131
7.2.1	Asprokremmos Reservoir (oligotrophic)	132
7.2.2	'Alyki'- Larnaca's Salt Lake (shallow lake - algal bloom observed).....	140
7.2.3	Karla Lake (mesotrophic - eutrophic lake).....	144
7.2.4	Coastal Areas.....	146
8	DISCUSSION AND CONCLUSIONS	148
8.1	Conclusions	148
8.2	Thesis Original Research Contribution	150
8.3	Discussion & Recommendations.....	151
	REFERENCES.....	153

TABLE OF TABLES

Table 4. 1: Field campaign data referred to sampling date and conditions during each campaign occurred for the years 2010, 2011 and 2012-2013 over Asprokremmos Reservoir.	86
Table 4. 2: Turbidity.	96
Table 4. 3: SDD and lnSDD.	96
Table 4. 4: Satellite images processed in the current study.	97
Table 6. 1: Values of correlation coefficient (R^2) for correlation $k_{d(\lambda_1-\lambda_2)}$ with corresponding Secchi Disk Depth values (power series) as well as $k_{d(\lambda_1-\lambda_2)}$ with corresponding TSI values (exponential series). Table illustrated the waveband range used for calculation of $k_{d(\lambda_1-\lambda_2)}$	127
Table 7. 1: Field campaign data acquired during 2010 over Asprokremmos Reservoir referring to sampling date: turbidity, SDD, TSI values; and sky conditions for sampling station 2 (low-turbidity values area) and sampling station 9 (high-turbidity values area).	134
Table 7. 2: Field campaign data acquired during 2011 over Asprokremmos Reservoir referring to sampling date: turbidity, SDD, trophic state index (TSI) values; and sky conditions for sampling station 2 (low-turbidity values area) and sampling station 12 (high-turbidity values area).	135

TABLE OF FIGURES

Figure 1. 1: Freshwater Resources - Long-term annual average (*The minimum period taken into account for the calculation of long term annual averages is 20 years) (Source: Eurostat 2010).....	23
Figure 1. 2: Map of the major Dams in Cyprus (Source: WDD 2010).	28
Figure 1. 3: Geographical distribution of precipitation in Cyprus (Source: http://environ.chemeng.ntua.gr/ineco/Default.aspx?t=288).....	29
Figure 1. 4: The Mediterranean divided into four regions (Source: UNEP-MAP 2010).	30
Figure 2. 1: (i) The components of radiance reaching a passive sensor - remote sensing signal: (1) Radiation reflected from the bottom of the water body (2) Radiation upwelling from the water volume and contains information relative to water quality (3) Radiation reflected by the air-water interface (4) Radiation scattered to sensor by the atmosphere between water and sensor.	48
Figure 2. 2: (i) Absorption spectra of two types of chlorophyll extracted in acetone (Source: Hall and Rao 1987) and (ii) Modelled reflectance spectra of chlorophyll concentration of 1, 10, 50, 100 and 250 mg m ⁻³ , respectively (Source: Rijkeboer et al. 1998).....	53
Figure 3. 1: Full scene / Partial scene: Landsat TM image of Cyprus focuses on the Study Area - Asprokremmos Reservoir.	60
Figure 3. 2: Picture of Asprokremmos focused in the (a) Outlet Area & (b) Inlet Area of the Dam.	60
Figure 3. 3: Map of the Catchment Area of Asprokremmos.	62
Figure 3. 4: Map presented the Geology of the Study Area.	63
Figure 3. 5: Maps of the sampling station network used during the field campaigns in Asprokremmos Reservoir during (a) 2010 & (b) 2011, respectively.	64

Figure 3. 6: Map of Lake Karla, located in Volos District area / Thessaly, Greece. Black squares show points of inflowing water for reconstruction purposes. Centre of the lake is at 39°29'00" N, 22°49'00" E (Reproduced from Oikonomou et al. 2012).	66
Figure 3. 7: Pictures taken during the first sampling campaign at the Karla Lake were dead fish were all over the water surface of the Lake.....	67
Figure 3. 8: Map of the sampling stations used during the field campaigns in Karla Lake.....	68
Figure 3. 9: Pictures of the sampling station located near Tekkes Mosque (a) high dryness observed and (b) lower dryness observed.	71
Figure 3. 10: Unusual algal bloom at the sampling station located near Tekkes Mosque.....	71
Figure 3. 11: Map of the sampling stations used during the field campaigns in the coastal area of Limassol and Paphos District.	73
Figure 3. 12: Sampling campaign in Asprokremmos Dam in Paphos District, Cyprus.	74
Figure 3. 13: Sampling campaign in Lake Karla in Thessaly Region, Greece.....	74
Figure 3. 14: Sampling campaign in Larnaca main Salt Lake (Alyki) in Larnaca District, Cyprus.....	75
Figure 3. 15: Sampling campaign in Limassol & Paphos District coastal areas, Cyprus.....	75
Figure 3. 16: Standard spectralon panel (Lambertian surface) used as reference value for the downwelling irradiance.	76
Figure 3. 17: Handheld field spectroradiometer GER1500 covering the UV-Vis-NIR area of the spectrum.	77
Figure 3. 18: (a) Fibre optic probe adjusted on GER1500 for underwater measurements of the upwelling radiance and (b) Macam diffuser 1 which	

incorporates a mirror and attaches to the fibre optic cable for underwater measurements of the downwelling irradiance.....	77
Figure 3. 19: A Secchi Disk used during the field campaigns to measure the Secchi Disk Depth.....	80
Figure 3. 20: (a-c) The portable Palintest Micro 950 Waterproof used to determine the turbidity level at several water samples during <i>in situ</i> campaigns.....	80
Figure 3. 21: Floating sensor platform.....	81
Figure 3. 22: Schematic diagram of methodology.....	84
Figure 4. 1: In situ reflectance measurement procedure: (a) Measuring the upwelling radiance $L_u(\lambda)$ at depth 0 ⁻ ; (b) Measuring the downwelling radiance $L_d(\lambda)$ at depth 0 ⁺ ; (c) Measuring the downwelling radiance $L_d(\lambda)$ at depth 0 ⁻	88
Figure 4. 2: Plots of the correlation coefficients (R^2) derived from the linear regression analysis against wavelengths. Correlation coefficients (R^2) were calculated for every single wavelength (350–1050 nm with a bandwidth of 1.5 nm) after correlating (a) turbidity (NTU), (b) SDD, and (c) $\ln(\text{SDD})$ values with the corresponding field reflectance values for each wavelength of the handheld spectroradiometer GER1500.	91
Figure 4. 3: Schematic representation of the spectral bands of CHRIS/Proba, Envisat-1 /MERIS and Landsat ETM+ multispectral scanning radiometers, and GER1500 field spectroradiometer using a typical water spectral signature collected in the 2 nd of July 2010 at sampling station 2 during the <i>in situ</i> sampling campaigns over the Asprokremmos Reservoir.....	93
Figure 4. 4: Schematic representation of correlation observed between the mean “in-band” reflectance and the SDD, $\ln\text{SDD}$ and TSI variables for the three examined satellite sensors.	96

Figure 4. 5: Sampling station network used during field campaigns divided into four groups – “Areas” and selected Areas Of Interest (AOI’s) used for the processing of the satellite data to retrieve the DN of the corresponding “Areas” 100

Figure 4. 6: Comparison of reflectance values retrieved from the satellite image versus the reflectance values acquired using the field spectroradiometer. 103

Figure 4. 7: Turbidity values retrieved from the satellite images versus ground truth turbidity values measured during the field campaigns over Asprokremmos Reservoir. 103

Figure 5. 1: Examined water bodies located in Cyprus, (1) Asprokremmos Reservoir, Paphos District; (2) Larnaca main Salt Lake (Alyki), Larnaca District and (3) Coastal area of Limassol District (3.1 Zugi, 3.2 Vassiliko Cement Works & 3.3 Old Harbour). 108

Figure 5. 2: Correlation between TSI_{SD} and several Landsat ETM+ one and two-band combinations derived using the ground truth measurements acquired during the extended field campaigns in Asprokremmos dam, in Paphos District. 111

Figure 5. 3: Comparison of a simple linear and two exponential regression models used to describe the relationship between our variables of interest, TSI_{SD} and the ratio Band2/Band3, derived from the ground truth measurements acquired during the extended field campaigns in Asprokremmos dam, in Paphos District. The linear model appears on the diagram as a dashed line, the exponential model is displayed as a continuous line and the exponential model with an intercept of 100 is displayed as a dotted line. 112

Figure 5. 4: A simple linear and the two exponential regression models used to describe the relationship between our variables of interest, TSI_{SD} and the ratio Band2/Band3, derived from the ground truth measurements acquired during the extended field campaigns in Asprokremmos dam, in Paphos District. The linear model appears on the diagram as a dashed line, the exponential model is displayed as a continuous line and the exponential model with an intercept of 100 is displayed as a dotted line. Data acquired from four different water bodies, Asprokremmos

dam in Paphos District; Larnaca main Salt Lake (Alyki); coastal area of Limassol and Karla Lake in Volos District, Thessaly, Greece are also shown. The empty circles represent measurements taken at the Asprokremmos dam; the empty triangles represent the measurements taken at the Larnaca main Salt Lake (Alyki); the empty squares referred to the measurements taken at the Karla Lake and the filled squares correspond to data acquired at the coastal area of Limassol. 112

Figure 5. 5: Correlation between TSI_{SD} and ratio Band2/Band3 of the mean “in-band” reflectance of ETM+ derived from the ground truth measurements performed over four different water bodies, Asprokremmos dam in Paphos District; Larnaca main Salt Lake (Alyki); coastal area of Limassol and Karla Lake in Volos District, Thessaly, Greece. The two exponential regression models used to describe the relationship between our variables of interest are shown. The exponential model is displayed as a continuous line and the exponential model with an intercept of 100 is displayed as a dotted line. The empty circles represent measurements taken at the Asprokremmos dam; the empty triangles represent the measurements taken at the Larnaca main Salt Lake (Alyki); the empty squares referred to the measurements taken at the Karla Lake and the filled squares correspond to data acquired at the coastal area of Limassol. 114

Figure 5. 6: Relation between the model-based and the field-based values of TSI_{SD} . (a) Represent the correlation resulted using only the “dependent” data-set that was used to develop the model and (b) represent the correlation resulted using only the “independent” data-set that was not included in the data-set used to develop the model. These data was acquired during the field campaigns in Asprokremmos Reservoir during 2011 and 2012. 116

Figure 5. 7: Correlation between SDD and turbidity (NTU) acquired during the field campaigns in Asprokremmos dam, in Paphos District. 117

Figure 6. 1: Diagram of various possible radiance fluxes: 1) Emergent flux: affected by the IOPs of the water and contains information relative to water quality; 2) Portion of the emergent flux: reflected back into the water body before passing

through the surface; 3) Reflection of the surface of direct solar radiance; 4) Reflection from the surface of diffuse sky radiance (Reproduced from Source: Lindell et al. 1999)..... 120

Figure 6. 2. In situ reflectance measurement procedure: (a) Measuring the downwelling radiance $L_d(\lambda)$ at depth 0⁺; (b) Measuring the downwelling radiance $L_d(\lambda)$ at several depths bellow water surface (0⁻, -10, -30, -50 & -100cm). 123

Figure 6. 3: Plots of $k_d(\lambda_1-\lambda_2)$ versus Secchi Disk Depth values using all possible wavebands presenting on Table 6. 1..... 127

Figure 6. 4: Diagram illustrating the correlation coefficients corresponding to correlation between k_d versus Secchi Disk, for wavebands ranging from 400 to 700 nm with different “band-steps” (a) 150 nm; (b) 100 nm and (c) 50 nm. 128

Figure 7. 1: Spectral signatures of Asprokremmos Reservoir correspond to different turbidity values acquired using the field spectroradiometer GER1500. 132

Figure 7. 2: Spectral signatures of Asprokremmos Reservoir correspond to different water depths below water surface acquired using the field spectroradiometer GER1500..... 133

Figure 7. 3: Map of the sampling station network used during the field campaigns over Asprokremmos Reservoir - Distinguish areas referred to turbidity variations are indicated. 136

Figure 7. 4: Landsat TM Image focused in the area of Asprokremmos Reservoir pointed out the two study areas of the Reservoir; Inlet & Outlet. 137

Figure 7. 5: Comparison of the spectral signatures corresponds to the Areas 1 to 4 of the Asprokremmos Reservoir..... 139

Figure 7. 6: Turbidity increasing trend across the Reservoir Areas..... 139

Figure 7. 7: Spectral signatures of Salt Lake (1st Sampling Campaign) where sampling points correspond to different dryness level were studied..... 141

Figure 7. 8: Water’s spectral signatures acquired during 3 different sampling campaigns over the Salt Lake correspond to different turbidity levels (3: 29.30 NTU; 1: 18.42 NTU and 2: 11.90 NTU). 142

Figure 7. 9: Diagram of the ideal bloom conditions (Source: Ian.umces.edu 2005). 143

Figure 7. 10: Water’s spectral signatures acquired during the 3rd Sampling campaign over the Salt Lake (a) correspond to different turbidity levels and to an algal bloom (1: 9.30 NTU; 2: 6.50 NTU, 3: 4.85 NTU and 4: Algal Bloom) and (b) representing the spectral signatures retrieved at different depths below the water surface during the algal bloom. 143

Figure 7. 11: Water’s spectral signatures acquired during the Sampling campaigns over Lake Karla in Thessaly; (a-b) corresponds to high chl-*a* concentration – more than 200µg/L and (c) to lower chl-*a* concentration – less than 60µg/L. 146

Figure 7. 12: Water spectral signatures acquired during the Sampling campaigns over several coastal areas in Paphos and Limassol; (a) represents two examples of waters differ on suspended solids concentration; (b) corresponds to coastal water having different bottom reflections – rocks & sand; and (c) illustrates the spectral signatures correspond to rocky surfaces covered with seaweed and surfaces covered with seaweed / algae plants. 147

TABLE OF ABBREVIATIONS & SYMBOLS

ABBREVIATIONS	
AOI	Area Of Interest
AOP's	Apparent Optical Properties
CDOM	Coloured Dissolved Organic Matter
chl- <i>a</i>	chlorophyll- <i>a</i>
DN	Digital Numbers
DOM	Dissolved Organic Matter
DP	Darkest Pixel
EU	European Union
FO	Fibre Optic
GER	Geophysical Environmental Research
GPS	Global Position System
IOP's	Inherent Optical Properties
Landsat ETM+	Landsat Enhanced Thematic Mapper
Landsat MSS	Landsat Multispectral Scanner
Landsat TM	Landsat Thematic Mapper
MCM	Million Cubic Meters
MERIS	Medium-Resolution Imaging Spectrometer
MODIS	Moderate-Resolution Imaging Spectroradiometer
MSS	Mineral Suspended Sediment
NIR	Near Infrared
NTU	Nephelometric Turbidity Units

ABBREVIATIONS

PAR	Photosynthetically Available Radiation
RS	Remote Sensing
RSR	Relative Spectral Response
SD	Secchi Disk
SDD	Secchi Disk Depth
SPM	Suspended Particulate Matter
SS	Suspended Sediment
TP	Total Phosphorus
TSI	Trophic State Index
TSM	Total Suspended Matter
TSS	Total Suspended Sediments
Vis	Visible
WDD	Water Development Department
WFD	Water Framework Directive
WQP	Water Quality Parameters

SYMBOLS

$\alpha_{(\text{CDOM})}$	absorption coefficients of Coloured Dissolved Organic Matter
$\alpha_{(\text{phyt})}$	absorption coefficients of phytoplankton pigments
$\alpha_{(\text{SM})}$	absorption coefficients of suspended material
$\alpha_{(\text{water})}$	absorption coefficients of water
$b_{b(\text{phyt})}$	backscattering coefficients due to phytoplankton pigments
$b_{b(\text{SM})}$	backscattering coefficients due to suspended material
$b_{b(\text{water})}$	backscattering coefficients due to water
E	irradiance
E_d	downwelling irradiance
E_u	upwelling irradiance
L	Radiance
L_d	downwelling radiance
L_u	upwelling radiance
R	Reflectance
k_d	diffuse attenuation coefficient
λ	Wavelength
N:P	Nitrogen : Phosphorus

1 Introduction

1.1 Water Resources Management: A Global View

It is widely recognized that at the dawn of the 21st century, many countries are entering a new era - an era of water scarcity and severe water shortage (Seckler et al. 1998). Water demand is driven by the rapid increase of world population as well as other stresses (Radif 1999). According to the 2012 Revision of the official United Nations population estimates and projections, the world population of 7.2 billion in mid-2013 is projected to increase by almost one billion people within the next twelve years, reaching 8.1 billion in 2025, and to further increase to 9.6 billion in 2050 and 10.9 billion by 2100 (United Nations, Dept. of Economic & Social Affairs 2013). Water availability is a key factor in many societies, shaping cultures, economies, history and national identity. This is especially true in the Mediterranean, where water resources are limited and very unevenly distributed over space and time (Roson and Sartori 2010).

Differences regarding water availability could be exacerbated by climate changes, with decreasing amounts of rain but more intense rainfall events predicted to occur in southern Europe coupled with more summer droughts, and increasing rainfall in central and northern Europe (EEA 2009a). Specifically, Finland and Sweden recorded the highest freshwater annual resources per inhabitant (around 20 000 m³ or more). By contrast, relatively low levels per inhabitant (below 3 000 m³) were recorded in the six largest Member States (Italy, France, the United Kingdom, Spain, Germany and Poland), as well as in Romania, Belgium and the Czech Republic, with the lowest levels in Cyprus (405 m³ per inhabitant) and Malta (188 m³ per inhabitant) (Eurostat European Commission 2010).

Freshwater availability in a country is determined not only by climate conditions but also by geomorphology, land uses and trans-boundary water flows (i.e. external inflows). Therefore, significant differences can be observed among freshwater resources over countries (Figure 1. 1), with Germany, France, Sweden,

Italy and the UK being the Member States with the highest amount of freshwater resources, with a long-term annual average between 164 300 and 188 000 million m³ and Malta, Cyprus and Luxembourg with the lowest amount of freshwater resources, with a long-term annual average of 100, 300 and 1600 million m³, respectively (Eurostat European Commission 2010; Eurostat 2010).

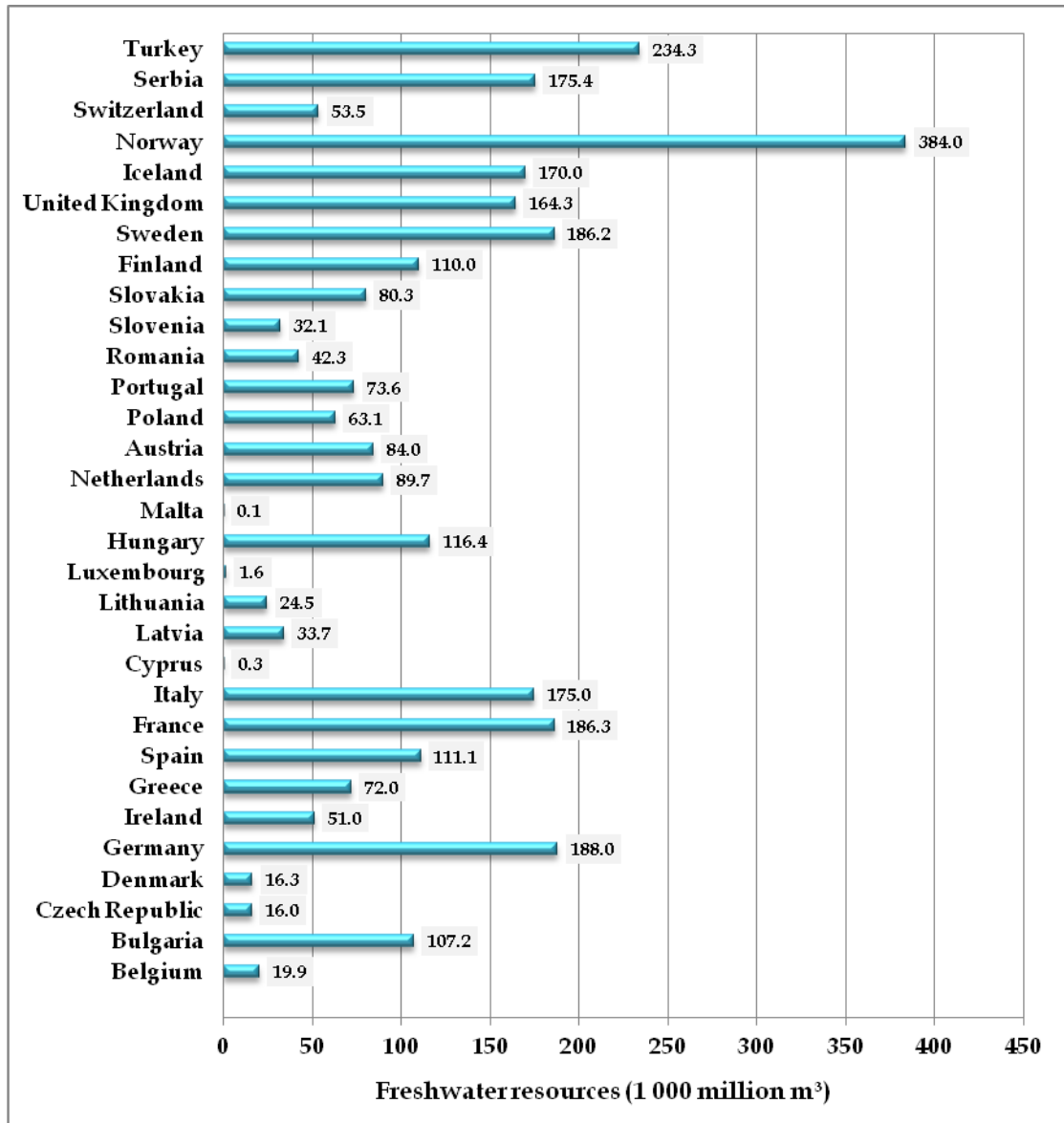


Figure 1. 1: Freshwater Resources - Long-term annual average (*The minimum period taken into account for the calculation of long term annual averages is 20 years) (Source: Eurostat 2010).

The increasing demand by citizens and environmental organizations for cleaner rivers and lakes, groundwater and coastal beaches has been evident for considerable time within the European Union (EU). This demand is one of the main reasons why the European Commission has made water protection one of the priorities of its work. Sustainable resource management requires that we maintain the natural capital stocks that deliver the most effective and efficient array of services. Sustainable management of water resources is essential in order to overcome the serious problems of pressures and impacts of water scarcity (EEA 2012; García-Ruiz et al. 2011).

The challenge of water quality management associated with the principle of sustainable development has been of concern to many researchers and managers in the last decade (Huang and Xia 2001). Both human activities and natural activities can change the physical, chemical, and biological characteristics of water, and will have specific ramifications for human and ecosystem health. Water quality is affected by changes in nutrients, sedimentation, temperature, pH, heavy metals, non-metallic toxins, persistent organics and pesticides, and biological factors, among many other factors (Carr and Neary 2008; United Nations Environment Programme (UNEP) 2010). Water quality is affected by materials delivered to a water body from either point or nonpoint sources. Point sources can be traced to a single source, such as a pipe or a ditch. Nonpoint sources are diffuse and associated with the landscape and its response to water movement, land use and management, and/or other human and natural activities on the watershed. Agriculture, industrial, and urban areas are anthropogenic sources of point and nonpoint substances. Polluting substances that lead to deterioration of water quality affects most freshwater and estuarine ecosystems in the world (Dekker et al. 1995; Ritchie et al. 2003).

By now, all European freshwater and coastal marine ecologists should be familiar with the *European Directive 2000/60/EC* establishing a framework for Community action in the field of water policy, which is commonly referred to as the *Water Framework Directive (WFD)*. The purpose of the directive is to establish a

framework for the protection of inland surface waters, transitional waters, coastal waters and groundwater. The directive aims to provide the mechanisms to prevent further deterioration, and it protects and enhances the status of aquatic ecosystems and, with regard to their water needs, of terrestrial ecosystems and wetlands directly depending on aquatic ecosystems (Irvine 2004).

The WFD establishes a framework for the protection of groundwater, inland surface waters, estuarine waters, and coastal waters and it will be the main international water law for the European countries in the coming decades. It requires a regular assessment of surface water and groundwater status using extensive reporting based upon vast monitoring efforts, including surveillance monitoring, operational monitoring and investigative monitoring. In this context, "status" is defined as an integrated assessment of chemical, hydrological, ecological and morphological water quality elements (Borja et al. 2006; Dworak et al. 2005).

The WFD constitutes a new view of water resources management in Europe based mainly upon ecological element; by obliging Member States to achieve the objective of at least "good ecological quality status" for all surface- and groundwater bodies by 2015 and requiring them to assess it by using biological elements, supported by hydro-morphological and physicochemical aspects (Birk and Hering 2006; Borja et al. 2006). The analyses of pressures and impacts must consider how pressures would be likely to develop, prior to 2015, in ways that would place water bodies at risk of failing to achieve ecological good status, if appropriate programmes of measures were not designed and implemented (Borja et al. 2006). Future scenarios for water resources in the Mediterranean region suggest (1) a progressive decline in the average streamflow including a decline in the frequency and magnitude of the most frequent floods due to the expansion of forests; (2) changes in important river regime characteristics, including an earlier decline in high flows from snowmelt in spring, an intensification of low flows in summer, and more irregular discharges in winter; (3) changes in reservoir inputs and management, including lower available discharges from dams to meet the water

demand from irrigated and urban areas and (4) hydrological and population changes in coastal areas, particularly in the delta zones, affected by water depletion, groundwater reduction and saline water intrusion (García-Ruiz et al. 2011). Since water resources become increasingly scarce the necessity of improving water management, water pricing and water recycling policies is requisite aiming both to ensure water supply and reduce tensions among regions and countries.

1.2 The Case of Cyprus

Cyprus is situated at the north-eastern part of the Mediterranean basin (33° east of Greenwich and 35° north of the Equator), and is the third largest island in the Mediterranean with an area of 9 251 square kilometres. It has a typical Mediterranean climate with mild winters, long hot, dry summers and short autumn and spring seasons.

In the region of Mediterranean the per capita consumption rates of water resource are already among the lowest in the world, but municipal and industrial requirements are expected to double and even triple over the next few years. Specifically, the values for the case of Cyprus regarding the surface and groundwater availability in m³ year⁻¹ person⁻¹ was 600 in 1971 and reduced into 300 in 2000. Moreover, Cyprus possesses the lowest amount of annual freshwater resources per capita in the EU (Araus 2004; EEA 2010; Eurostat 2010).

It is expected that a global climatic change will bring about increased temperatures and decreased precipitation adding a whole new dimension to the food and water challenge (Araus 2004; Mannion 1995; Postel 1999). Climate change projections for the Mediterranean region derived from global climate model driven by socio-economic scenarios show an increase of temperature (1.5 to 3.6°C in the 2050s) and precipitation decrease in most of the territory (about 10% to 20% decrease, depending on the season in the 2050s) (Iglesias et al. 2000, 2007; IPCC 2001).

According to (Hamdy et al. 1995) the Mediterranean countries are classified into three major groups with regard to future water problems. Cyprus belongs to the

countries whose water resources are currently sufficient but will decrease in the future, although these countries will be able to continue to meet their needs through water resource development provided per capita withdrawals do not increase significantly (Hamdy et al. 1995).

Great attention was given and continues to be given by the Water Development Department (WDD) in the rational exploitation of the water resources in reservoirs and ponds and in the development of water policy regarding the water resources management in Cyprus. Measures and strategic actions were taken by local water stakeholders (e.g., the Cyprus WDD) aiming to make the water resources management more sustainable. In Cyprus, the appearance of low rainfall periods is a rule and not an exception. Subsequently, these critical periods have to be faced with readiness and without causing deficits to the islands water systems. One way to achieve this is by storing and wisely managing the reserves so as to accommodate for the low rain seasons (Sofroniou and Bishop 2014).

Since the 1960s, Cyprus has followed a supply-side management approach that aimed at decreasing water shortages through the construction of dams and conveyance infrastructure. The motto of this management era was “No drop of water to the sea”. The freshwater storage capacity of the island was increased by 50 times: from 6 to 300 million cubic meters (MCM). According to the criteria of the International Commission of Large Dams (ICOLD) there are currently about 7000 large dams in Europe (i.e. dams higher than 15 m or reservoir with a capacity greater than 3 hm³). Nowadays Cyprus ranks as one of the countries with the highest dam development in the world. Water storage capacity in Cyprus is about twice the average annual runoff. The major dams of Cyprus are shown in Figure 1. 2 and it is worth noting that Cyprus is ranked first in the ICOLD register, in the area of Europe, with a ratio of fifty large dams for every 10 000 square kilometres (Delipetrou et al. 2008; EEA 2009b; WDD n.d.).

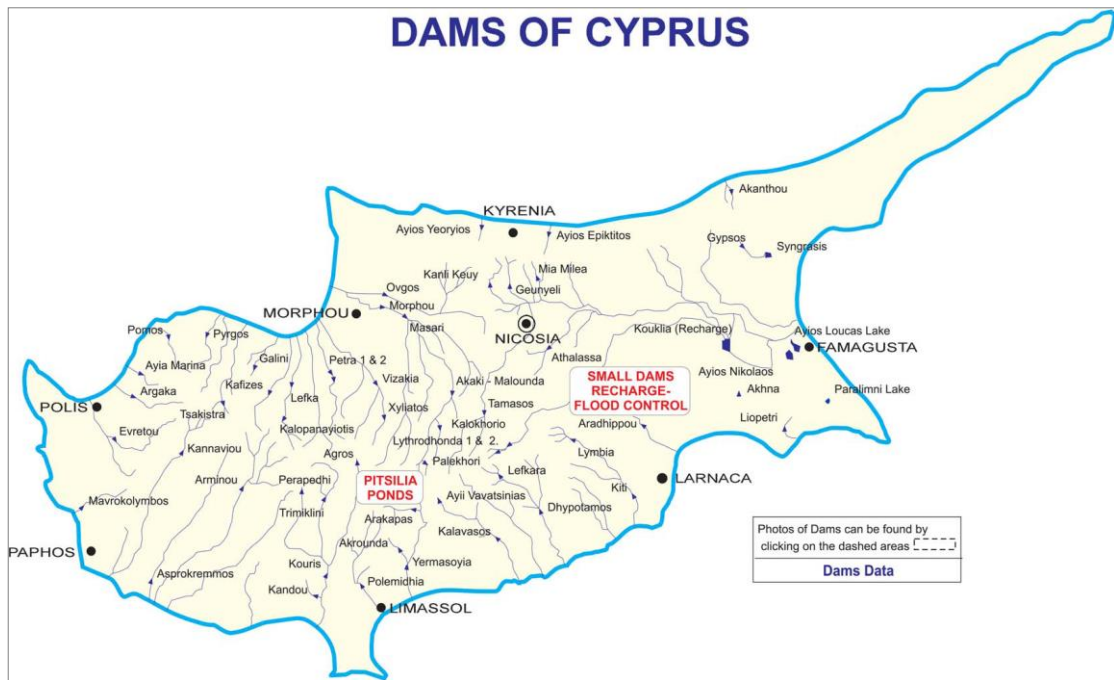


Figure 1. 2: Map of the major Dams in Cyprus (Source: WDD 2010).

Until 1997 the main source of water in Cyprus was rainfall. According to a long series of observations, the mean annual precipitation, including snowfall was estimated at 503 mm, and from 2000 until now has been reduced to 463 mm. The quantity of water falling over the total surface area of the free part of Cyprus is estimated at 2.750 MCM, but only 10% or 275 MCM is available for exploitation, since the remaining 90% returns to the atmosphere through direct evaporation and transpiration.

The rainfall is unevenly distributed geographically with the highest located in the two mountain ranges and the lowest in the eastern lowlands and coastal areas (Figure 1. 3). Additionally there is great variation of rainfall with frequent droughts spanning from two to four years. The average annual net rainfall of 275 MCM is distributed between surface and groundwater storage with a ratio 1:3 respectively. From the underground storage approximately 1/3 flows into the sea.

Statistical analysis of rainfall in Cyprus reveals a decreasing trend of rainfall amounts in the last 30 years, contrary to temperature variations which show an

increasing trend. The rates of change of precipitation and temperature are greater during the second half of the century compared to those in the first half. In the last decades the number of years of low precipitation and drought is greater than before and the semi - arid conditions both in Cyprus and in the eastern Mediterranean have deteriorated. Also, most of the warmest years of the century were observed in the last 20 years. Specifically, the total yearly average precipitation during the period 1961-1990 is about 500 mm. A lowest value of 182 mm was observed in 1972/73 and a highest of 759 mm occurred in 1968/69. The mean annual precipitation increases in the south-western windward slopes from 450 mm to nearly 1,100 mm at the top of the central massif of Troodos. On the leeward slopes, precipitation decreases steadily northwards and eastwards to between 300 and 350 mm in the central plain and the flat south eastern parts (the Kokkinochoria area) of the island (Iacovides 2011; Rossel 2001).

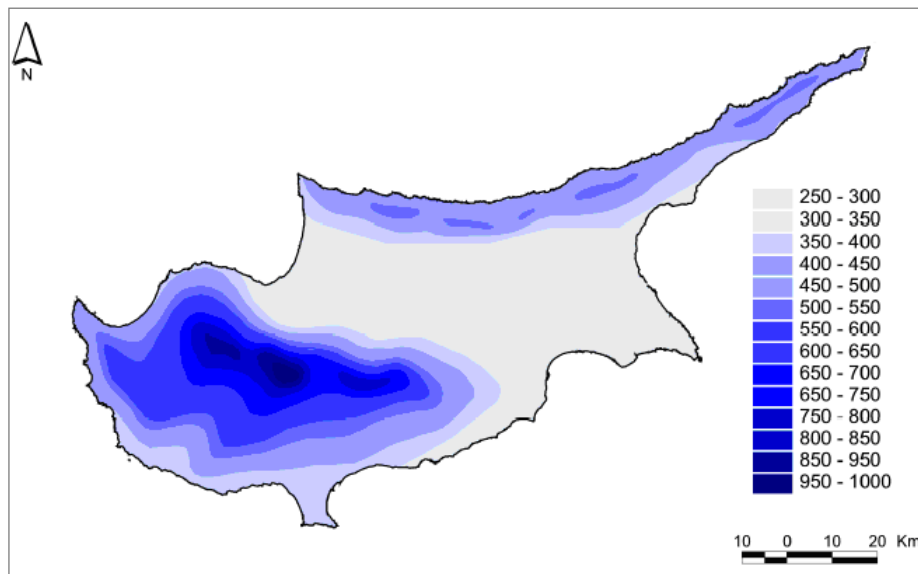


Figure 1. 3: Geographical distribution of precipitation in Cyprus (Source: <http://environ.chemeng.ntua.gr/ineco/Default.aspx?t=288>).

Moreover Cyprus' coastline measures approximately 735 km of which 50% is under the control of the Republic of Cyprus and 50% under Turkish occupation. As an island, the vulnerability of the coastal strip is extremely high in Cyprus,

since all land-based activities have a direct impact on this narrow strip. A well balanced coastal policy, based on an integrated approach and involving all the stakeholders is a demand of high priority for Cyprus, at least if the target is sustainable development is to be achieved.

For the purpose of identifying the important properties and assessing the state of the Mediterranean ecosystems and the pressure exerted on them, the Mediterranean Sea was subdivided into four regions. Such operational subdivision was the result of a consensus based on biogeographic and oceanographic considerations (2nd Meeting of Government-designated Experts on the Application of the Ecosystem Approach, Athens, 9-10 July 2008). The four regions identified (Figure 1. 4) are (i) Region 1: Western Mediterranean; (ii) Region 2: Adriatic Sea; (iii) Region 3: Ionian Sea and Central Mediterranean; and (iv) Region 4: Aegean Sea-Levantine Sea (UNEP-MAP 2010).

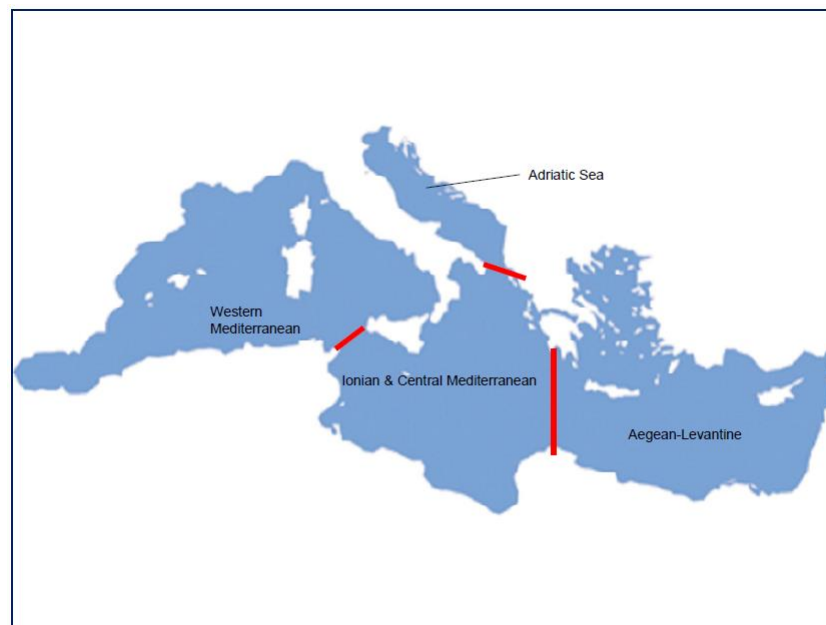


Figure 1. 4: The Mediterranean divided into four regions (Source: UNEP-MAP 2010).

The ultra-oligotrophic character of this region as well as the unusual Nitrogen : Phosphorus (N:P) ratios in its deep waters have stimulated a discussion on the major sources of nutrients (especially N and P). A recent review by Krom et al.

(2010) indicates that the major external sources of nutrients in the region are atmospheric dust input, direct anthropogenic input and fluvial (riverine) effluent. Estimates of the impact of these external nutrient sources (including anthropogenic sources) suggest that most of the production, 70-85 %, is actually regenerated production (Carbo et al. 2005; Yogeve et al. 2011). Approximately half of the new production is most likely due to mixing and entrainment from deeper layers, while most of the remainder is attributed to atmospheric dust inputs. A small fraction is due to riverine inputs, while nitrogen fixation is increasingly thought to be negligible in the Levantine basin (Petrou et al. 2012; Yogeve et al. 2011).

Cyprus is the largest island in the eastern Mediterranean and hosts many human activities around its coastline. Human activities such urbanization, industrial activities, tourism, maritime activities and others may induce increased nutrient concentrations and eutrophication in the coastal waters through land based pollution, sewage and urban runoff. Another problem is the increasing population in coastal areas that presents a potential (but localized) threat to the coastal sea grass resources caused by domestic sewage disposal which degrades water quality. Poor coastal planning signifies the anarchical coastal urbanization and the loss of natural resources (water quality, degradation / destruction of the coastal communities, over-frequentation). Potential impacts need to be studied and taken into account so as to minimize impacts (e.g., physical destruction of habitats, pollution, lights etc.). Apart from the Integrated Coastal Area Management, some impact mitigation measures could be applied to restore and / or to avoid negative effects on the marine habitats and biodiversity. This is the case of some of the main impacts on marine habitats (new marinas, dredging, breakwaters, desalination plants) (Howarth et al. 2000; UNEP-MAP 2007).

The WFD was put in force in 2000 by the EU and is focused on preserving, protecting and improving the quality of all water environments (groundwater, surface water and coastal water). Member States of the EU are obliged to achieve and maintain healthy water ecosystems by 2015. Chlorophyll is highly sensitive

indicator of nutrient, by which it is controlled and hence nutrient-enhanced, production and physical forcing of coastal ecosystems. In Cyprus maximum chlorophyll-*a* (chl-*a*) values measured in winter to early spring (November-March) when phytoplankton bloom occurs following the deep winter mixing. Site based chl-*a* values have been monitored within the WFD program for the period 2007-2010 and they are lower than 0.1 µg L⁻¹ which is set as boundary between “high” and “good” Ecological Status Classes. According to present methodology a possible minimum deviation from the reference conditions is acceptable. However, since the spatial scale used is different from the WFD this boundary limit can be modified in the future (Petrou et al. 2012; WFD_L164/19 2008; WFD_L232/14 2010).

1.3 Remote Sensing as a Supporting Monitoring Tool

New technologies and innovative practices play a central role in ensuring that society can meet its needs for goods and services without exceeding them. However, because of expense and time requirements for monitoring based on field campaign programs, it is impractical to monitor more than a small fraction of water bodies in a low frequency by conventional *in situ* methods. On the other hand, remote sensing technology is a promising tool that can potentially be used on a systematic basis to gather- and fill- the gaps, in terms of collecting data needed for water clarity assessments, in rich surface water bodies areas like Cyprus. It can provide robust data and indicators to water resource managers since it is a cost-effective solution which can act as a supporting tool for monitoring several surface water bodies simultaneously. It can provide water quality information data on a systematic basis having the advantage of synoptic coverage compared to the classic method of sampling campaign and analysis. Various projects have reported the development of empirical algorithms in order to monitor Case-2 waters' status such as chl-*a*, Secchi Disk Depth (SDD), turbidity, temperature etc. using several satellite sensors such as Landsat, MODIS, MERIS and others (Dekker et al. 2002; Miller and McKee 2004).

Coupling satellite observations with predictive models will provide better management of coastal areas for mitigation in areas of public health, invasive species, fisheries management and water resources. Therefore the development and improvement of satellite remote sensing technologies and applications for water quality observations rely on the needs of sustainable water strategies and new policies for water management (Coble et al. 2004).

Various studies have been reported on the usefulness of remote sensing as a tool in monitoring of water quality (Dekker et al. 2002; Ritchie and Charles 1996; Ritchie et al. 1990; Schalles et al. 1998). Remote Sensing can be defined as a science and the art of obtaining information about an object, area, or phenomena through the analysis of data acquired by device that is not in contact with the object, area, or phenomena under investigation (Thomas et al. 2004). Remote sensing of monitoring water quality has been started in the early 1970's (Usali and Ismail 2010). According to Diofantos G. Hadjimitsis et al. (2010), the high availability of cloud-free images increases the potential for using satellite remote sensing technologies for monitoring water quality in large dams and irrigation demand in Cyprus.

1.4 Problem Statement

Water reservoirs have been widely used in Cyprus for rain water storage while water scarcity and droughts are becoming more frequent events. From this point of view, systematic water quality monitoring of the reservoirs' water resources is of vital importance and must be implemented for efficient water resource management in order to achieve, maintain and protect "good status" for surface waters.

The WDD is responsible for implementing the water policy of the Ministry of Agriculture, Natural Resources and Environment, to provide effective protection, rational development and sustainable management of water resources in Cyprus. In this context, the WDD implements the necessary measures to prevent the

qualitative and quantitative deterioration of water bodies from contamination, pollution and uncontrolled exploitation (WDD 2009).

According to the WDD's annual reports in the framework of the water quality monitoring program for the implementation of Article 8 of Directive 2000/60/EC concerning rivers, lakes/reservoirs and groundwater 11 reservoirs were systematically monitored in 2009 (WDD 2009). During 2010 the national monitoring program for small reservoirs was expanded, in the context of which water samples for the determination of physicochemical parameters were taken at about 20 water reservoirs in a frequency of three times per annum (WDD 2009, 2010). The National Monitoring Program of the small reservoirs continued in 2011 as well, in collaboration with the District Offices of the Department. In 2011 one dam was added to the relevant monitoring network which now includes 22 water reservoirs. All of these reservoirs were sampled for physicochemical parameters with a frequency of 3 times a year (WDD 2011). In 2012 only 13 reservoirs were included in this monitoring program with a frequency of 4 to 6 times a year while 60 water samples were collected. In the context of biological classification of aquatic systems a contract for the analysis of samples of biological quality element "phytoplankton" in water reservoirs has been completed. Furthermore, 42 samples of phytoplankton were collected from reservoirs at different depths using a boat (WDD 2012).

The overall aim of this PhD thesis is to develop predictive models for monitoring water turbidity, SDD and Trophic State Index (TSI) in Cyprus' reservoirs from space using field spectroscopy. This would become a very useful tool in the case of Cyprus since a large number of reservoirs exist. Systematic monitoring of temporal and spatial variations over such water bodies based on remotely sensed images would be more efficient. In order to achieve this task, field spectroscopy has been used to identify the spectral regions where the best correlations of reflectance and Water Quality Parameters (WQP) are observed and can assist to the development of future satellite sensors based on such campaigns. Field spectroradiometric measurements are useful for validating satellite-derived

measurements as well as for supporting the removal of atmospheric effects from satellite images (Hadjimitsis et al. 2004).

The results presented in this work are part of a three year project which was ongoing from 2010 to 2012. This is the first time that an extensive field campaign has been implemented in Cyprus aiming to examine the variations of the WQP over large reservoirs using field spectroradiometric data. Specifically, the WQP that were determined is the turbidity and the SDD and the case study was the Asprokremmos Reservoir.

In this PhD thesis we will present the outcomes of the field spectroradiometric campaigns over Asprokremmos Reservoir and the methodology been used for the development of the predictive models for monitoring the WQP based on the analysis of the water spectral signatures. Useful information regarding saline or fresh water bodies can be gained from the analysis of a spectral signature. Field spectroradiometric data are processed in order to retrieve the at-satellite mean “in-band” reflectance values correspond to different satellite sensors having different spectral and spatial characteristics in order to develop the predictive algorithms correspond to each sensor and WQP. It is important to highlight that turbidity is a vital monitoring parameter for the Cyprus WDD, since any high concentrations of suspended solids (SS) may cause serious problems in water filtration processes.

Additionally, the thesis highlights the importance of studying the spectral signatures acquired over different water bodies (inland reservoirs, lakes and coastal) aiming to further test the extracted models. For this purpose additional field campaigns were performed over the Karla Lake in Greece which is a eutrophic lake high in nutrients, several coastal areas in Cyprus which are characterized as oligotrophic water bodies and over the Larnaca main Salt Lake (Alyki) in Cyprus which is a shallow lake high in nutrients. These additional data can be very useful since they may cover different areas of the model and help us to better understand the behaviour of the model including also some extreme values. Moreover, the examination of their spectral data can assist in collecting additional

information regarding the water optical characteristics and subsequently their quality characteristics such as the concentration of SS, chl-*a* and others.

1.5 Overall Structure of the Thesis

The structure of this thesis can be described as shown below:

- ❑ Chapter 1: “Introduction”: An overview of the global view and the case of Cyprus regarding Water Resources availability and management is given in this chapter. Furthermore, the problem statement and some introductory aspects on the importance of using Remote Sensing as a supporting tool are presented. Finally, the structure of the PhD thesis is presented.
- ❑ Chapter 2: “Literature Review: Water Quality Management and Monitoring of Surface Water Bodies using Field Spectroscopy and Remote Sensing Techniques”. In this Chapter, a review of the use of remote sensing techniques for the estimation of several WQP such as turbidity, SDD and chl-*a* is presented. Furthermore the theoretical background of the optical properties of water and the use of field spectroscopy in order to extract useful information regarding water quality status of a water body is discussed extensively.
- ❑ Chapter 3: “Resources and Methodology”. In this chapter, a summary on the resources used for the aim of this study as well as an outline of the developed methodology required to reach the goals are described.
- ❑ Chapter 4: “Development of Water Quality Predictive Models for Asprokremmos Reservoir”. In this chapter, an analytical description of the basic outcomes derived by processing of the field derived data (subsurface reflectance and water quality measurements) over Asprokremmos Reservoir is provided. Additionally based on the field spectroradiometric measurements the at-satellite mean reflectance values are calculated and the suitable bands for the calculation of the examined WQP are estimated for several distinct satellite sensors. Lastly, eight available Landsat satellite

images were processed aiming to examine the efficiency of the predictive algorithm.

- ❑ Chapter 5: “Development of the Trophic State Index (TSI) Predictive Algorithm for Case-2 Water Bodies”. In this Chapter, a description regarding the development of a predictive model aiming to assess the TSI over surface water bodies using the Landsat satellite sensor is given. For this implementation, field spectroradiometric measurements acquired over 4 different Case-2 water bodies are used.
- ❑ Chapter 6: “Diffuse Attenuation Coefficient (k_d) over Asprokremmos Reservoir”. In this Chapter the field spectroradiometric data acquired during the field campaigns in Asprokremmos Reservoir are processed in order to calculate the Diffuse Attenuation Coefficient values over different bandwidths ($k_{d(\lambda_2-\lambda_1)}$). These values were then correlated to the corresponding water quality values, aiming to detect the optimal spectral region which gives the best correlation between k_d and TSI or SDD, respectively.
- ❑ Chapter 7: “Examining the Spectral Characteristics of Different Water Bodies using Field Spectroscopy”. In this Chapter, an analysis on how spectral signatures of different water bodies can be affected by the optical properties of water is presented. An analysis of the differences and the main characteristics observed on the patterns of the spectral signatures corresponding to water bodies which differ on their trophic status are finally discussed.
- ❑ Chapter 8: “Discussion and Conclusions”. In this chapter, a brief discussion regarding the main outcomes and the most important conclusions derived from the PhD thesis is presented. Furthermore, the opportunities of using smart techniques from the stakeholders to assure the sustainable water resources management and possible areas of future work are highlighted. The original research contribution of this thesis is presented as well.

2 Literature Review: Water Quality Management and Monitoring of Surface Water Bodies using Field Spectroscopy and Remote Sensing Techniques

In this Chapter a concise review regarding the use of both field spectroradiometric data as well as airborne and satellite remotely sensed data for the water quality assessment over fresh and coastal water bodies is presented. An analysis on how optically active substances can affect the reflectance data is discussed. Finally, a description of several statistical methodologies used to retrieve algorithms assisting to calculate the main WQP using remotely sensed data is presented.

2.1 Remote Sensing for Monitoring Case-2 Water Bodies

In many developed countries the standard traditional mapping and monitoring techniques of water bodies have already become too expensive compared to the amount of information obtained for environmental use. More recently, the importance of coastal zone and inland water applications, such as pollution monitoring, combined with a new generation of satellite sensors has led to a surge of interest in the inversion of remotely sensed data for Case-2 waters (Östlund et al. 2001; Ruddick et al. 2000). Synoptic, multi-sensor satellite data products and imagery have become increasingly valuable tools for the assessment of water quality in inland and near shore coastal waters. Significant research and development activities and related user-driven applied efforts are underway in both developed and developing nations to generate products and information of interest for managers and decision makers (GEO 2007).

The traditional means of water quality analysis are based on point-by-point sampling and laboratory analysis of water samples. Besides being time-consuming and expensive, conventional methods of studying water quality (e.g. water sampling by boat) frequently fail to adequately represent heterogeneous and patchy areas. The increase in the spatial and temporal frequency of the

measurements is usually limited by time and cost. Efficient monitoring of the coastal water quality cannot be achieved using only water samples taken in vast coastal area. Since the 1980s satellite Remote Sensing represents an opportunity for synoptic and multi-temporal viewing of water quality. Satellite and airborne scanner data are useful in mapping some of the important WQP such as turbidity, SS and chl-*a* providing a better spatial knowledge of environmental variables. Therefore an integration of remote sensing technique and seawater sampling is more appealing and worth pursuing (Baban 1999; Büttner et al. 1987; Flink et al. 2001; Giardino et al. 2007; Khorram et al. 1991; Koponen et al. 2002; Liu et al. 2003; Östlund et al. 2001; Pulliainen et al. 2001; Su et al. 2008).

Satellite images are valuable tools for environmental assessment because they allow for daily or weekly collection of data, depending on satellite overpass frequency, rather than monthly as done by traditional sampling campaigns. Moreover the availability of low price satellite images enables the extended use of remote sensing for monitoring water quality in coastal areas. Finally the use of satellite imagery offers the advantage of providing spatially continuous data, rather than information relating only to sampling points (Chen et al. 2010; Lavender et al. 2002; Su et al. 2008; Wang et al. 2004).

Over the past few decades, remotely sensed data have been acquired through a range of airborne and space-borne sensors. The number of sensors and their capability diversity has increased over time. At present, a large number of satellite sensors observe the Earth surface at wavelengths from visible to microwave, at spatial resolutions from sub-meters to kilometres and at temporal frequencies ranging from 30 min to weeks or months. Furthermore, archives of remote sensing data are increasing, providing a unique, but not complete, series of Earth surface observations during the most recent time period (Rosenqvist et al. 2003). With this enormous data resource, there seems to be a potential for remote sensing to assist EU member states and candidates meet their obligations under the WFD (Chen et al. 2004a).

Successful remote sensing quantification of WQP is affected not only by the type of waters under investigation, but also by the sensor used. A classification scheme, according to which oceanic waters are partitioned into Case-1 or Case-2 waters, was introduced by Morel and Prieur (1977), and refined later by Gordon and Morel (1983) (Prieur and Sathyendranath 1981; Sathyendranath and Morel 1983; Sathyendranath et al. 1989). By definition, Case-1 waters are those waters in which phytoplankton (with their accompanying and co-varying retinue of material of biological origin) are the principal agents responsible for variations in optical properties of the water, refer to Open Ocean Waters. On the other hand, Case-2 waters are influenced not just by phytoplankton and related particles, but also by other substances, that vary independently of phytoplankton, notably inorganic particles in suspension and yellow substances, refer to Coastal and Inland Waters (IOCCG 2000). Paradoxically Case-2 waters cannot be satisfactorily studied from ocean observation satellite data such as Coastal Zone Colour Scanner (CZCS) and Sea-viewing Wide-Field-of-View (SeaWiFS) because of their coarse spatial resolution. Instead, the majority of quantification has to rely on meteorological (e.g., Advanced Very High Resolution Radiometer or AVHRR) and Earth resources satellites data such as Landsat, SPOT and IRS, even though they are designed primarily for terrestrial observations (Liu et al. 2003).

MERIS, SeaWiFS and MODIS/Aqua have been widely used by several researchers for monitoring water quality of coastal water bodies (Attila et al. 2013; Doron et al. 2011; Froidefond et al. 2002; Gitelson et al. 2007). As mentioned by Attila et al. (2013) the MERIS-instrument on the ENVISAT-satellite with its enhanced spatial resolution in full-resolution (FR) mode can offer more than MODIS and SeaWiFS do for the meandering coastline in the northern parts of the Baltic Sea. Also the spectral band combination of MERIS is well suited to this type of water body, as demonstrated by (Härmä et al. 2001).

Since the 1970s, many researchers have attempted to develop a robust algorithm for monitoring inland waters quality from several satellite sensors such as Landsat TM or ETM+ data (Chen et al. 2004b; Khorram et al. 1991; Lavery et al. 1993; Wang

et al. 2004), SPOT HVR data (Bhatti et al. 2011; Dekker et al. 2002; Doxaran et al. 2002; Kaiser et al. 2010; Ouillon et al. 1997; Su et al. 2008), MODIS TERRA data (Dall'Olmo and Gitelson 2005; Doxaran et al. 2009; Hellweger et al. 2004; Hu et al. 2005; Miller and McKee 2004; Wu et al. 2009), NOAA AVHRR data (Althuis and Shimwell 1995; Carrick et al. 1994; Chen et al. 2004b; Prangma and Roozkrans 1989; Van Raaphorst et al. 1998; Ruhl et al. 2001; Woodruff et al. 1999), MERIS data (Alikas and Reinart 2008; Bresciani et al. 2014; Koponen et al. 2002; Kratzer et al. 2008, 2014; Kutser et al. 2006; Ruiz-Verdú et al. 2008), ASTER data (Kishino et al. 2005; Nas et al. 2009), IRS-1C and -P6 data (Sheela et al. 2011; Thiemann and Kaufmann 2000; Xu et al. 2010), Hyperion data (Giardino et al. 2007; Kutser et al. 2005; Wang et al. 2005), IKONOS and QuickBird data (Ekercin 2007; Oyama et al. 2009; Sawaya et al. 2003).

There are numerous multi-spectral satellite sensors (e.g., MODIS, MERIS) that can provide optically-derived products such as pigment and dissolved/suspended matter concentrations or aerosol properties, but again these are primarily focused on the global domain which leads to limitations in their spatial and/or temporal resolution (IGOS 2006). The accounting of atmospheric effects in satellite images is an important step prior to any direct correlation between the at-satellite reflectance against WQP. In the case that atmospheric effects are not considered, the produced correlations are doubtful and not accurate (Hadjimitsis et al. 2004).

The retrieved water leaving spectral reflectance is related with water turbidity *in situ* measurements, using the atmospherically corrected satellite data in combination with the corresponding limnological data (Hadjimitsis and Clayton 2011; Hadjimitsis 2008; Rijkeboer et al. 1998; Sathyendranath et al. 2001). Many studies referred that with the development of remote sensing technology, remotely sensed data have been utilized to assess Secchi Disk Transparency (SDT) and Total Suspended Matter (TSM) (Dekker et al. 2002; Dewider and Khedr 2001; Hadjimitsis et al. 2006; Hadjimitsis, Clayton, et al. 2010; Pozdnyakov et al. 2005; Wang et al. 2004; Zhang et al. 2008). Field spectroscopy can support the remote sensing users to establish effective regression models since the measurements are

acquired on spot and no effect from the atmosphere is taken place (Hadjimitsis and Clayton 2011; Hadjimitsis et al. 2004).

2.2 Field Spectroscopy

Spectroradiometric measurements play an important role in the development of remote sensing applications. Field-based spectroradiometric measurements are necessary in remote sensing studies for three reasons; 1) they are required for determining underwater reflectance $R(0^-)$ from the Remote Sensing Radiance L_{rs} measurement; 2) they are essential for determining the atmospheric effect between the airborne sensor and the ground and 3) they may be used to predict the potential performance of existing or planned remote sensing instruments. *In situ* spectroradiometric measurements of reflectance and water quality analyses are of great importance for the development of predictive algorithms since they can provide critical information for the comprehension of spectral signatures over different water bodies functioning as a bridge between laboratory optical measurements and remote sensing measurements.

Field spectroscopy can support the remote sensing users to establish effective regression models since the measurements are acquired on the spot and no effect from the atmosphere is taken place. Moreover it can assist to identify and classify the at-satellite water reflectance and therefore improve or develop new algorithms and methodology to determine WQP using remotely sensed data (Hadjimitsis and Clayton 2011; Hadjimitsis et al. 2004; Papoutsas, Retalis, et al. 2014). However, one of the major difficulties is to define in advance the optimal or suitable bandwidths and spectral and radiometric resolution in which WQP should be retrieved so as to eliminate any errors in the development of predictive statistical models or equations (Papoutsas and Hadjimitsis 2013; Papoutsas, Hadjimitsis, Themistocleous, et al. 2010). In this manner spectroradiometric measurements can be a cost-effective way of determining the relevance of application of a remote sensor for a specific task, as illustrated by Dekker et al. (1990, 1991, 1992 b-d) and Dekker and Peters (1993) (Dekker 1993).

Spectroscopy is the study of the interaction between electromagnetic radiation and matter. According to Milton (1987) in remote sensing we are primarily concerned with electromagnetic radiation that has interacted with the object of interest and therefore carries information about the composition of the object or the nature of processes occurring within it. Spectral data are typically obtained for small areas at ground level using portable field spectroradiometers which provide highly detailed spectral information of known targets identified in the field (Milton 1987; Teillet 1995).

Nicodemus et al. (1977) introduced the term of a reflectance factor, being the “ratio of the radiant flux actually reflected by a sample surface to that which would be reflected into the same reflected-beam geometry by an ideal (lossless) perfectly diffuse (Lambertian) standard surface irradiated in exactly the same way as the sample”.

Field spectroradiometers measure the amount of energy reflected from a ground area or object of interest over different wavelengths, and these measurements can be converted to spectral radiance values if appropriate equipment calibration factors exist. The processing of raw field spectra into calibrated reflectance forms an important part of most remote sensing projects which use ground spectroradiometric data in support of airborne or satellite image analysis (Milton 1987; Peddle et al. 2001).

The use of a simultaneous dual-beam spectroradiometer offers the most efficient means of collecting field measurements of spectral reflectance (Duggin and Philipson 1982; Duggin 1980, 1981). In this configuration, the reference and target sensors are triggered simultaneously, minimizing the impact of changes in atmospheric state on the derived reflectance measurement (Rollin and Milton 1998). It is important to underline the need for an accurately defined field inter-calibration procedure in order to improve the quality of reflectance data collected using a dual-beam spectroradiometer system (Anderson et al. 2006).

The most common method used in field spectroscopy is referred as the “single beam” and involves sequential measurements of the spectral radiance from the target of interest followed by that from a calibrated reference panel. Typically, target measurements are “sandwiched” between two reference panel measurements made several minutes apart, and the irradiance at the time that the target is measured is estimated by linear interpolation (Robinson and Biehl 1979; Walter-Shea and Biehl 1990). This assumes that the irradiance varies continuously and linearly between the two reference panel measurements, which is not the case if sub-visual patches of water vapour pass through the direct solar beam, for example. Often, the best that can be done is to make the target and reference panel measurements in quick succession, typically within 1 min and assume that the irradiance is virtually unchanged (Milton and Rollin 2006).

White reference panels are required to obtain reflectance or absorbance values from radiance measurements. It is important to calibrate the reference panel over time (Pfitzner et al. 2005). This can be achieved by comparing the field panel to a non-contaminated laboratory panel. Based on such measurements, a wavelength-dependent ratio can be calculated which subsequently can be used to correct field spectra to the ‘true’ white reference standard. The laboratory reference itself should be calibrated against some national or international standard on a regular basis. This procedure will again yield correction ratios (Hueni et al. 2009; Pfitzner et al. 2006).

Through the components of light absorption and scattering coefficients, the water body controls the ratio between light scattering and absorption values, thus determining the subsurface reflectance and, in turn, the emergent flux that will be sensed by radiometers. Because the medium composition affects the absorption and scattering coefficients differently at various wavelengths, the resulting spectral distribution can be mathematically modeled and/or measured by a spectroradiometer from above and under the water’s surface, and thus can be used to provide information about the water body (Jupp et al. 1994; Senay and Shafique 2001a).

2.3 The Underwater Light-field

Radiative transfer theory is the framework that connects the optical properties of water with the ambient light field. The distinction of optical properties between the two mutually exclusive classes of properties (Inherent Optical Properties (IOPs) and Apparent Optical Properties (AOPs)) was made clear by Preisendorfer. These two classes can be related through the radiative transfer equation, which after mathematical manipulations is explicitly used in analytical methods or is simulated by use of a probabilistic approach known as the forward Monte Carlo method.

IOPs: are those properties that depend only upon the medium and therefore are independent of the ambient light field within the medium. The two fundamental IOPs are the *absorption coefficient* and the *volume scattering function*. Other IOPs include the *attenuation coefficient* and the *single-scattering albedo*. **IOPs are defined to be independent of the ambient light field and are not directly measurable in the field.** All parameters of bio-optical models can be referred back to the IOPs that theoretically express the bulk optical properties of natural waters in terms of: i) the absorption coefficients, ii) the backscattering coefficients of the visible water constituents, and iii) the phase function, which describes the angular behaviour of scattering processes.

The four intrinsic optical quantities, explaining the behaviour of light in water, which are all functions of the wavelength of light, λ (Jerlov 1968) are presented analytically below:

$a(\lambda)$: the absorption coefficient which quantifies light attenuation by transformation of the energy of photons;

$b(\lambda)$: the scattering coefficient which quantifies light attenuation by scattering of photons;

$c(\lambda)$: the attenuation coefficient, $c=a+b$ which quantifies the extinction of a collimated beam of light; and

$\beta(\theta,\lambda)$: the volume scattering function, which quantifies the dependence of scattered light intensity on scattering angle, θ .

Specification of the values of any 2 of $a(\lambda)$, $b(\lambda)$, or $c(\lambda)$ as well as $\beta(\theta,\lambda)$ completely characterizes a water in optical terms and, at least in principle, allows prediction of the behaviour in the water of any incident light field and thus prediction of the water appearance.

AOPs: are those properties that depend both on the medium (the IOPs) and on the geometric (directional) structure of the ambient light field and that display enough regular features and stability to be useful descriptors of the water body. Commonly used AOPs are the *irradiance reflectance*, the *average cosines*, and the *various attenuation functions (k functions)*. **AOPs such as spectral reflectance and the apparent water colour (the dominant wavelength) are directly measurable.** The radiative transfer equation provides the connection between the IOPs and the AOPs. The physical environment of a water body such as the waves on its surface, the character of its bottom, the incident radiance from the sky etc. enters the theory via the boundary conditions necessary for solution of the radiative transfer equation.

Remote sensing of water-constituent concentrations is based on the relationship between the remote-sensing reflectance, $R_{rs}(\lambda)$, and the IOPs of total absorption (a) and backscattering (b_b) coefficients:

$$R_{rs} = f \frac{b_b(\lambda)}{a(\lambda) + b_b(\lambda)} \quad (2.1)$$

Where λ is the wavelength (nm) and f is dependent on the geometry of the light field emerging from the water body.

$a(\lambda)$ is the sum of the absorption coefficients of phytoplankton pigments (a_{phyt}), coloured dissolved organic matter (a_{CDOM}), tripton or suspended material (a_{SM} , non-algal particles) and pure water (a_{water}). $b_b(\lambda)$ is the sum of the backscattering coefficients due to phytoplankton pigments ($b_{b(\text{phyt})}$), tripton or suspended

material (b_b (SM), non-algal particles) and pure water (b_b (water)) (Gitelson et al. 2008; Gordon et al. 1988; Papoutsas, Hadjimitsis, and Alexakis 2010):

$$a(\lambda) = a_{phyt}(\lambda) + a_{CDOM}(\lambda) + a_{SM}(\lambda) + a_{water}(\lambda) \quad (2.2)$$

$$b_b(\lambda) = b_b(phyt)(\lambda) + b_b(SM)(\lambda) + b_b(water)(\lambda) \quad (2.3)$$

For saline or fresh waters, however, two principal terms of consequence to understanding photon propagation entering, interacting with, and exiting from the water body are radiance (L) and irradiance (E). Radiance is defined as the amount of radiant energy per unit time per unit solid angle (i.e. towards a certain direction) per unit of projected area of the source (i.e. its unit is $W\ m^{-2}\ sr^{-1}$). Spectral radiance is the radiance per unit wavelength interval at a given wavelength (unit $W\ m^{-2}\ sr^{-1}\ \mu m^{-1}$). The radiance detected by the sensor in Figure 2.1 (L_d) can be expressed as

$$L_d = T_{atm}(L_w + L_s + L_b) + L_a + L_1 \quad (2.4)$$

Where L_w , L_s , L_a , L_b , and L_1 are the radiance components from the water volume (at depth $z = +0$, just above the surface), water surface (depth $z = +0$), atmosphere, bottom and adjacent areas, respectively, and T_{atm} is the transmittance of the atmosphere (the portion of the radiation that propagates through the atmosphere) (Koponen 2006).

Volume Reflectance: The dimensionless bulk water reflectance, $R(z,\lambda)$, is defined by the ratio of E_{up} to E_{down} , both measured at the same distinct water depth, z . The required reflectance for remote sensing studies, the volume reflectance, $R_{vol}(0^-, \lambda)$, is defined directly at the subsurface (0^-):

$$R_{vol}(0^-, \lambda) = \frac{E_{up}(0^-, \lambda)}{E_{down}(0^-, \lambda)} \quad (2.5)$$

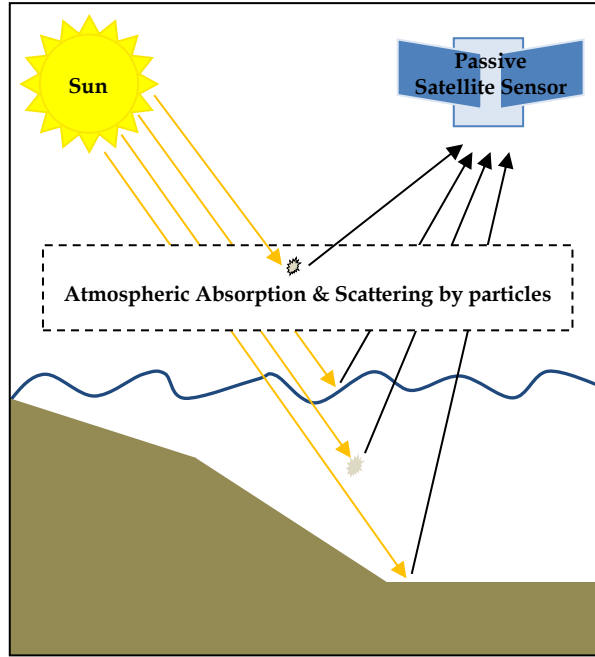


Figure 2. 1: (i) The components of radiance reaching a passive sensor – remote sensing signal: (1) Radiation reflected from the bottom of the water body (2) Radiation upwelling from the water volume and contains information relative to water quality (3) Radiation reflected by the air-water interface (4) Radiation scattered to sensor by the atmosphere between water and sensor.

There are physical restrictions on the measurement of $E_{up}(\lambda)$ and $E_{down}(\lambda)$ directly beneath the subsurface (0^-). In water, the irradiance at a particular depth, $E(z, \lambda)$, is a function of the intensity at the surface, $E(0^-, \lambda)$, and to the exponent of the negative-extinction coefficient, k , at the depth, z , (assumed constant over the interval 0^- to z):

$$E(0^-) = E(z) \times e^{kz} \quad (2.6)$$

Remote Sensing Reflectance: This widely used reflectance for water remote sensing studies is defined as the ratio of the water-leaving radiance, $L_w(0^+, \lambda)$, to $E_{down}(0^+, \lambda)$, directly at the water surface (0^+):

$$R_{rs}(0^+, \lambda) = \frac{L_w(0^+, \lambda)}{E_{down}(0^+, \lambda)} \quad (2.7)$$

The underwater light field was measured within a depth range of 1–5 m based on the Smith and Baker (1983) method; simultaneously, the downwelling incident irradiances $E_{down}(E)[0^+]$ were measured on-board ship. These irradiance values were transferred below the water surface after (Gordon et al. 1988) using:

$$E_{down}(\lambda)[0^-] = E_{down}(\lambda)[0^+] * 0.96 \quad (2.8)$$

2.4 Optical Properties

Some of the substances found in water contribute to the way in which optical radiation interacts with water bodies (through wavelength-dependent scattering and absorption). These optically significant substances change the colour of water. Remote sensing instruments using certain channels in the optical region of the spectrum can detect the changes and estimate the amount of optically significant substances (Koponen 2006). However, the use of remote sensing in marine and freshwater studies is limited at a relatively narrow region of electromagnetic spectrum comparing with the other ground targets. This is caused by a combination of factors, but mainly because of low solar irradiance reaching the earth's surface at wavelengths shorter than 400 nm and the combination of low solar energy with the steep increase of electromagnetic energy absorption by water at wavelengths larger than 850 nm. *Thus, the spectral range between 400 nm and 850 nm has been chosen by researchers to develop methods for estimating parameters of water quality by remote sensing.* Remote Sensing (RS) techniques of surface waters, using the Visible (Vis) and Near-Infrared (NIR) ranges of the electromagnetic spectrum, have contributed greatly to the understanding of large scale marine processes and to the assessment of the quality of water bodies (Dekker et al. 1994).

We now turn our attention to the way that each of the water constituents can affect the electromagnetic energy and as a result affects the signal reaching the remote sensor from a water body. The appearance of water colour can be determined through the analysis of the retrieval spectral signatures. Constituents and their concentration in the water can directly affect the optical properties of the water so

optical properties values can be used in order to evaluate the type of water and to determine WQP such as turbidity.

Substances in surface water can significantly change the backscattering characteristics of surface water. Remote sensing techniques depend on the ability to measure these changes in the spectral signature backscattered from water and relate these measured changes by empirical or analytical models to a WQP. The optimal wavelength used to measure a WQP is dependent on the substance being measured, its concentration and the sensor characteristics (Jerlov 1976; Kirk 1983; Ritchie et al. 2003).

Some water constituents can be estimated directly by RS techniques, as they have a direct effect on the optical properties of the examined water body; e.g. phytoplankton pigments, and particularly chl-*a* and phycobilins, Suspended Particulate Matter (SPM) and gilvin (Herut et al. 1999; Jupp et al. 1994). Other water characteristics can be estimated by the evident correlation that they show with an optically active water constituent, e.g., chl-*a* and phosphorus concentration (Kutser et al. 1995).

A comprehensive study of the absorption and scattering properties of the main visible water constituents has been given in Gordon and Morel (1983). They conclude that the water-leaving remote-sensing signal is mainly a function of:

- ❑ Absorption by phytoplankton pigments and detritus, where the photosynthesis pigment chl-*a* is of major importance
- ❑ Backscattering by SPM
- ❑ Absorption by Coloured Dissolved Organic Matter (CDOM)
- ❑ Fluorescence by CDOM and the phytoplankton pigment groups of billiproteins and chlorophylls (unlike absorption, fluorescence is directly linked to the physiological state of the photosynthetic system)
- ❑ Scattering by water molecules at short wavelengths and Raman scattering at intermediate wavelengths

The spectral absorption will cause a reduction in $R(0^-)$ while the spectral scattering will cause an increase in $R(0^-)$. The subsurface irradiance reflectance $R(0^-)$ is an essential parameter in the development of multi-temporal remote sensing algorithms. $R(0^-)$ acts as the link between: 1) laboratory-based determination of inherent optical properties; 2) *in situ* measured parameters of the (ir)radiance field and 3) the remotely sensed upwelling radiance signal. Overall, according to Kirk 1994, essentially all the light absorption which takes place in natural waters is attributable to four components of the aquatic ecosystem: the water itself, dissolved yellow pigments, the photosynthetic biota (phytoplankton, and macrophytes where present) and inanimate particulate matter (tripton) (J. T. O. Kirk 1994).

2.4.1 Pure Water

During an investigation of remote sensing in water bodies, it is first helpful to understand how the *pure water* absorbs and/or scatter selectively incident radiation or sunlight downward in the water column. Still, it is important to consider how the incident light is affected when the water column is not pure but contains organic and inorganic materials. The most notable pure water feature is the minimum amount of absorption and scattering of incident light in the water column (thus, the best transmission) occurs in the region of the wavelength of blue (400 to 500 nm). In the following wavelengths, light is very well absorbed by water and little scattering occurs.

Smith and Baker (1981) and Pope and Fry (1997) provide absorption spectra of pure water derived from laboratory investigations. Ocean Optic Protocols propose the absorption spectra of Sogandares and Fry (1997) for wavelengths between 340 nm and 380 nm, Pope and Fry (1997) for wavelengths between 380 nm and 700 nm, and Smith and Baker (1981) for wavelengths between 700 nm and 800 nm. Buiteveld et al. (1994) investigated the temperature dependant water absorption properties. Morel (1974) provides spectral values of the pure water volume scattering coefficient at specific temperatures and salinity, and the phase function.

2.4.2 Phytoplankton

Phytoplankton cells are strong absorbers of visible light and therefore play a major role in determining the absorption properties of natural waters. Chlorophylls and carotenoids are always present in micro- and macro algae. The main photosynthetic pigment is chl-*a*, the chlorophylls b, c and d are antenna pigments and coexist in species-specific variations. All chlorophylls absorb in the short blue wavelength range, and chl-*a* considerably in the red-wavelength range. The group of carotenoids is composed of a variety of pigments that serve as antenna pigments or protect the organism, and absorb in the blue-to-green wavelength range. The antenna pigment group of phycobilins is bound to phycobiliproteins and includes red pigments (e.g., phycoerythrin, phycoerythrocyanin) and blue pigments (e.g., phycocyanin). *The main variations in spectral shape occur in the blue to green wavelength range, where the accessory pigments show the maximum absorption* (Figure 2. 2). The phytoplankton scattering varies according to cell and colony sizes and shows lower backscattering probability with increasing cell size (Sathyendranath et al. 1995).

Absorption by phytoplankton occurs in various photosynthetic pigments, of which the chlorophylls are best known to non-specialists. *Absorption by chlorophyll itself is characterized by strong absorption bands in the blue and in the red (peaking at ≈ 430 and 665 nm, respectively, for chl-*a*), with very little absorption in the green.* Semi-empirical algorithms rest on the knowledge on how the optical properties of optically active variables affect the reflectance at the applied wavelengths. Chl-*a*, for example, can be estimated with the blue/green reflectance ratio in the case of oceans (O'Reilly et al. 1998) and with NIR/red ratio (Gitelson et al. 2002; Yacobi et al. 2011) in lakes. Both algorithms utilize the locations of absorption maximums of phytoplankton.

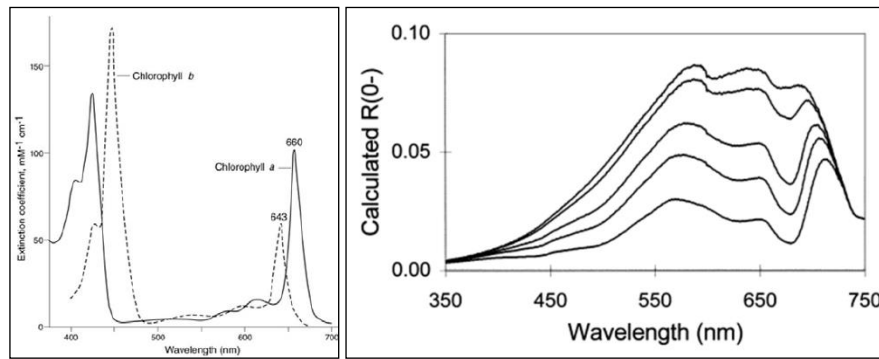


Figure 2. 2: (i) Absorption spectra of two types of chlorophyll extracted in acetone (Source: Hall and Rao 1987) and (ii) Modelled reflectance spectra of chlorophyll concentration of 1, 10, 50, 100 and 250 mg m⁻³, respectively (Source: Rijkeboer et al. 1998).

2.4.3 SPM

The main influence of turbidity is the limitation of light penetration in the water column, which is a factor that controls primary production. The signal becomes more complicated in coastal and estuarine turbid waters in which terrestrial substances, such as CDOM and SS, are present in addition to phytoplankton.

However, according to (Doxaran et al. 2002) results obtained with a reflectance model also showed that appropriate reflectance ratios are slightly influenced by variations of sediment types and that invariant and accurate relationships may be established between R_{rs} ratios (ratios between near-infrared and visible wavelengths) and the SPM concentration.

Concerning the lower SPM (<100 mg l⁻¹), the signal measured in the near infrared was weak, and the R_{rs} maximum was observed around 580 nm. Over 100 mg l⁻¹, the R_{rs} maximum was located around 700 nm, and a second maximum appeared at 800 nm. For the highest SPM concentrations (>300 mg l⁻¹), the measured R_{rs} signal was far from zero in the near-infrared wavelengths (700–1000 nm).

Relationships with high correlations were obtained between reflectance ratios of near infrared and visible bands and SPM. In fact, these reflectance ratios were almost insensitive to variations of sediment type that occur in estuaries and to changing illumination conditions. As a result, invariant relationships were

established between reflectance ratios and SPM, including all measurements carried out in the Gironde Estuary during a 6-yr period.

Turbidity can have a significant influence on aquatic communities. Turbidity is caused by a variety of water constituents, including SS, minerals, CDOM and algae. A frequently used approach involves regression of the blue and red optical bands (or their ratio) versus *in situ* water clarity data. The basis for this method is that as turbidity increases, red reflectance increases, while blue reflectance either decreases or does not increase as quickly as red, depending on the particular water constituents causing turbidity (e.g., CDOM versus sediment). This interaction between the red and blue bands has been shown to be a robust indicator of water clarity (Knight and Voth 2012).

There has been little agreement to date between published SS algorithms (Mitchelson-Jacob 1999), possibly because of variations in the range of Mineral Suspended Sediment (MSS) concentrations, particle size distributions, particle shape or mineralogy, as well as errors incurred through the presence of co-varying in-water constituents such as chlorophyll and yellow substance (Binding et al. 2003; Novo et al. 1989).

Suspended particles (sediments, phytoplankton) increase the energy reaching the sensor at all visible and near-infrared wavelengths, because the particles themselves are reflecting (Büttner et al. 1987). Quibell (1991) investigated the additive effects of sediments on the upwelling radiance from pure algal cultures and found that the addition of particulates increased reflectance at wavelengths longer than 550 nm. Dekker et al. (1991) analysed spectral curves collected on two of the Loosdrecht Lakes in the Netherlands and found that the best estimates of optical water quality (including algal chlorophyll) were made by using ratios at wavelengths between 600 and 720 nm (Han and Rundquist 1997).

In the visible and near-infrared spectral regions, and especially in the near-infrared, most of the backscattering is caused by suspended matter in comparison to other major colour-producing constituents in water (Ruddick et al. 2006;

Teodoro et al. 2007). Mahtab et al. (1998) investigated the responses of remote-sensing reflectance (R_{rs}) to different C_{TSM} according to the simulated spectra, and concluded that TM Band 4 (TM4) was the best for retrieving C_{TSM} . Gitelson et al. 1993 pointed out that the reflectance at 700–900 nm was sensitive to TSM, and these bands were the best for retrieving C_{TSM} from reflectance (Ma et al. 2011).

Although, Band4 can be used only for high turbidity levels since water itself highly absorbs in this region. According to the findings of Harrington et al. 1992; exo-atmospheric reflectance measures referred to (1) Landsat MSS Band 1, are highly sensitive to low SS concentrations and reflectance quickly saturates with increasing sediment loads; (2) Landsat MSS Band 3 provides the greatest ability to monitor the range of SS levels that are of most concern in lake resource management (i.e., 0-500 mg L⁻¹) and 3) Landsat MSS Band 4 is most sensitive to very high SS loads. A greater precision can be obtained with estimates of SS concentration based on the use of Landsat MSS Band 3 (Harrington et al. 1992).

2.4.4 CDOM

“Gelbstoff” as an important aquatic group was first introduced by Kalle (1937; 1949). In limnological literature, this complex group is also called gilvin, while in remote-sensing terms, it is known as yellow substance (Bricaud et al. 1981), aquatic humus (Dekker 1993) and CDOM (Schwarz et al. 2002). Fulvic and humic acids in varying attributions constitute the main part of CDOM and represent the coloured fraction of dissolved organic carbon in natural waters (Theng 1987). These complex dissolved organic substances are autochthonous, originating from decaying phytoplankton biomass, and allochthonous, coming from river input and coastal erosion (Heim 2005).

Their common optical behaviour is that they strongly absorb in the ultraviolet to blue wavelength region, causing the yellowish to brownish colours in organic-rich waters. The minimal influence of yellow substance at longer wavelengths suggests that an MSS algorithm may have a greater probability of success if the wavelengths are selected from the red region of the spectrum. This is confirmed

by the greater proportion of explained variance in the relationship between MSS and Reflectance at longer wavelengths (represented by the R^2 values) (Binding et al. 2005).

2.5 Analysis of Reflectance Data

Several statistical techniques have been used to investigate the correlation between spectral wavebands or waveband combinations and the desired water quality parameters in order to develop suitable predictive models correspond to each WQP and satellite sensor. The retrieval of concentrations of different water quality factors from remote sensing measurements is based on the analysis of hyperspectral data. Several different computational approaches and bio-optical models have been proposed; see e.g. (Ammenberg et al. 2002; Gordon and Morel 1983; Hakvoort et al. 2002; Malthus and Dekker 1995; Pope and Fry 1997; Tanaka et al. 2004). Some researchers used only direct regression analysis with WQP without employing any full-scale *in situ* spectroradiometric measurements (Alparslan et al. 2007, 2010; Hadjimitsis et al. 2006).

In general, the development of empirical relationships between spectral properties and WQP has been widely used from several researchers using several satellite, airborne or field spectroradiometric data. For the development of high spectral resolution remote sensing applications, both imaging and non-imaging (either line or point measurements) data are of interest. Ground-based surface and subsurface spectral measurements may serve as surface calibration and as the link between the remotely sensed signal and the inherent optical properties.

Ritchie et al. (1974) developed an empirical approach to estimate SS. The general forms of these empirical equations are:

$$Y = A + BX \text{ or } Y = AB^X \quad (2.9)$$

Where Y: is the remote sensing measurement (i.e., radiance, reflectance, energy) and X: is the WQP of interest (i.e., SS, chlorophyll). A and B are empirically

derived factors. In empirical approaches statistical relationships are determined between measured spectral/thermal properties and measured WQP. Often information about the spectral/optical characteristic of the WQP is used to aid in the selection of best wavelength(s) or best model in this empirical approach. The empirical characteristics of these relationships limit their applications to the condition for which the data were collected. Such empirical models should only be used to estimate WQP for water bodies with similar conditions (Ritchie et al. 1974, 2003).

Gitelson et al. (1993) determined regressions of the form shown in Equation 2.10 in order to relate the reflectance data to constituent concentrations.

$$C_k = aZ^b \quad (2.10)$$

Where Z : is a *normalized reflectance function* that is maximally sensitive to constituent k , and least sensitive to disturbing effects (including survey and irradiance conditions, equipment parameters, variations in other constituent concentrations and so on), C_k : is the constituent concentration, and a and b are regression coefficients that, hopefully, do not vary between systems.

To emphasize the specific relative contribution of constituent inherent optical properties (such as absorption and scattering coefficients) to reflectance, the dimensionless reflectance function Z can be found through a normalization process, that relates the reflectance at a wavelength that is sensitive to constituent variation (R_{active}), to the reflectance at wavelengths that are relatively insensitive to constituent variation ($R_{reference}$). There are two alternative normalizations that have been found effective:

Reflectance ratio:

$$z = R_{active}/R_{reference} \quad (2.11)$$

Reflectance difference ratio:

$$z = [(R_{active} - R_{reference}) / (R_{active} + R_{reference})] \quad (2.12)$$

Note that R_{active} and $R_{reference}$, will depend almost equally on the survey conditions and parameters of the radiometer.

3 Resources and Methodology

In this Chapter, a brief description of the selected study areas and an outline of the materials and methods used for the aims of this research are presented. Moreover, the meteorological, hydrological and geological characteristics of the main study area; as well as how the sampling station network was designed and how field measurements were conducted are described. Finally, the overall methodology and the goals of this PhD are illustrated in a comprehensive diagram.

3.1 Main Study Area

Asprokremmos Reservoir in Paphos District was the pilot study area selected for our sampling campaigns. The deepest area of the reservoir is located at 32°33'18.30"E and 34°43'38.40"N. Asprokremmos Dam is built at an altitude of about 80m above sea level and is located 16km east of the city of Paphos. It was completed in 1982 and is the second largest reservoir in Cyprus with a maximum capacity of 52,375,000m³. It is an earth-fill dam consisting of the main embankment, spillway, tunnels and galleries and geotechnical works. Due to poor rainfall the dam rarely overflows. Xeros River which flows into the dam runs only during winter and spring. Water is used for both potable and irrigation purposes. Figure 3. 1 shows a partial scene of Asprokremmos Dam acquired from Landsat TM satellite sensor and Figure 3. 2 presents the two areas of the reservoir where extreme conditions are observed (Outlet Area: lower turbidity values & Inlet Area: higher turbidity values).

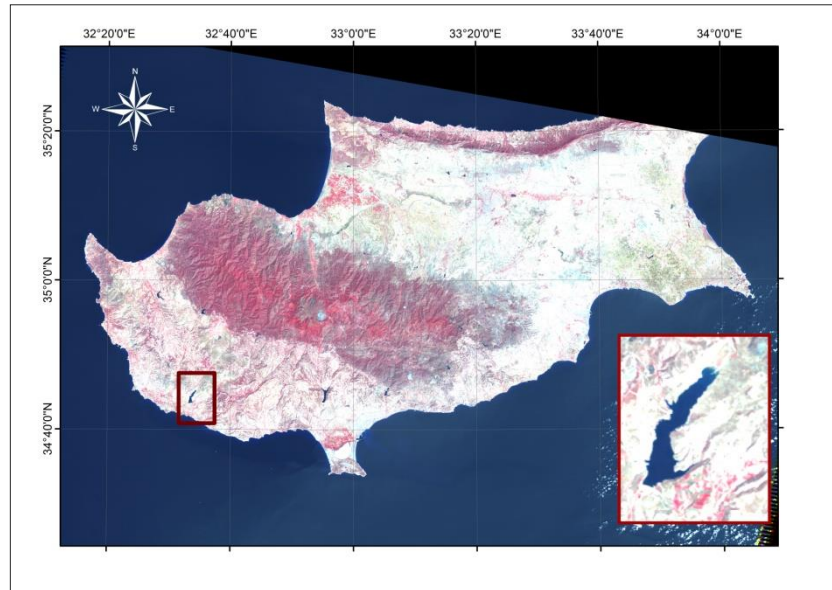


Figure 3. 1: Full scene / Partial scene: Landsat TM image of Cyprus focuses on the Study Area - Asprokremmos Reservoir.

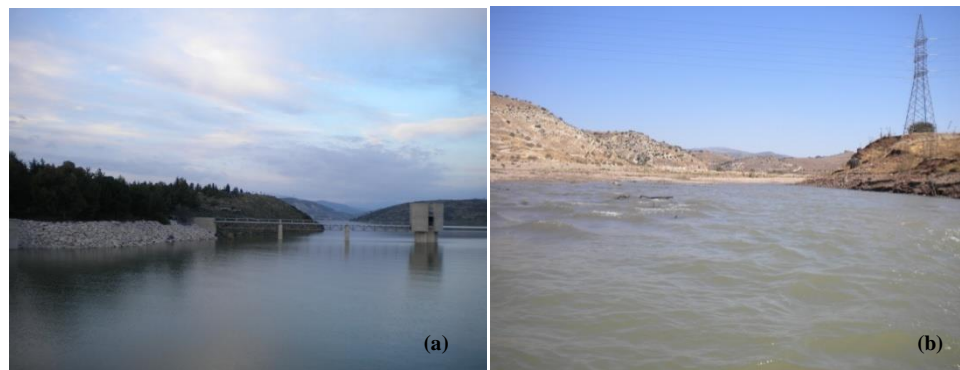


Figure 3. 2: Picture of Asprokremmos focused in the (a) Outlet Area & (b) Inlet Area of the Dam.

3.1.1 Meteorological and Hydrological Data of Study Area

It is important to highlight that when the reservoir reaches its maximum capacity (overflows) the deepest point is at about 55m height. The Reservoir area at this condition is about 25,925,000m² and the measured height at the tower (sampling station 1) is about 50m.

According to WDD annual reports the Water situation in 2010 was improved compared to previous years, due to higher rainfall on the one hand resulting in the inflow of larger quantities to the dams, and to the construction of new desalination units on the other, with total capacity reaching 180 000 m³/day at the end of 2010 when the Paphos desalination plant was put into operation. Precipitation in 2010 reached 546 mm or 109% of average rainfall. Inflow to the dams during 2010 (Jan.-Dec 2010) reached 119 MCM. Reservoir storage on 01/01/2010 was 95,6 MCM or 32,9% of total capacity, while on 31/12/2010 it was 139,3 MCM or 48% of total capacity (WDD 2010).

The water situation in 2011 was worse than previous year; this is due to the reduced rainfall, followed by reduced amounts of water inflow to the dams. The maximum water storage in the dams during May 2011 was 182.2 MCM while during 2010 was 195.5 MCM. The rainfall reached 464 mm or 92% of the normal. The inflow to the dams from January to December 2011 was only 65.5 MCM. The water storage in the dams on 1/1/2011 was 139.3 MCM or 48% of the total storage capacity while on 1/1/2012 was 124.9 MCM or 43% of the total storage capacity (WDD 2011).

During 2012, the water situation in Cyprus was much better, compared to the previous year, due to the high rainfall levels and the increased amounts of water inflows into the dams. The water reserves in the dams were 125 MCM, or 43% of their capacity, on 1/1/12 and reached 274 MCM, or 94.2% of their capacity, by mid-April. In 2011 the maximum amount of reserves was 182 MCM, or 62.6% of the dams capacity. The total water inflow into the dams during the calendar year 2012 was 239 MCM, which is the greatest flow ever recorded in a single year. The rainfall was 654 mm or 131% of the mean rainfall (Wdd 2012; WDD 2012).

3.1.2 Catchment Area & Geology of Study Area

Within the spatial limits of Asprokremmos basin nine villages are established (Figure 3. 3). The upstream area is rather hilly (485 m height) compared to the downstream which is part of Paphos district extensive coastline. The basin is

covered by an extensive dendritic drainage network with Xeros River to be the higher order stream of the network.

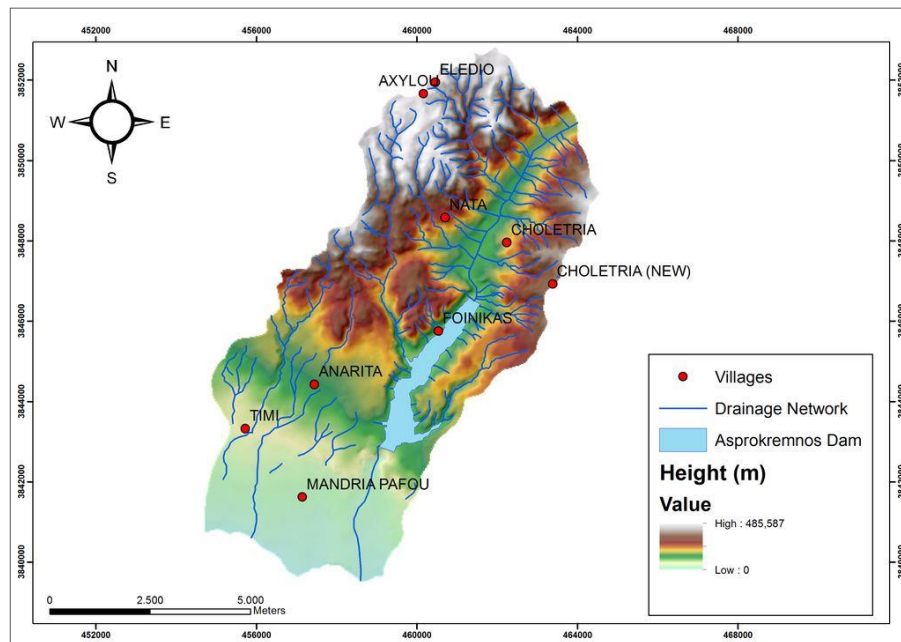


Figure 3. 3: Map of the Catchment Area of Asprokremnos.

Concerning the geological igneous, sedimentary and metamorphic rocks, ranging in age from Middle regime, the main part of the catchment area is covered by the Lefkara and Mamonia Complex formations (Figure 3. 4). The Lefkara Formation includes pelagic marls and chalks with characteristic white colour, with or without cherts. The Mamonia Complex constitutes a diverse and structurally complex assemblage of allochthonous Triassic to Upper Cretaceous (230-75 Ma). Overlying the Mamonia Complex rocks, there is an allochthonous sedimentary formation, known as Kathikas Melange, The lower south-western part of the basin is mainly covered by terrace deposits and Pakhna and Kalavasos formations. Pakhna Formation (Miocene, 22 Ma), consists mainly of yellowish marls and chalks. The deposition of the evaporates of the Kalavasos formation followed in the Upper Miocene (Messinian, 6 Ma) as a result of the closure of the Mediterranean Sea from the Atlantic Ocean and the evaporation of its waters. The Formation is composed

of gypsum and gypsiferous marls (Newman 2013, 2014; Robertson and Woodcock 1979).

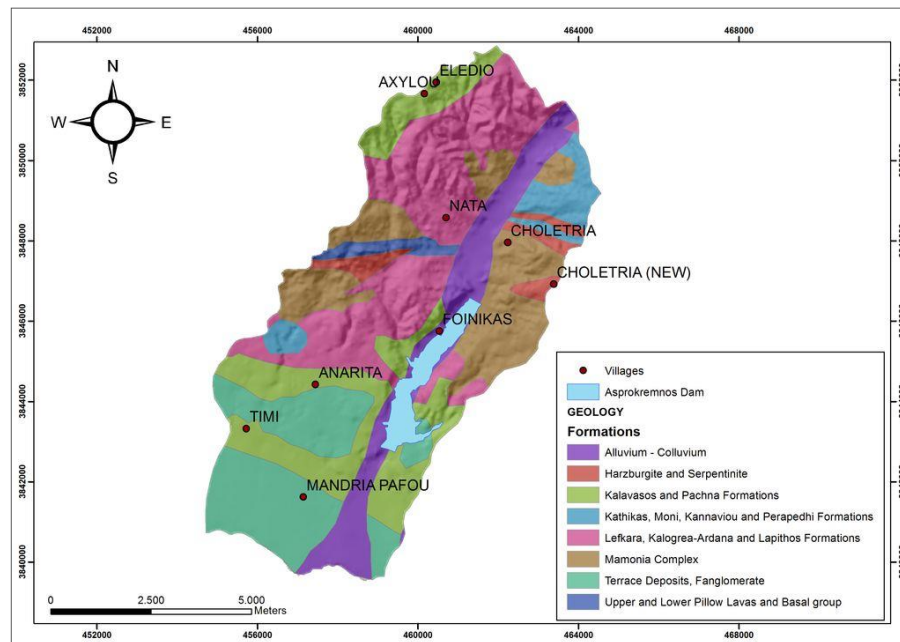


Figure 3. 4: Map presented the Geology of the Study Area.

3.1.3 Sampling Campaigns & Sampling Station Network

This study is focused on the Asprokremmos Reservoir where both spectroradiometric measurements and image analysis were acquired. The results presented in this thesis are part of a complex project lasted from 2010 to 2013 aiming to develop a systematic image-based tool for assessing water quality over large reservoirs in Cyprus. Outcomes from the process of data (spectroradiometric & turbidity data) acquired during the field campaigns which lasted for three years are going to be presented. An ideal sampling station network in the area of Asprokremmos Dam was designed for the aims of this study. The main goal was to have an adequate number of sampling stations positioned in all directions for the proper and adequate coverage of the study area. Finally, the sampling station network used for the field campaigns during the years 2010 (11 sampling stations) and 2011/2012 (12 sampling stations) are respectively shown in Figure 3. 5(a) and (b).

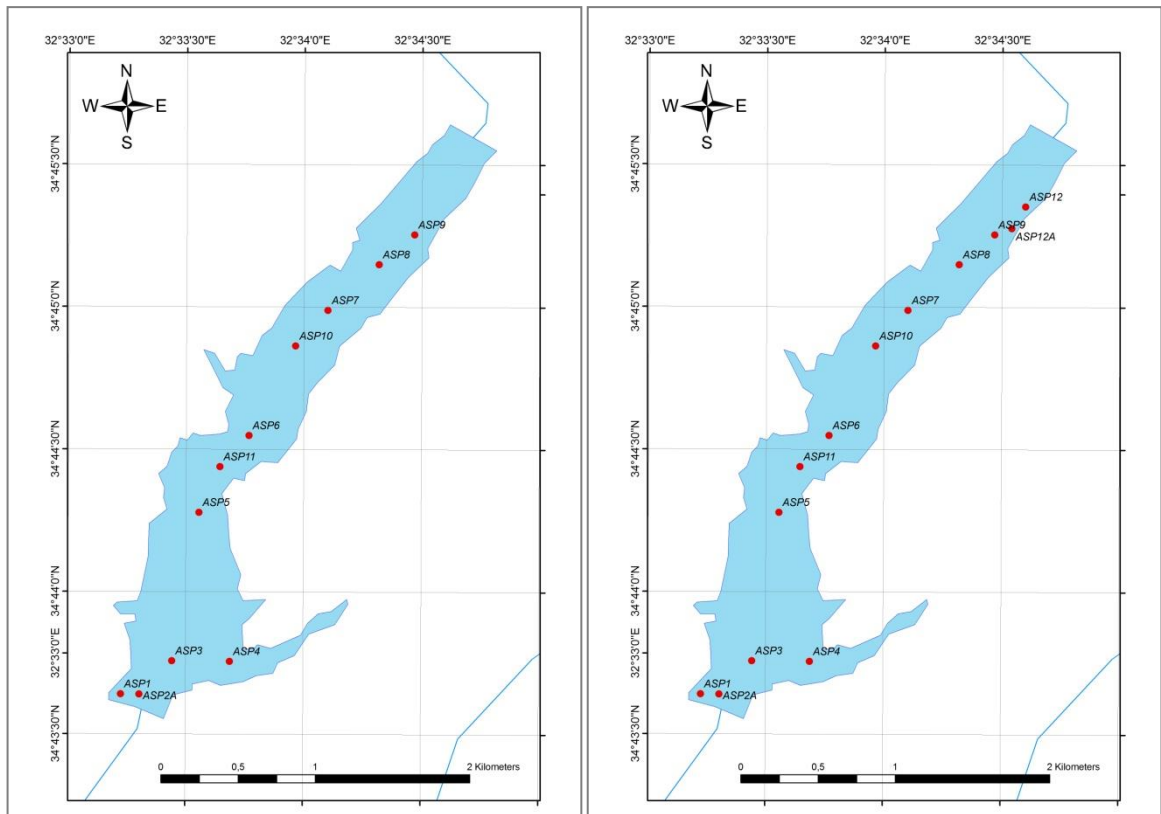


Figure 3. 5: Maps of the sampling station network used during the field campaigns in Asprokremmos Reservoir during (a) 2010 & (b) 2011, respectively.

In situ spectroradiometric data together with *in situ* water turbidity readings were collected during the satellite overpass in order to enhance the statistical analyses for retrieving the cross-correlation of spectroradiometric data and water turbidity. *In situ* spectroradiometric data were obtained by using a field spectroradiometer GER (Geophysical Environmental Research) 1500 equipped with a Fibre Optic (FO) probe and *in situ* determination of water turbidity was achieved by using both a portable turbidity meter (Palintest Micro950) and a Secchi Disk (SD).

All *in situ* campaigns for the years 2010 and 2011 were arranged according to Landsat TM and ETM+ acquisition schedule. In order to schedule the optimal time frame for the *in situ* campaigns two additional parameters were taken into consideration; the ideal weather conditions and the period of high water demand. In collaboration with the Cyprus Water Development Department the optimal

period was defined to be from late-April to late-October 2010 and late-March to mid-November 2011. During the period 2012/2013, 7 sampling campaigns were implemented in order to verify the developed regression model based on measurements acquired for years 2010 and 2011. Finally, a total of forty two sampling campaigns have been carried out during the period 2010-2013.

3.2 Other Study Areas

Alongside the sampling campaign in Asprokremmos Dam, three additional study areas were selected for a limited run of measurements. The aim was to collect data from water bodies with different Trophic State and investigate the changes in spectral signatures.

3.2.1 Lake Karla (Thessaly, Greece)

Lake Karla, is located in the plain of Thessaly, in Volos District area, in Greece (Figure 3. 6) and was selected as a case study because it appears high values of nutrients concentrations (such as chl-*a* and phosphates) compared to those observed in Cyprus water bodies. Lake Karla was chosen due to its particularity as until 1962, there was a natural lake in Lake Karla basin sustained by Pinios River winter flood flows and basin runoff which was drained through an ambitious reclamation project, mainly for agricultural purposes. Lake Karla occupied, until 1962, most of the eastern part of Thessaly plain in central Greece. It was one of the most important wetlands in Greece and a natural reservoir, which provided significant water storage. The lake area fluctuated from 40 to 180 km² due to the very gentle land slope and the inflow-outflow balance. For this reason, significant area of the surrounding farmland was often inundated facing soil salinity problems (Kokkinos and Mylopoulos 2007; Loukas et al. 2005; Oikonomou et al. 2012; Papadimitriou et al. 2011).

Quite shortly after the completion of the land reclamation project, it became evident that it was a failure, which created bigger problems than the ones it was supposed to solve. The decision to restore part of the former lake has only recently

been made by the Greek government, although numerous studies for the construction of a reservoir have been made throughout the period following lake drainage. Currently a project for the partial restoration of the Karla Lake is under progress. According to the scheme, a water reservoir with a size of 3,800 Ha will be created in the lowest part of the old lakebed (Moustaka et al. 2002; Oikonomou et al. 2012; Papadimitriou et al. 2011).

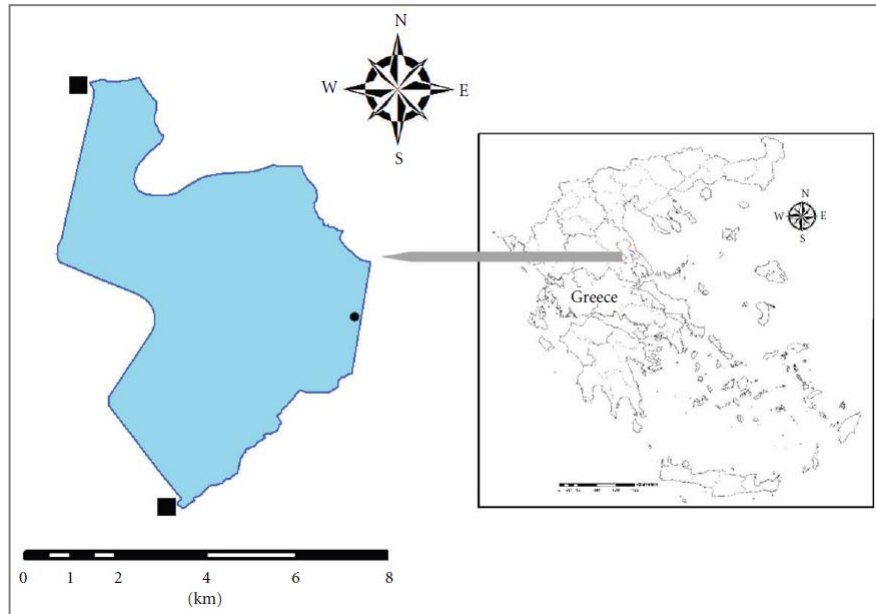


Figure 3. 6: Map of Lake Karla, located in Volos District area / Thessaly, Greece. Black squares show points of inflowing water for reconstruction purposes. Centre of the lake is at $39^{\circ}29'00''$ N, $22^{\circ}49'00''$ E (Reproduced from Oikonomou et al. 2012).

3.2.1.1 Sampling Campaigns & Sampling Station Network

Eleven *in situ* sampling campaigns have been occurred in Lake Karla. The sampling campaigns lasted from early April 2012 to early October 2012. During the campaigns spectroradiometric field measurements were collected using a handheld GER1500 field spectroradiometer equipped with a FO probe in order to retrieve the spectral signature of the lake's water. Field measurements of SDD and several physicochemical parameters were obtained at every sampling point (Temperature, pH, Conductivity, Dissolved Oxygen). Furthermore, water samples

were collected for laboratory analysis for the determination of nutrients (Total Phosphorus & chl-*a*) and SPM. *In situ* campaigns were carried out with the collaboration of the Department of Civil Engineering, University of Thessaly, Volos, Greece; the Management Body of the Eco-Development Area of Karla, Mavrovouni, Kefalovriso and Velestino and the Department of Civil Engineering and Geomatics, Cyprus University of Technology (Remote Sensing Lab), Limassol, Cyprus.

Since 2009 hundreds of dead fish were found in the Karla Lake. Governmental authorities and universities were investigated the reason of those phenomena. An eventuality is a possible pollution or lack of oxygen occurred from the water outfall into Lake Karla from Pinios River. Pinios River is heavily influenced by pesticides and nitrates from fertilizers used on crops that outfall along the river from industries and cheese-dairies wastewaters and agricultural wastes (crops leachate generation). Furthermore, according to the findings of a study undertaken by the Aristotle University of Thessaloniki it has been reported the existence of toxic phytoplankton (cyanobacterium) in the water body of Lake Karla. During the first sampling campaign at the Karla Lake we came up against this woeful phenomenon as all over the surface of the Lake dead fish were lie (Figure 3. 7) (Econews.gr 2009).



Figure 3. 7: Pictures taken during the first sampling campaign at the Karla Lake were dead fish were all over the water surface of the Lake.

During the firsts sampling campaigns to Lake Karla it was very difficult to reach the three sampling station as there were theoretically preselected so as to estimate the trophic state of the lake as there was not available a power engine boat. The

problem of the boat was overcome due to the good turn of a resident of a nearby village named Kanalia who offered to help us with the sampling campaigns as he was the owner of a small power engine boat and to whom we express our grateful thanks. Finally three samplings stations were selected located near the inflowing water points as shown at Figure 3. 8.



Figure 3. 8: Map of the sampling stations used during the field campaigns in Karla Lake.

3.2.2 Larnaca main Salt Lake (Alyki)

Larnaca Salt Lake Complex is one of the most important natural standing water bodies in Cyprus and is of international ecological significance (declared as a protected area by a decision of Council of Ministers (1997), Ramsar Site, Natura2000 Site, Special Protected Area under Barcelona Convention, Important Bird Area). It consists of four main lake water bodies, the main Salt Lake (Alyki), Orphani, Soros and the small so-called Airport Lake, which was part of the Orphani Lake but was cut off when the airport runway was constructed (Hadjichristophorou 2008). This wetland area in south-eastern Cyprus is in one of the driest parts of the island. The three most important climatic factors determining the development of salt lakes are temperature, net evaporation and precipitation (Williams 2002).

The wetland area also includes the extensive halophytic communities on the shores of the lakes and in the area between the lakes and the sea. Two small forests one by the Tekke and the other on the east bank of Alyki add diversity to the area. Our research field campaigns focused in Alyki, which is the main Salt Lake, having a very high salinity regime, hence its use in the past for salt collection (Hadjichristophorou 2008). The hyper-salinity of Larnaca's salt lake is inhospitable to many life forms and only the specialized adapted forms can survive (Wharton 2002).

The alga that forms the basis of the food chain here is *Dunaliella salina*, a brick red unicellular alga, which is a very salt tolerant species. On this alga feeds *Artemia salina*, the Brine shrimp. This shrimp can withstand very large salinity fluctuations (from 15‰-280‰) but usually thrives at salinities of about 100‰, that is to say about 2.5 times higher than that of the sea. *Branchinella spinosa*, the Fairy shrimp, a close relative of *Artemia salina*, lives in the other Larnaca lakes, which are less salty, as well as in the Akrotiri Salt Lake, which also has a lower salinity regime.

Both *Artemia* and *Branchinella* start laying cysts at the end of the season, when the salinity rises and reaches a certain threshold. This is usually in early summer. The cysts have a hard, resistant shell and can stay alive for several years in very hostile and extreme conditions (in the salt deposits, at very high temperatures). They will hatch when the conditions are right, which is after the lake is full of water again and the salinity of the lake drops to about 25‰. These shrimps are the main food of the Flamingo and of other birds in these lakes. On average about 1000-2000 Flamingo overwinter here each year where in peak years, such as 1995 and 2005, there may be as many as 7000 (Demetropoulos 2006; Hadjichristophorou 2004).

The other Larnaca lakes are less salty than the main Salt Lake and they are more similar, ecologically, to Akrotiri Lake in many respects. The system is however more complex as the lakes at Larnaca, are in some ways, interrelated. *There is for example a small but significant inflow of low salinity water into the main Salt Lake from the Airport Lake and Orphani.* This low salinity water helps trigger the hatching of the cysts. In some years, a lower than normal salinity in Alyki, caused by

unusually high precipitation, can result in *Branchinella* multiplying in this lake together with *Artemia* and other species (e.g., Ostracods) (Manolaki n.d.).

3.2.2.1 Sampling Campaigns & Sampling Station Network

Three *in situ* sampling campaigns have been occurred in the main Salt Lake (Alyki). The first sampling campaign was obtained on the 7th of July 2011, the second on the 20th of January 2012 and the third on the 10th of May 2012. During the campaigns spectroradiometric field measurements were collected using a handheld GER1500 field spectroradiometer equipped with a FO probe in order to retrieve the spectral signature of the lake's water. Turbidity values were determined using a portable turbidity meter and water samples were collected for laboratory analysis for the determination of nutrients, Total Suspended Solids and physicochemical parameters. Field monitoring will complement by satellite image analysis.

This first campaign includes the water analysis in two different locations. The two under study locations were distinguished by the depth of the water. During the first sampling campaign Alyki was almost dry and at the first sampling station which is located near Tekkes Mosque, the depth of the water was not adequate to show the spectral signature of the water. Although several points in this area were selected in order to collect spectroradiometric measurements. Those points differed regarding their dryness and as a result different salinity levels can be observed. On Figure 3. 9(a) and (b) an example of two lake's surface points of different salinity level is given; (a) corresponds to points of high dryness which are covered with a layer of salt and (b) to points of lower dryness where the salt layer is not visible. The second sampling station is located on the Northeast side next to the environmental park. This is the deepest area of the salt lake and some spectral signatures of the salt lake's water body were obtained over this area.

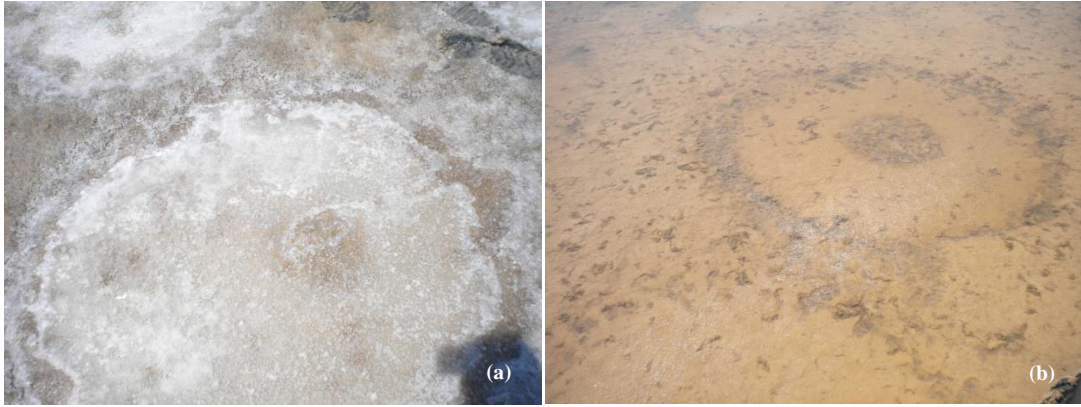


Figure 3. 9: Pictures of the sampling station located near Tekkes Mosque (a) high dryness observed and (b) lower dryness observed.

During the 2nd and 3rd sampling campaign Alyki was filled with water and water spectral signatures were collected. During the 3rd sampling campaign an unusual algal bloom was observed at the sampling station located near Tekkes Mosque (see Figure 3. 10).



Figure 3. 10: Unusual algal bloom at the sampling station located near Tekkes Mosque.

3.2.3 Coastal Areas in Cyprus (Limassol & Paphos District Areas)

The coastal area of Cyprus is under pressure due to economic/urban development particularly tourism, recreation, urban and infrastructure development and to a lesser extent, agricultural and industrial development. Indeed, the rapid socio-economic growth of Cyprus, especially in the 1980s, beside its desired effects, has also caused strains on the natural fabric of the coastal area. The most serious coastal planning problems today relate to the sudden expansion of the main

coastal urban centre of Limassol, Larnaca and Paphos and have mostly been caused by the type and speed of development (Demetropoulos 2002).

The Ministry of Agriculture, Natural Resources is responsible for the control of the pollution of water and soil, which is a result of human activities. Studies are being undertaken on the impact of pollution on marine ecology, as well as of the impact of aquaculture on marine biodiversity. Moreover, for the assessment of ecological status of coastal waters a relevant monitoring is being implemented within the Water Framework Directive (2000/60/EC), while within the MED POL Program a monitoring on the quality of the coastal waters, including the assessment of pollutants (heavy metals etc.) in fish is carried out. However excessive use of fertilizers has resulted in high nitrate levels in the aquifer in some areas, leading in some cases to increased nutrient concentration at few beaches which resulted, combined with other synergistic factors, to the occasional occurrence of the ephemeral macroalgae *Cladophora spp.* (Department of Environment 2010).

Our objective is to develop a monitoring tool for Case-2 water bodies, which includes the coastal zone, aiming to provide useful information to the stakeholders regarding some WQP such as the turbidity, the SDD and the TSI. Such a tool would be very beneficial for the protection and conservation of the marine environment with the overall aim of promoting sustainable use of the seas and conserving marine ecosystems, as defined by the Marine Strategy Framework Directive 2008/56/EC.

3.2.3.1 Sampling Campaigns & Sampling Station Network

All the sampling campaigns and the *in situ* measurements were carried out with the collaboration of the Department of fisheries and marine research of Cyprus, Nicosia, Cyprus; the Maritime Institute of Eastern Mediterranean, Limassol, Cyprus; and the Department of Civil Engineering and Geomatics, Cyprus University of Technology (Remote Sensing Lab), Limassol, Cyprus.

During all the *in situ* campaigns field spectroradiometric data together with water turbidity, SDD and water samples for laboratory analyses were obtained. Three

coastal areas were selected in collaboration with the Department of fisheries and marine research of Cyprus in order to examine the coastal water quality in Cyprus. The study areas are positioned in Limassol District which is located on the southern part of the island of Cyprus. Three different sampling stations were selected (Figure 3. 11), where 3.1 is the area of the Zugi Harbour, 3.2 is the area of the Vassiliko Cement Works and 3.3 is the area of the Limassol Old Harbour. Further some *in situ* campaigns were arranged along the coastline of Paphos as illustrated in Figure 3. 11(1b) in the context of protecting the quality of water resources which has been a high priority since this area includes many bathing sites need to be monitored and classified for environmental protection purposes and protection of human health.

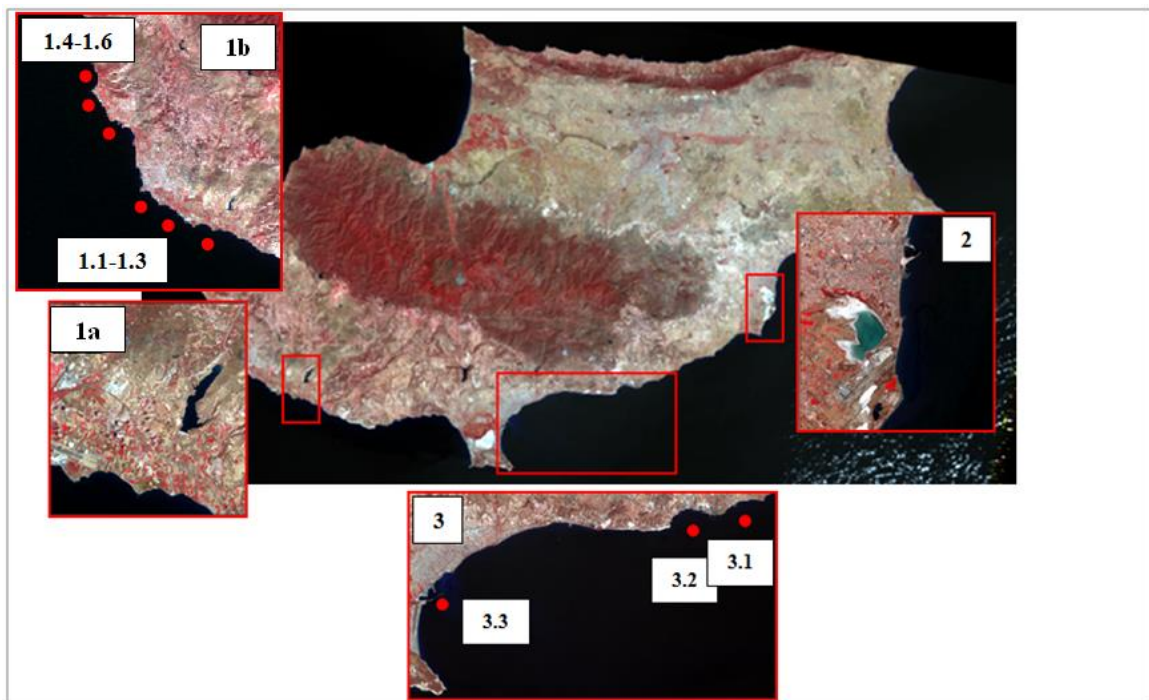


Figure 3. 11: Map of the sampling stations used during the field campaigns in the coastal area of Limassol and Paphos District.

During the *in situ* campaigns carried out with the collaboration of the Department of fisheries and marine research of Cyprus it was very difficult to reach areas very close the coastline as the available boat used for the purpose of field campaigns was very big. More sampling campaigns at areas very close to the coastline of

Limassol and Paphos District were carried out using a smaller boat with the collaboration of the Maritime Institute of Eastern Mediterranean.

3.3 Resources

3.3.1 Boat & GPS

A power-engine boat was used to support the *in situ* campaign in the Asprokremmos Dam in Paphos (see Figure 3. 12). A small boat was used to support the in situ campaign in the Karla Lake in Thessaly region, in Volos, in Greece (see Figure 3. 13). A canoe boat was used in order to carry out the sampling campaigns in Larnaca main Salt Lake (Alyki) in Larnaca District, Cyprus (Figure 3. 14). A ship was used in order to carry out the sampling campaigns in Limassol and Paphos District coastal areas, in Cyprus (Figure 3. 15).

A Global Position System (GPS) Garmin GPS72 and a differential Leica Viva GPS, to better pointing accuracy were also used in order to track the locations of the selected sampling stations during all the sampling campaigns.



Figure 3. 12: Sampling campaign in Asprokremmos Dam in Paphos District, Cyprus.



Figure 3. 13: Sampling campaign in Lake Karla in Thessaly Region, Greece.



Figure 3. 14: Sampling campaign in Larnaca main Salt Lake (Alyki) in Larnaca District, Cyprus.



Figure 3. 15: Sampling campaign in Limassol & Paphos District coastal areas, Cyprus.

3.3.2 Field Spectroradiometer

The GER1500 field spectroradiometer (Figure 3. 17) is a light-weight, high performance, single-beam field spectroradiometer. It is a field portable spectroradiometer covering the ultraviolet, visible and near-infrared wavelengths from 350 nm to 1050 nm. It uses a diffraction grating with a silicon diode array. The silicon array has 512 discrete detectors that provide the capability to read 512 spectral bands.

The instrument is very rapidly scanning, acquiring spectra in milliseconds. The spectroradiometer provides the option for standalone operation (single beam hand-held operation) and the capability for computer assisted operation through its serial port, which offers near real-time spectrum display and hard disk data transfer. The maximum number of scans (512 readings), can be stored for

subsequent analysis, using a personal computer and GER licensed operating software.

For the purpose of the current study which aims to monitor WQP in the Asprokremmos Dam the GER1500 field spectroradiometer equipped with a FO probe and a diffuser as shown in Figure 3. 18(a) and (b), was used to measure the spectral signatures for certain depths below water surface. The data are stored in ASCII format for transfer to other software. GER1500 specifications can be found at SVC (2002).

A standard spectralon panel (Figure 3. 16) was also used in order to measure the downwelling irradiance each time just before to start measuring the spectral upwelling irradiance of the target. The measured upwelling irradiance value taken on the standard spectralon panel is almost equal to the downwelling irradiance as the reference spectralon panel is a Lambertian surface reflecting almost 100% of the downwelling irradiance and as a result is taken as a reference value regarding the downwelling irradiance. Stability of the light field is always an issue in field measurements because sky conditions are not always stable.



Figure 3. 16: Standard spectralon panel (Lambertian surface) used as reference value for the downwelling irradiance.



Figure 3. 17: Handheld field spectroradiometer GER1500 covering the UV-Vis-NIR area of the spectrum.

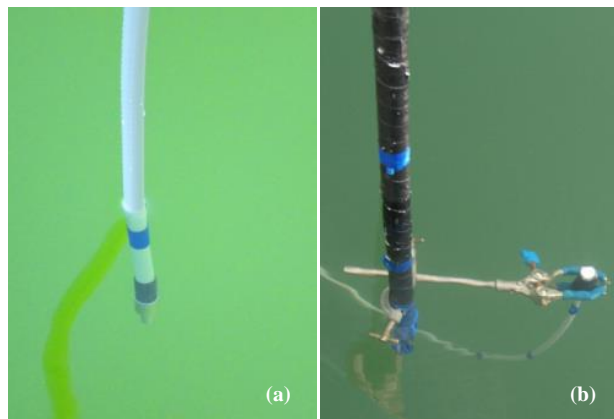


Figure 3. 18: (a) Fibre optic probe adjusted on GER1500 for underwater measurements of the upwelling radiance and (b) Macam diffuser 1 which incorporates a mirror and attaches to the fibre optic cable for underwater measurements of the downwelling irradiance.

Since reflectance requires a pair of measurements; the upwelling radiance (L_u) and the downwelling irradiance (E_d), if a single spectrometer is used to measure both L_u and E_d and the light field changes between measurements, then one cannot compute a reliable reflectance. On the other hand, if a pair of spectrometers is used to make the two measurements simultaneously, they must be cross-calibrated. While it is more efficient in the field to have the two calibrated spectrometers, it can be less expensive and sufficient to use a single spectrometer and move fast. The spectral irradiance reflectance (or irradiance ratio), $R(z, \lambda)$, has been determined during our campaigns using a 10-meter FO probe adjusted on the

GER1500 field spectroradiometer in order to enhance the subsurface reflectance values at different depths below water surface. Spectral irradiance reflectance is defined as the ratio of spectral upwelling to downwelling plane irradiances:

$$R(z, \lambda) = \frac{E_u(z, \lambda)}{E_d(z, \lambda)} \quad (3.1)$$

Moreover a diffuser was adjusted on the end of the FO probe and the downwelling irradiance was also determined for different depths.

McLoy (1995) describes the technique for measuring the reflectance factors using a control stable surface with known characteristics. This is the method that was followed in this research for the spectroradiometric measurements. Many scientists (Anderson and Milton 2006; Anderson et al. 2006; Beisl 2001; McLoy 1995; Schaepman 2007) highlight the advantages of using control surfaces in the measurement of reflectance factors (Bruegge et al. 2001). In this study, the control surface was a commercially available "Labsphere" compressed "Spectralon" white panel (Figure 3. 16). There is evidence that these types of panels are more consistent and retain their calibration better than painted panels (Beisl 2001; Jackson et al. 1992).

Spectralon diffuse reflectance targets are ideal for laboratory and field applications such as field validation experiments, performed to collect remote sensing data due to their special features and properties which are summarised below:

- ❑ durable and washable
- ❑ high reflectance: have typical reflectance values of 95% to 99% and are spectrally flat over the UV-VIS-NIR spectrum
- ❑ impervious to harsh environmental conditions
- ❑ chemically inactive

3.3.3 Digital Turbidity Meter & Secchi Disk

A SD and a portable digital turbidity meter (Palintest Micro950) (see Figure 3. 19 and Figure 3. 20a-c) were used in order to measure the turbidity levels observed in the Asprokremmos Reservoir.

SDT is a commonly used, low-cost technique that measures water clarity (Specifically, a black and white disk is lowered into the lake until it can no longer be seen). Water clarity is related to the quantity of phytoplankton in the water, although non-algal turbidity and tannic acids also can reduce water clarity (Fuller et al. 2002, 2011). SDD measurements were always taken over the shady side of the boat. SDD is a measure of water clarity by human eyes and all optically active substances in water affect it (SDD decreases as the concentration of chl-*a*, CDOM, and other substances increases). As eyes use the whole visible band and the combined effect of all optically active substances over this region is complex, it may be difficult to find conclusive reasons for using some particular wavelengths for its retrieval (Koponen et al. 2002).

The Palintest Micro 950 Waterproof Turbidity-Meter is a portable micro-processor controlled turbidity meter used to determine the turbidity level at several water samples during *in situ* campaigns. Turbidity is an important measurement, particularly on clean water systems such as natural and drinking water. To provide a precise method of determination, the turbidity is measured using the nephelometric principle. A beam of light is passed into the water sample and the amount scattered by particles present is detected at right angles (90°) to the incident beam.



Figure 3. 19: A Secchi Disk used during the field campaigns to measure the Secchi Disk Depth.



Figure 3. 20: (a-c) The portable Palintest Micro 950 Waterproof used to determine the turbidity level at several water samples during *in situ* campaigns.

An important feature of this instrument is the LED IR light source at a wavelength of 850 nm. The use of a near infrared light source is in accordance with the recent British, European and International standards on the determination of turbidity (ISO 7027). Measuring the turbidity at this specific wavelength ensures precision and eliminates any interference from inherent colour in the water.

The calibration of the turbidity-meter is easy. The calibration procedure was applied just before each survey starts. Four turbidity standards of various turbidity level, 0.02, 20, 100, and 800NTU, were used. The turbidity-meter's display guides the user step-by-step through the calibration process. The instrument is capable of measuring test samples with a quick and stable response and readings are displayed on a large custom LCD together with units, and status codes. When the calibration process is completed water sample is collected in an empty vial with light shield cap and turbidity level is determined (Palintest 2003).

3.3.4 Smart Buoy Monitoring System

The data buoy, loaded with various water quality sensors, has been deployed in the Asprokremmos Reservoir, for real time monitoring of water quality as shown in Figure 3. 21. The design and development of an innovative, energy-autonomous floating sensor platform that is installed in the dam and will have the ability, through wireless network, to transfer data to a remote central database has been made. An innovative low-cost sensor which measures the turbidity of water, based on the concentration of micro-particles is installed in the floating platform. The sensor is based on optical technology and has the ability to record turbidity measurements as well as to communicate with the central platform either through wires or through a wireless sensor network acting as an energy autonomous node.



Figure 3. 21: Floating sensor platform.

The smart-buoy platform was installed in the Outlet area of the Asprokremmos Reservoir, which is the region where the water is pumped to the water treatment plant. The acquired data were used for calibration purposes of the turbidity predictive model which was developed based on the *in situ* data collected during the field campaigns along the Reservoir. The need for continuously monitoring of

the turbidity levels in this area is of high priority since it provides raw water for treatment, and is essential to ensure that the water meets the required abstraction standards before it passes to the water treatment plant.

3.4 Methodology

During this study an effort was given in order to develop a regression model for monitoring water turbidity and Trophic State Index in Cyprus' reservoirs using satellite remote sensing. In order to achieve this task, the main study area of Asprokremmos Reservoir in Paphos District was selected and several field campaigns took place in order to collect both the spectroradiometric data and at the same time the corresponding WQP of turbidity and SDD. During the sampling campaigns both several sampling stations were selected covering various areas over the reservoir, and different dates were selected covering different weather conditions aiming to take into account both the spatial and the temporal variations being observed over the reservoir.

Moreover, additional field measurements were acquired over other water bodies such as several coastal areas over Limassol and Paphos District in Cyprus, Karla Lake in Thessaly District in Greece and Salt Lake in Larnaca District in Cyprus. All the *in situ* SDD values were used to calculate the Carlson's Trophic State Index and all the spectroradiometric measurements acquired using a handheld field spectroradiometer (GER 1500) were filtered using the Relative Spectral Response (RSR) filters in order to retrieve the mean reflectance values corresponding to Landsat satellite sensor. After applying regression analysis using data collected over 4 different types of water bodies, several regression models were developed and evaluated based on the determination factor (R^2) in order to retrieve the best algorithm predicting the TSI using the Landsat's band reflectance values.

For the aim of this study the following methodological steps were applied:

- Selection of the study area and design of a sampling station network in the area of interest - Asprokremmos Reservoir

- ❑ Use of a power engine boat and a GPS to support the *in situ* campaign in the Reservoir. Sampling campaigns started in April 2010 and last until October 2012 including 42 sampling campaigns. A handheld GER1500 field spectroradiometer equipped with a FO probe was used in order to retrieve the spectral signatures at several different depths below water surface. Reflectance was calculated as a ratio of the target radiance to the reference radiance
- ❑ WQP of turbidity and SDD were collected simultaneously to the *in situ* spectroradiometric data aiming to cover various water quality statuses
- ❑ Statistical analysis of the field derived data was performed in order to retrieve the model with the best correlation coefficient (coefficient of determination). The spectral regions where the best correlation between the reflectance and each of the WQP (turbidity, SDD or TSI) were identified
- ❑ All the *in situ* spectroradiometric data were processed in order to retrieve the mean “in-band” reflectance values regarding both the Landsat and the Chris-Proba satellite sensors and the appropriate spectral bands for each sensor were identified

Additional measurements were acquired over different water bodies (coastal areas of Cyprus, Karla Lake in Greece and Larnaca’s Salt Lake in Cyprus) in order to 1) build-up a spectral library including different water bodies and 2) further test our model. A well-fitting predicting model of the TSI for all the water bodies including in this thesis was developed.

In conclusion we can say that the ultimate goal of the current study is the development of several models based on a large data set of field observations, which can be used in accordance with the satellite data availability, which will enable the monitoring of the turbidity level at several inland water bodies on a systematic base based only on satellite observations without the need of time-consuming field campaigns. The methodology steps followed during the current study are illustrated in Figure 3. 22.

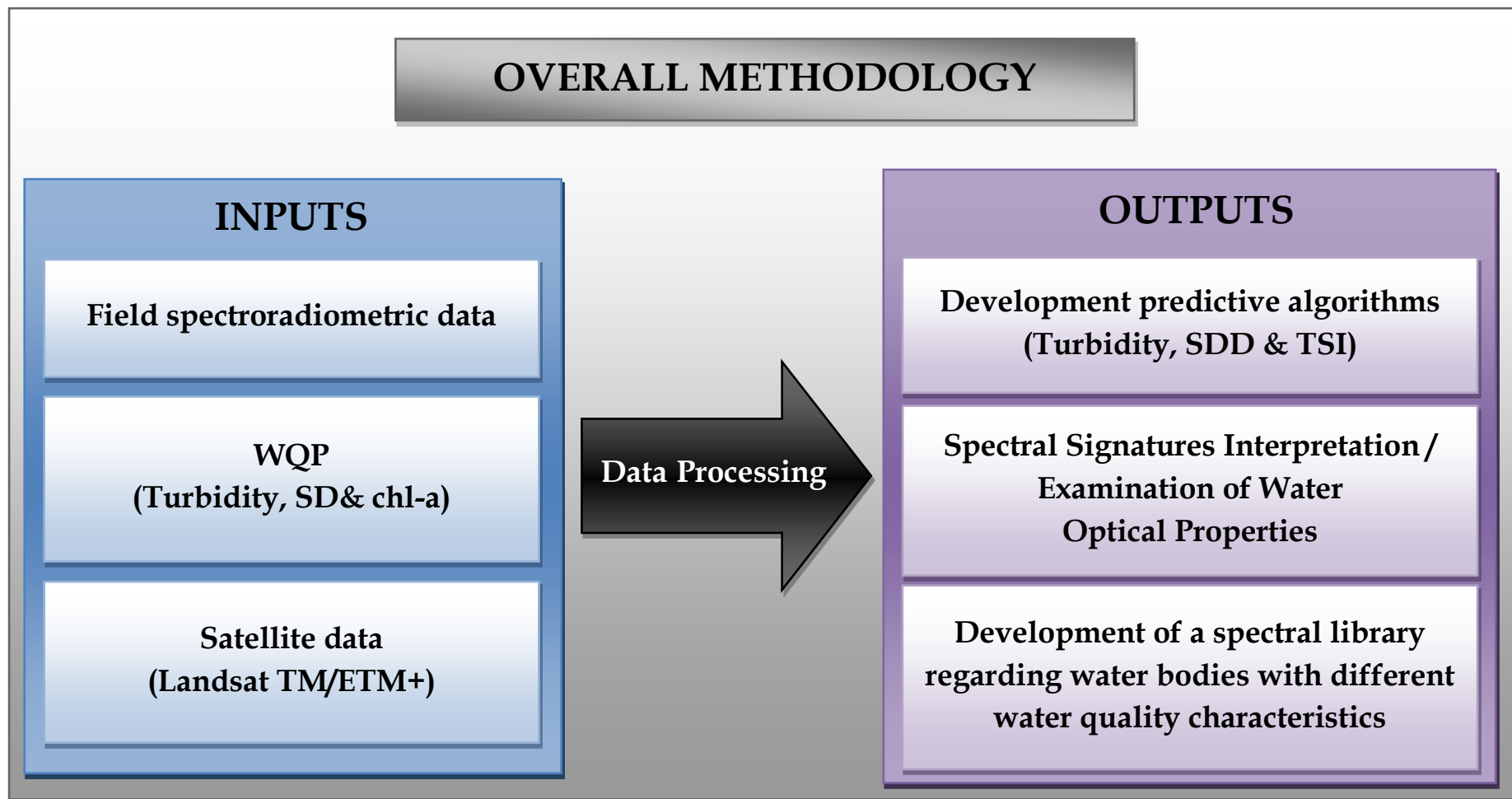


Figure 3. 22: Schematic diagram of methodology.

4 Development of Water Quality Predictive Models for Asprokremmos Reservoir

In this Chapter, are presented the results derived by the processing of the ground truth subsurface reflectance and the water quality measurements conducted over Asprokremmos Reservoir. Field campaigns were taken place during the period 2010 to 2012 and lasted for 3 years. The results from the regression analysis between the subsurface reflectance using the handheld field spectroradiometer GER1500 with a bandwidth of 1,5nm and both the water turbidity and the SDD values are also presented. Finally, based on the field spectroradiometric measurements the at-satellite mean reflectance values were calculated and the suitable bands for the calculation of the above-mentioned WQP were estimated regarding several satellite sensors. A comparison of the three examined satellite sensors; Landsat TM/ETM+, Chris-Proba and MERIS based on the obtained results is provided.

4.1 Field Campaigns

All the *in situ* campaigns implemented in this study were scheduled according to Landsat TM and ETM+ acquisition schedule aiming to obtain field and satellite data simultaneously. The number of the implemented sampling campaigns was reduced comparing to Landsat's acquisition schedule since cloud free conditions and boat availability were requisite. All the field campaigns started at about 8am and lasted for about 4hours since the scene centre scan time for Cyprus is at 10:13am (standard time). During 2010 finally 18 sampling campaigns were carried out lasted from April 2010 to October 2010 and during 2011 17 sampling campaigns lasted from end of March 2011 to early November 2011. During the period 2012/2013, 7 sampling campaigns were carried out which were used to verify the developed regression model based on measurements acquired throughout the extended field campaign during the years 2010 and 2011. The dates of the *in situ* campaigns during the years 2010, 2011 and 2012/2013 are analytically presented on Table 4. 1.

Table 4. 1: Field campaign data referred to sampling date and conditions during each campaign occurred for the years 2010, 2011 and 2012-2013 over Asprokremmos Reservoir.

2010		Condition	2011		Condition	2012 - 2013		Condition
No	Sampling Date	1-6 *	No	Sampling Date	1-6 *	No	Sampling Date	1-6 *
1	29-Apr-10	1	1	31-Mar-11	1	1	30-April-12	1
2	07-May-10	1	2	02-May-11	1, 5	2	08-Jun-12	1
3	15-May-10	1	3	10-May-11	1	3	29-Jun-12	1
4	31-May-10	1	4	10-Jun-11	1	4	23-Aug-12	1
5	10-Jun-10	3	5	27-Jun-11	1	5	18-Sep-12	1
6	16-Jun-10	1	6	05-Jul-11	1	6	27-Oct-12	1
7	24-Jun-10	2	7	13-Jul-11	1, 6	7	10-Jun-13	1
8	02-Jul-10	1	8	29-Jul-11	1			
9	18-Jul-10	1	9	22-Aug-11	1, 6			
10	03-Aug-10	1	10	30-Aug-11	3 to 4			
11	11-Aug-10	1	11	15-Sep-11	1			
12	19-Aug-10	1	12	23-Sep-11	1			
13	27-Aug-10	1	13	30-Sep-11	1			
14	20-Sep-10	1	14	10-Oct-11	1			
15	28-Sep-10	1	15	17-Oct-11	1			
16	06-Oct-10	1	16	2-Nov-11	4 (NO GER1500)			
17	14-Oct-10	1	17	10-Nov-11	1			
18	22-Oct-10	1						
*1: clear			*2: thin clouds			*3: partly cloudy		
*4: cloudy			*5: dusty			*6: yellow particles		

4.1.1 Sampling

An ideal sampling station network over the area of Asprokremmos Reservoir was designed to achieve the aims of this study. In order to design an efficient and effective water quality monitoring sampling station network over the reservoir, a preliminary plan was established in order to investigate whether significant variations in turbidity values were observed. Two different sampling scenarios were compared using for example either a grid of 30×30 m or one of 10×10 m. Turbidity measurements collected at the centre of each grid. The findings of this preliminary study revealed no significant variations within those areas. Moreover, comparing the turbidity values measured at several sampling points in relation to their distance from the river inlet higher variations were observed as the distance to the river inlet decreases.

Finally, the sampling station network used during our field campaigns consisted of 11 sampling stations for the year 2010 and 12 sampling stations for the years 2011 and 2012 positioned in all directions for the proper and adequate coverage of the study area. A new sampling station (12) was added to the sampling station network since the water level in the Asprokremmos Dam was increased during 2011. The Reservoir was overflowed during the winter period 2011/2012 which has been one of the wettest in recent years. The Asprokremmos Dam was overflowed for the first time since 2004 for two years continuously, on late-January 2012 and late-December 2012.

4.1.2 Field Spectroradiometric Measurements

All the *in situ* campaigns were carried out with the collaboration of the Cyprus Water Development Department and the Cyprus University of Technology (Remote Sensing Lab). Reflectance values were calculated as the ratio of the water irradiance to the reference irradiance (i.e. Spectralon reference panel) (see Figure 4. 1). In order to find the most representative reflectance value at the surface of the water body, the method suggested by Hadjimitsis and Clayton (2011) was followed. This method requires the acquisition of reflectance values at different depths (e.g. 0.10–1.50 m)

and the application of a linear regression between reflectance (at every depth) against depth (in meters). For the purpose of this study, reflectance measurements were acquired at the following depths: 0, 0.1, 0.3, 0.5, 1.0, and 1.5 m. Linear regression regarding the reflectance values at several depths was applied aiming to retrieve the surface reflectance values (Hadjimitsis and Clayton 2011).

A Spectralon reference panel (99.9% reflectance) was used as a reference target for the spectroradiometric measurements in order to calculate the target reflectance values for calibration purposes (Themistocleous et al. 2013). Reflectance measurements over the Spectralon reference panel were taken just before each reflectance measurement over the targets using the SVC GER1500 spectroradiometer equipped with a FO probe. During our field campaigns, one reflectance measurement was acquired at each depth. However, it is important to mention that each reflectance value was calculated from the average of five single measurements since the spectroradiometer was programmed to repeat every measurement five times and calculate the average reflectance value. All the SDD measurements were taken from the shaded side of the boat.

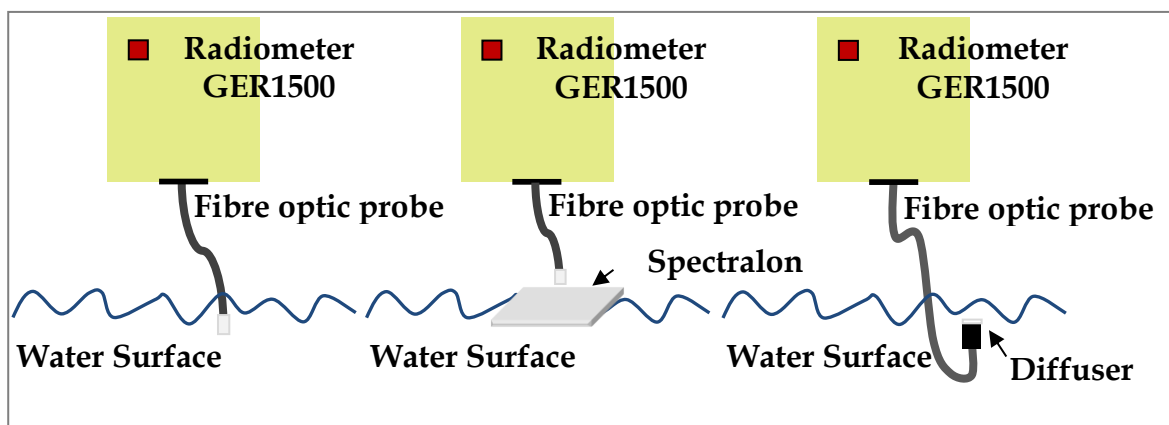


Figure 4. 1: In situ reflectance measurement procedure: (a) Measuring the upwelling radiance $L_u(\lambda)$ at depth 0; (b) Measuring the downwelling radiance $L_d(\lambda)$ at depth 0⁺; (c) Measuring the downwelling radiance $L_d(\lambda)$ at depth 0.

4.2 Statistical Analysis

The overall purpose of this study is the development of an algorithm which can assist to monitoring inland water bodies over several reservoirs in Cyprus. The main objective is to identify the spectral regions where the best correlation can be achieved between the reflectance and the WQP values such as the turbidity and the SDD. In order to create such an algorithm it is critical to examine the spectral characteristics and specify the properties of several waters including water bodies whose water quality values vary.

These findings can be of great assistance to the water quality monitoring of such water bodies using satellite remote sensing technology. Field spectroradiometric measurements are useful for validating satellite derived measurements as well as for supporting the removal of atmospheric effects from satellite images (Hadjimitsis et al. 2004). In fact, field spectroradiometric measurements can support the identification of appropriate spectral bands in which several other WQP can be retrieved. This can assist the development of future satellite sensors based on such campaigns (e.g. CHRIS/PROBA).

4.2.1 Regression Analysis using *In Situ* Reflectance Data

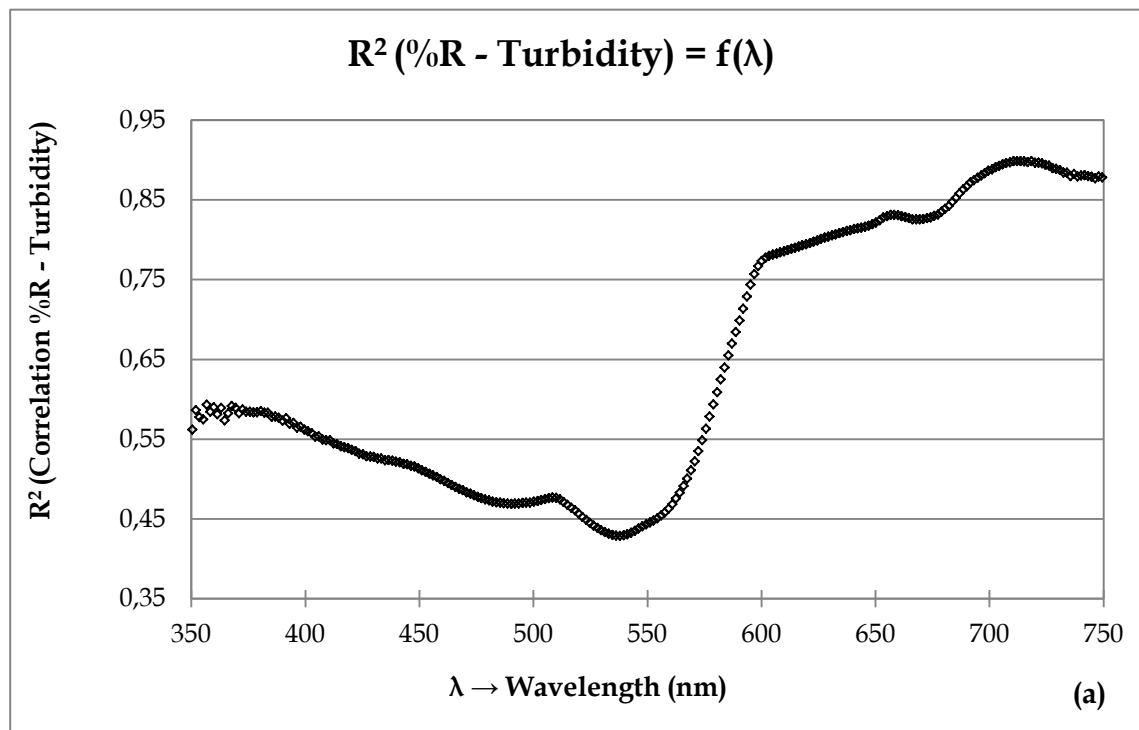
All the data acquired during the field campaigns over the Reservoir were statistically analysed in order to identify the spectral region where the best correlation can be derived. *In situ* reflectance data (GER1500) and the correspondence turbidity and SDD readings were processed in order to accurately assess the spectral wavelengths with the higher correlation.

The linear regression model was applied in order to model the relationship between the reflectance values and each of the WQP. Our goal was to identify the spectral wavelength where the best correlation could be achieved in order to develop the most suitable predictive algorithm for our study area. Figure 4. 2(a) and (b) show the wavelengths where the higher correlation coefficients (coefficients of determination) were observed after correlating the reflectance values at each wavelength of the

GER1500 (reflectance values recorded per 1.5 nm using field data) with the corresponding turbidity (NTU) and SDD values. For every single wavelength (with a bandwidth of 1.5 nm) a separate correlation coefficient was determined (reflectance against turbidity, SDD, and $\ln(\text{SDD})$). Figure 4. 2(a)–(c) show the plots of those correlation coefficients (R^2) against the correspondence wavelengths. The higher values for the coefficients of determination (squares of the correlation coefficient - R^2) were respectively achieved at wavelength $\lambda = 718.48$ nm for turbidity with $R^2 = 0.90$ (Equation 4.1 & Figure 4. 2(a)), at wavelength $\lambda = 597.00$ nm for SDD with $R^2 = 0.58$ (Figure 4. 2(b)), and at wavelength $\lambda = 605.13$ nm for $\ln(\text{SDD})$ with $R^2 = 0.77$ (Equation 4.2 & Figure 4. 2(c)).

$$NTU = 7.080(R_{718.48nm}) + 0.643 \quad R^2 = 0.90 \quad (4.1)$$

$$\ln SDD = -0.992 \ln(R_{605.13nm}) + 1.340 \quad R^2 = 0.85 \quad (4.2)$$



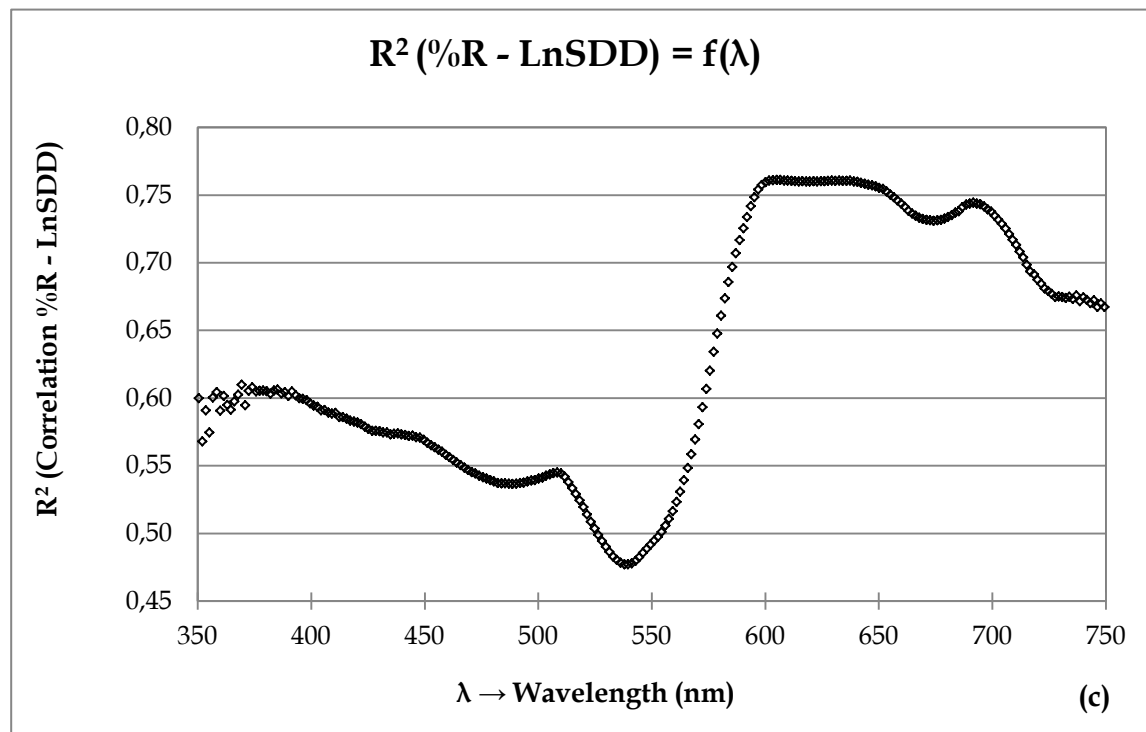
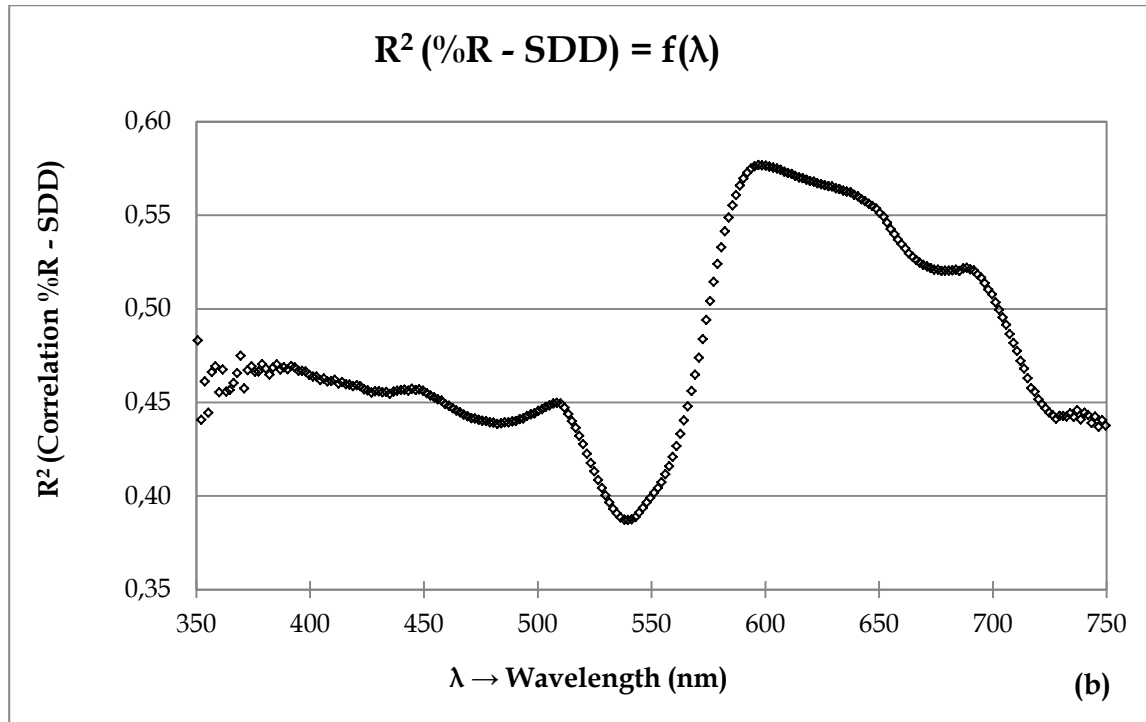


Figure 4. 2: Plots of the correlation coefficients (R^2) derived from the linear regression analysis against wavelengths. Correlation coefficients (R^2) were calculated for every single wavelength (350-1050 nm with a bandwidth of 1.5 nm) after correlating (a) turbidity (NTU), (b) SDD, and (c) Ln(SDD) values with the corresponding field reflectance values for each wavelength of the handheld spectroradiometer GER1500.

4.2.2 Definition of Optimum Satellite Bands based on Regression Analysis of GER1500 Data versus SDD and Turbidity

All *in situ* reflectance data were processed in order to retrieve the mean “in-band” reflectance values for the Landsat TM and ETM+ multispectral scanning radiometer Bands 1 to 4, the Envisat-1 / MERIS Medium Resolution Imaging Spectrometer Bands 1 to 15 and the CHRIS/Proba Compact High Resolution Imaging Spectrometer Bands A1 to A62. The mean “in-band” reflectance values for each sampling station were then correlated both with the corresponding turbidity and the SDD readings for all bands. This procedure was followed in order to identify both the optimal spectral regions for monitoring the inland water quality using Landsat TM/ETM+, Envisat-1 /MERIS and CHRIS-Proba sensors; and the differences between the sensors. In Figure 4. 3(a) typical spectral signature collected during the *in situ* sampling campaigns is presented indicating the corresponding spectral bands for the three above mentioned satellite sensors. As it can be seen referring to the spectral region ranging from 400 to 900 nm, the CHRIS/Proba sensor has 53 Bands (A1–A53) while the Envisat-1 MERIS has 15 Bands and Landsat TM has only 4 Bands. The GER1500 which was used during the field campaigns has 333 Bands corresponds for the same spectral region with a bandwidth of 1.5 nm.

All the examined satellites have different spatial and spectral acquisition characteristics. Specifically, the bandwidth range for Landsat TM/ETM+ ranged from 60 to 140 nm, for Envisat-1 MERIS from 2.5 to 10 nm and for CHRIS/Proba from 5 to 20 nm. Landsat and CHRIS/Proba were selected since they can provide frequent and freely available high-resolution images over the study area. Regarding CHRIS/Proba an image acquisition schedule can be made. On the other hand although Envisat-1 MERIS’ spatial resolution is relatively low comparing to the pre-mentioned satellite sensors it was selected due to its high spectral resolution.

The spectral range of the latter is restricted to the visible near-infrared part of the spectrum between 390 and 1040 nm and was designed to acquire 15 spectral bands. The spectral bandwidth is variable between 1.25 and 30 nm depending on the width

of a spectral feature to be observed and the amount of energy needed in a band to perform an adequate observation. Over open ocean an average bandwidth of 10 nm is required for the bands located in the visible part of the spectrum. Driven by the need to resolve spectral features of the Oxygen absorption band occurring at 760 nm a minimum spectral bandwidth of 2.5 nm is required (<http://www.crisp.nus.edu.sg/~research/tutorial/meris.htm>).

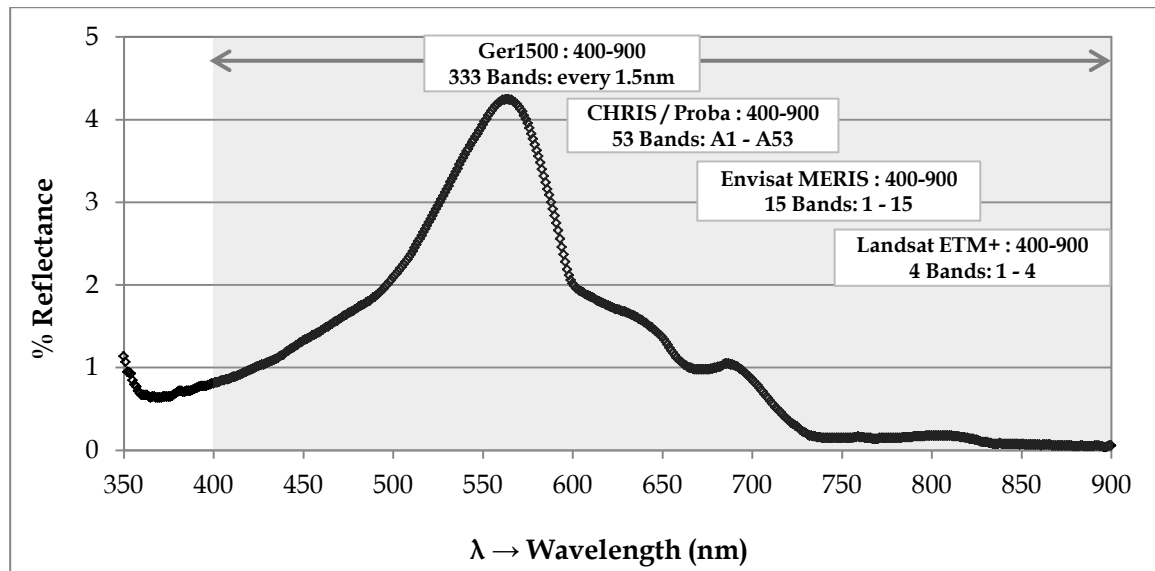


Figure 4. 3: Schematic representation of the spectral bands of CHRIS/Proba, Envisat-1/MERIS and Landsat ETM+ multispectral scanning radiometers, and GER1500 field spectroradiometer using a typical water spectral signature collected in the 2nd of July 2010 at sampling station 2 during the *in situ* sampling campaigns over the Asprokremmos Reservoir.

The results depicted better correlation regarding turbidity values and *in situ* mean reflectance values than SDD values and *in situ* mean reflectance values for all the sensors (CHRIS/Proba, Landsat TM/ETM+ and Envisat-1 MERIS). The highest correlations for the monitoring of turbidity were achieved for the CHRIS/Proba Band A31, the Landsat Band 3 and the Envisat-1 MERIS Band 12 (see Equations 4.3; 4.4 and 4.5).

The results derived using the Landsat TM/ETM+ spectral bands showed that there is a significant statistical correlation between turbidity values and Band 3 mean

reflectance values, with resulting correlation coefficients of $R=0.92$ and $R^2=0.85$. The ANOVA test with a confidence interval of $p=0.05$ (95%) was applied and the statistical F value of $F_{1,159} = 900.46$ was retrieved. Comparing the statistical F value with the correspondence critical value F^* , it is apparent that $F_{1,159} = 900.46$ is greater than $F^* = 3.91$ and as a result our model is significant. Statistical analyses indicated that a strong correlation between turbidity and reflectance can be obtained for Landsat Bands 3 and 4. However, Band 4 cannot be used for water reflectance measurements because the water absorption coefficient has a very high value (near to 1) after 800 nm (approximately) and thus, light is mostly absorbed and not reflected by water at wavelengths higher than 800 nm. As a result, the reflectance corresponding to Band 4 appears to have very low values, which can be mostly attributed to measurement errors despite the apparent high correlation. Data corresponding to Band 4 are not relevant and are thus not used for the purposes of this study. The very low reflectance values of water at Band 4 do not give an opportunity for remote sensing users to retrieve significant aspects of water quality.

$$NTU = 4.588(A31) - 0.515 \quad R^2 = 0.90 \quad (4.3)$$

$$NTU = 2.897(Band3) - 0.247 \quad R^2 = 0.85 \quad (4.4)$$

$$NTU = 17.330(Band12) + 1.134 \quad R^2 = 0.83 \quad (4.5)$$

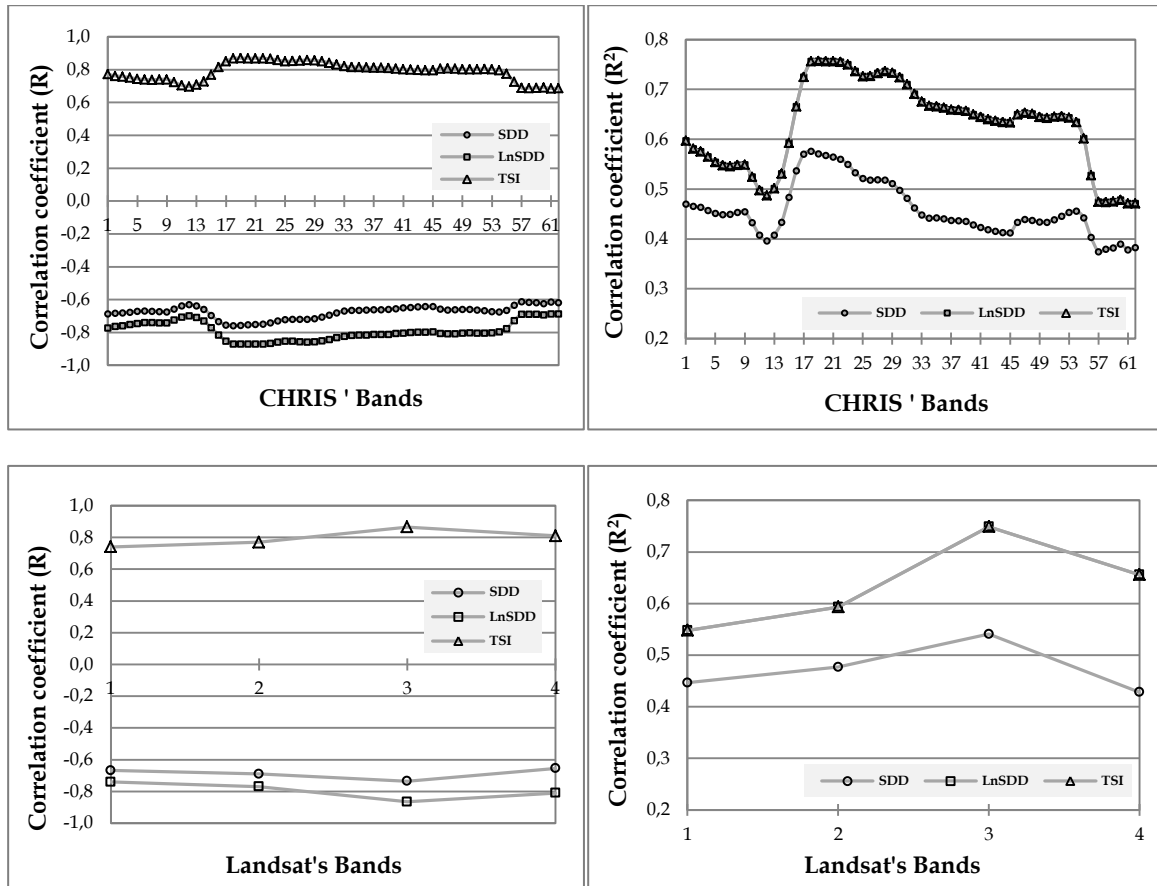
The results showed that the correlation between the mean “in-band” reflectance values and the SDD can be improved by using the natural logarithm relation ($\ln SDD$) regarding all the sensors (CHRIS/Proba, Landsat TM/ETM+ and Envisat-1 MERIS). The highest correlations for the monitoring of SDD and $\ln SDD$ were achieved for the CHRIS/Proba Band A18-A19, the Landsat Band 3 and the Envisat-1 MERIS Band 6 (Equations 4.6; 4.7 and 4.8).

$$\ln SDD = -0.968 \ln(A19) + 1.284 \quad R^2 = 0.78 \quad (4.6)$$

$$\ln SDD = -0.869 \ln(Band3) + 0.871 \quad R^2 = 0.79 \quad (4.7)$$

$$\ln SDD = -0.949 \ln(Band6) + 1.295 \quad R^2 = 0.74 \quad (4.8)$$

The correlation coefficients between the mean “in-band” reflectance values and both the SDD and the natural logarithm relation lnSDD corroborates the non-linear relationship between the variables. The squares correlation coefficients for the CHRIS/Proba were estimated for SDD equal to $R^2=0.58$ and for lnSDD $R^2=0.76$; for the Landsat TM/ETM+ for SDD $R^2=0.54$ and for lnSDD $R^2=0.75$; and for the Envisat-1 MERIS for SDD $R^2=0.49$ and for lnSDD $R^2=0.75$ (see Figure 4. 4).



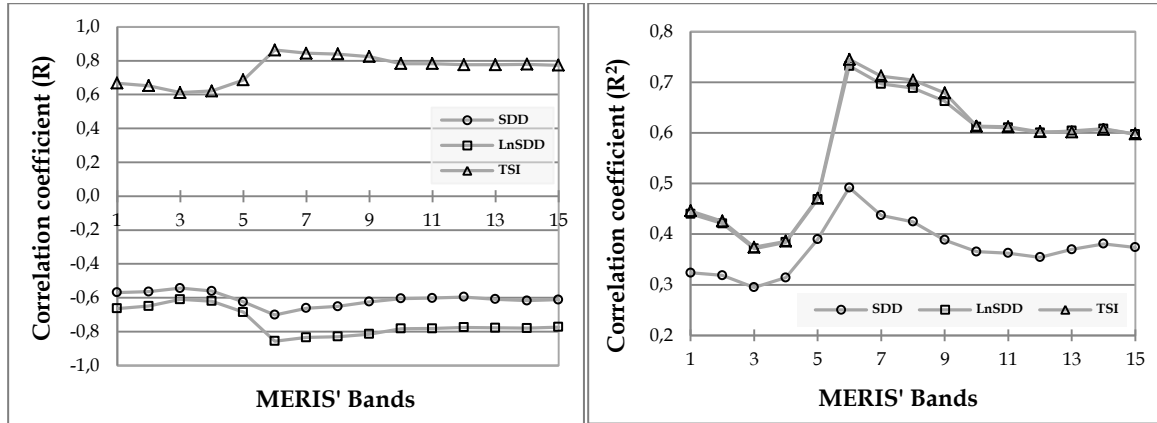


Figure 4. 4: Schematic representation of correlation observed between the mean “in-band” reflectance and the SDD, lnSDD and TSI variables for the three examined satellite sensors.

Table 4. 2: Turbidity.

Sensor	Bands info	Monitoring Turbidity	Centre band (Bandwidth (nm))	Max - R ²
GER1500	333 / 1.5	718.5	718.5 (1.5)	0.90
CHRIS/Proba	53 / 5 - 20	Band A31	706 - 712 (6)	0.90
Landsat TM/ETM+	4 / 60 - 140	Band 3	630 - 690 (60)	0.85
Envisat-1 MERIS	15 / 2.5 - 10	Band 12	768 - 782 (14)	0.83

*Bands info: Number of bands ranged from 400 to 900 nm / Bandwidth range

Table 4. 3: SDD and lnSDD.

Sensor	Bands info	Monitoring SDD / lnSDD	Centre band (Bandwidth (nm))	Max - R ²
GER1500	333 / 1.5	597.00 / 605.13	597.00 / 605.13 (1.5)	0.58 / 0.76
CHRIS/Proba	53 / 5 - 20	Band A18 Band A19	596 - 609 (13) 609 - 618 (9)	0.58 / 0.76
Landsat TM/ETM+	4 / 60 - 140	Band 3	630 - 690 (60)	0.54 / 0.75
Envisat-1 MERIS	15 / 2.5 - 10	Band 6	615 - 625 (10)	0.49 / 0.75

*Bands info: Number of bands ranged from 400 to 900 nm / Bandwidth range

In conclusion, the statistical analyses of all the above mentioned data indicated that a negative correlation is observed between the mean “in-band” reflectance and both the SDD and the lnSDD while a positive correlation is observed between the mean “in-band” reflectance and both the TSI and the turbidity (Papoutsas, Retalis, et al. 2014).

4.3 Satellite Images Analysis

The goal of this study is to assess the performance of Landsat remotely sensed data for estimating the turbidity level over the Asprokremmos Reservoir. For the aim of this study the field campaigns were coincident with Landsat overpasses, and finally an overall of eight cloud free Landsat satellite images were available. The acquisition dates and the satellite sensor of the satellite images used for the aim of the current study are depicted in Table 4. 4.

Table 4. 4: Satellite images processed in the current study.

A/A	Acquisition Date	Satellite Sensor
1	31/5/2010	Landsat ETM+
2	16/6/2010	Landsat ETM+
3	27/8/2010	Landsat TM
4	2/5/2011	Landsat ETM+
5	5/7/2011	Landsat ETM+
6	13/7/2011	Landsat TM
7	29/7/2011	Landsat TM
8	24/8/2012	Landsat ETM+

The available satellite images were processed in order to convert the Digital Numbers (DN) values recorded in the ETM+ and TM Bands 1 to 4 at the pixels corresponding to the ground-truth stations into radiance. Then, the remotely sensed radiances were corrected for the atmospheric effects using the Darkest Pixel method.

4.3.1 Pre-processing of Satellite Images

Pre-processing refers to those operations that precede the main analysis and include mainly geometric and radiometric corrections (Teillet 1986). Such processing steps include the geometric and radiometric correction of the satellite image.

Geometric correction of a satellite image is achieved by registration to the Universal Transverse Mercator (UTM) coordinate system using the nearest neighbour resampling method. For this application well-defined and well-distributed ground control points such as road intersections, airport runway intersections, bends in rivers, and corners of inland water bodies must be chosen as ground control points through careful selection of numerous points (Hadjimitsis et al. 2006).

Radiometric correction of a satellite image consists of two steps: a) the conversion of DN to radiance and reflectance and b) the atmospheric correction. Initially, satellite images are processed in order to convert satellite sensors' measurements from DN to spectral radiance using standard calibration values of the satellite image by applying the Equation 4.9. The methodology that based on the conversion of DN to at-satellite radiance (i.e., reflectance recorded at the satellite sensor) values using calibration offset and gain coefficients for each spectral band is well accepted. The information about sensor calibration parameters is usually supplied with the data (Mather 2004).

$$L_{sat} = DN \times Gain + Offset \quad (4.9)$$

The next step comprises the removal of atmospheric effects from satellite imagery. The objective of any atmospheric correction method is to determine the atmospheric effects. Any sensor that records electromagnetic radiation from the Earth's surface using visible or near-visible radiation will typically register a mixture of two kinds of energy. The value recorded at any pixel location on a remotely sensed image does not represent the true ground-leaving radiance at that point. Part of the brightness is due to the reflectance of the target of interest and the remainder is derived from the brightness of the atmosphere itself. The separation of contributions is not known a

priori, so the objective of atmospheric correction is to quantify these two components; in this respect, the analysis can be based on the corrected target reflectance or radiance values. Many atmospheric correction methods have been proposed for use with multi-spectral satellite imagery (Hadjimitsis et al. 2004; Papoutsas and Hadjimitsis 2013). The absolute radiometric correction aims to transfer the sensor detected radiance into ground surface reflectance using Equation 4.10.

$$\rho_{\text{surface}} = \frac{(L_{\text{sat}} - L_{\text{path}})\pi}{E\tau} \quad (4.10)$$

Here ρ_{surface} is the ground surface reflectance of the target. L_{path} is the path radiance, E is the irradiance on the ground target, and τ is the transmission of the atmosphere (Lillesand and Kiefer 1994). Absolute radiometric models use *in situ* measurements or reasonable estimation of atmospheric optical depth, solar zenith angle and satellite status to input parameters for calculating the ground surface reflectance (e.g. Chavez 1996; Chen et al. 2005; Song et al. 2001).

The Darkest Pixel (DP) atmospheric correction method, also known as the histogram minimum method, is the simplest atmospheric correction method provided a reasonable correction, at least for cloud-free skies which has been found to be a very effective algorithm especially for the visible part of the spectrum (Hadjimitsis et al. 2004). The principle of the DP approach is that most of the signal reaching a satellite sensor from a dark object is contributed by the atmosphere at Visible (Vis) and Near Infra-Red (NIR) wavelengths. Therefore, the pixels from dark targets are indicators of the amount of upwelling path radiance in that band. The atmospheric path radiance adds to the surface radiance of the dark target, giving the target radiance at the sensor. The surface radiance of the dark target is approximated as having zero surface radiance or reflectance. A recent adaptation of the DP method is to assume a known non-zero surface reflectance of the dark target (Hadjimitsis et al. 2003). Many studies have been shown that an atmospheric correction must be taken into account in the pre-processing of satellite imagery especially where images consist of dark

targets such as coastal waters or inland waters (Agapiou et al. 2011; Papoutsas and Hadjimitsis 2012).

4.3.2 Comparing Results of Different Areas over Asprokremmos Reservoir

For the comparison of the ground-truth data to the satellite data the ground stations were divided into four groups – “Areas” over the Asprokremmos Reservoir. The classification of the stations into groups was based on the distance of each station to the point where Xeros River flows into the Reservoir. Based on the distance criterion Area 1 consists of the sampling stations 1,2,3&4; Area 2 of the sampling stations 5,11&6; Area 3 of the sampling stations 10&7 and Area 4 of the sampling stations 8,9&12 (see Figure 4. 5). For the comparison of the field- to the satellite- data the average values for both the mean “in-band” reflectance (for Bands 1 to 4) and the turbidity for the stations belong to the same Area were calculated.

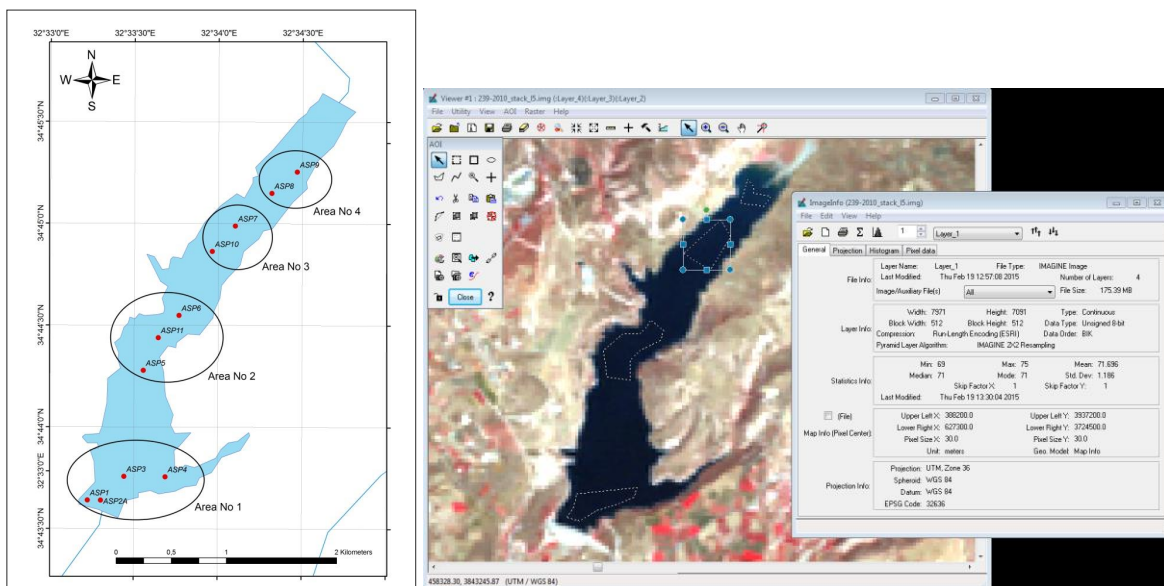
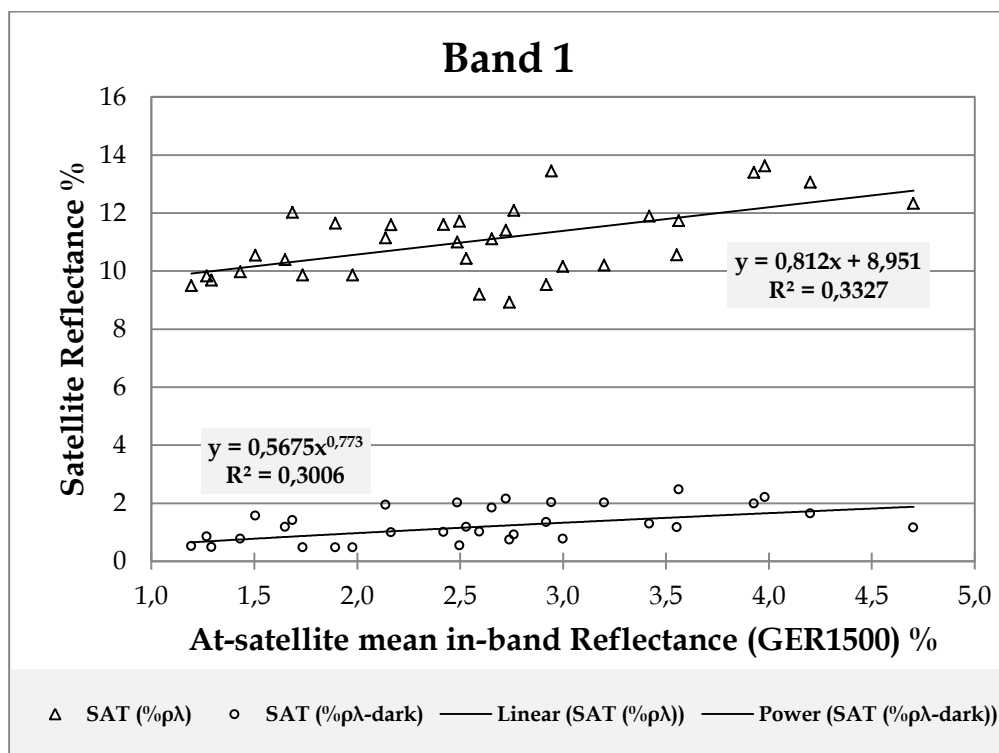


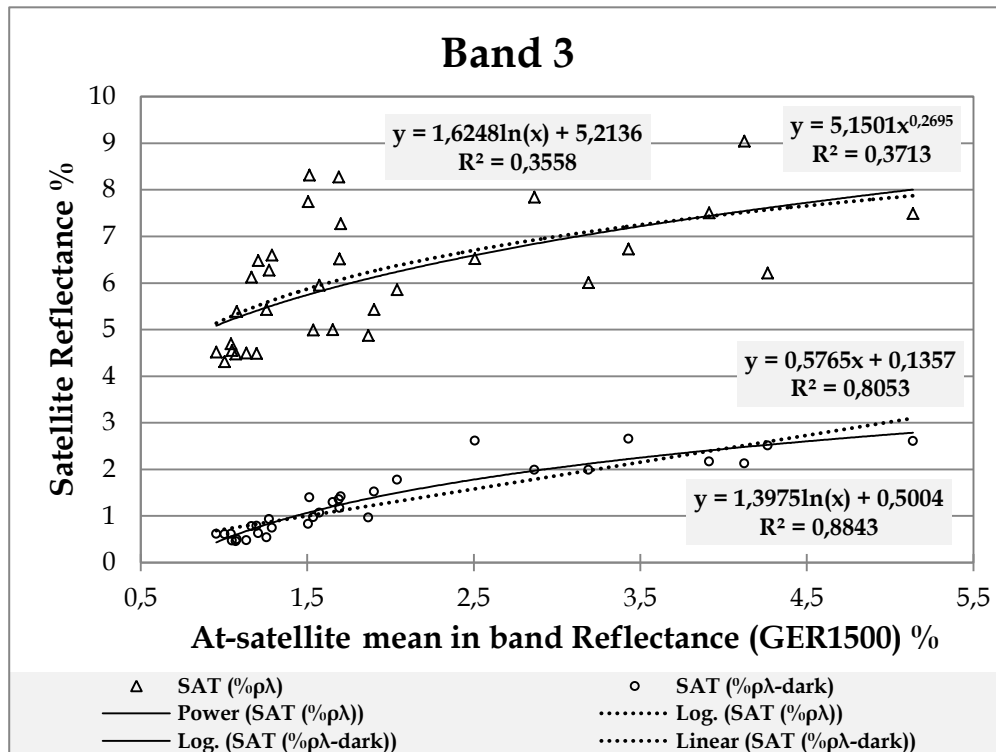
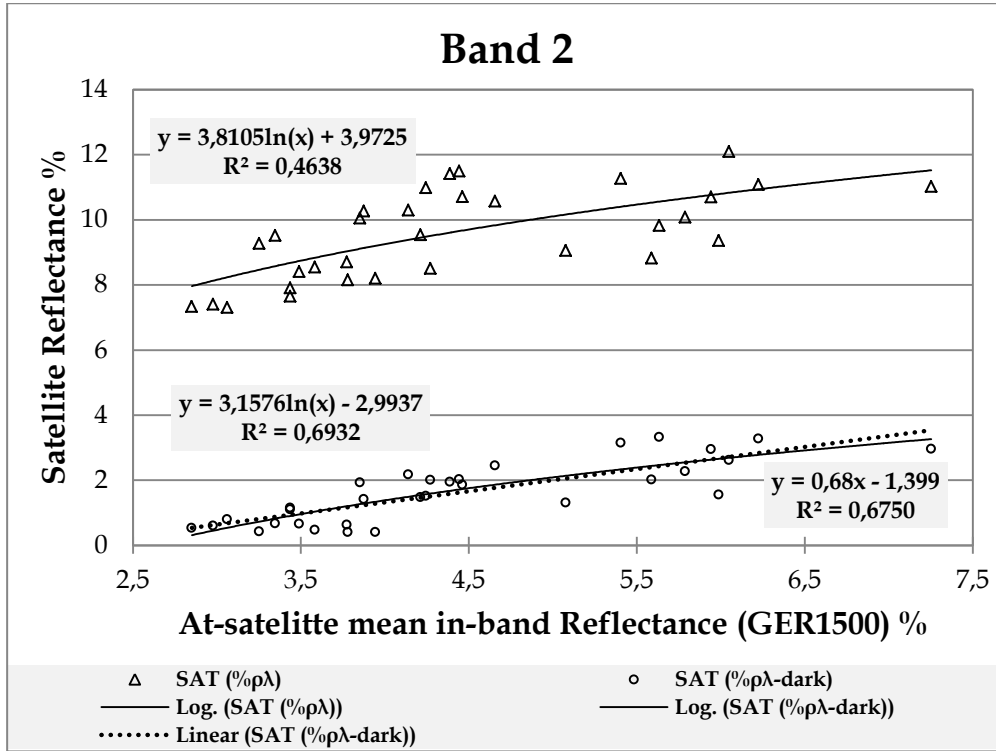
Figure 4. 5: Sampling station network used during field campaigns divided into four groups – “Areas” and selected Areas Of Interest (AOI’s) used for the processing of the satellite data to retrieve the DN of the corresponding “Areas”.

Comparison with ground-truth data collected for eight Landsat overpasses showed a satisfactory correspondence between measured concentrations and concentrations

retrieved from the ETM+ and TM data using the Darkest Pixel atmospheric correction procedures and the "local" turbidity predictive algorithm.

The comparison of the ground-truth mean "in-band" to the satellite reflectance values give better results for the satellite derived data after the atmospheric correction using the DP method with the best correlation coefficient observed for Band 3 (Figure 4. 6). Figure 4. 7 indicates the correlation between the turbidity values retrieved using the Landsat values correspond to Band 3; comparing to the ground truth values acquired at the same day during the field campaigns over the Reservoir. As it is shown, a good correlation can be observed between the estimated and the "true" turbidity values with a correlation coefficient of $R^2 = 0.8053$ correspond to the linear model and $R^2 = 0.8856$ to the logarithmic model ($R^2 = 0.8856$).





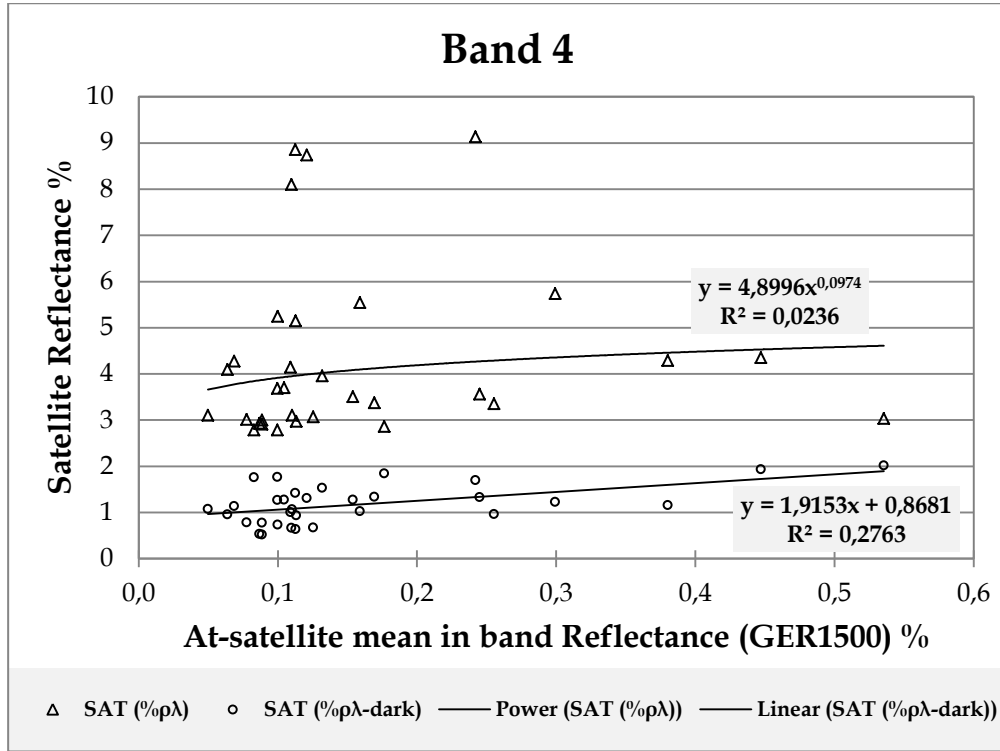


Figure 4. 6: Comparison of reflectance values retrieved from the satellite image versus the reflectance values acquired using the field spectroradiometer.

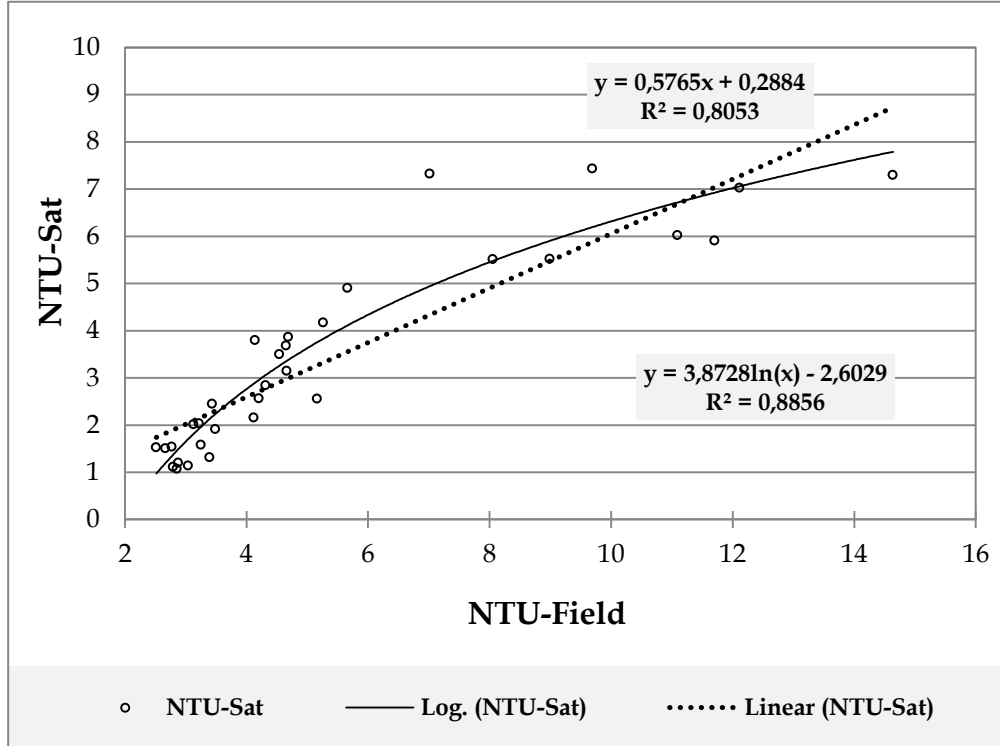


Figure 4. 7: Turbidity values retrieved from the satellite images versus ground truth turbidity values measured during the field campaigns over Asprokremmos Reservoir.

5 Development of the Trophic State Index (TSI) Predictive Algorithm for Case-2 Water Bodies

In this Chapter a description is provided regarding the development of a predictive model aiming to assess the TSI over surface water bodies using the Landsat satellite sensor. The data used for this implementation are based on the field spectroradiometric measurements acquired over 4 different Case-2 water bodies with the main study area of the Asprokremmos Reservoir. All the spectroradiometric data were processed in order to calculate the at-satellite mean reflectance values correspond to Landsat's bands. The algorithm was further test using the field spectroradiometric data obtained over the other 3 Case-2 water bodies, the Karla Lake in Greece, the Larnaca's salt-lake in Cyprus and coastal areas along Paphos and Limassol in Cyprus.

5.1 Theoretical Background

The European WFD establishes a framework for the protection of groundwater, inland surface waters, estuarine waters, and coastal waters. The WFD constitutes a new view of water resources management in Europe, based mainly upon ecological elements; its final objective is achieving at least 'good ecological quality status' for all water bodies by 2015. The analyses of pressures and impacts must consider how pressures would be likely to develop, prior to 2015, in ways that would place water bodies at risk of failing to achieve ecological good status, if appropriate programs of measures were not designed and implemented (Borja et al. 2006). Future scenarios for water resources in the Mediterranean region suggest (1) a progressive decline in the average stream flow (already observed in many rivers since the 1980s), including a decline in the frequency and magnitude of the most frequent floods due to the expansion of forests; (2) changes in important river regime characteristics, including an earlier decline in high flows from snowmelt in spring, an intensification of low flows in summer, and more irregular discharges in winter; (3) changes in reservoir

inputs and management, including lower available discharges from dams to meet the water demand from irrigated and urban areas and (4) hydrological and population changes in coastal areas, particularly in the delta zones, affected by water depletion, groundwater reduction and saline water intrusion. These scenarios enhance the necessity of improving water management, water pricing and water recycling policies, in order to ensure water supply and to reduce tensions among regions and countries (García-Ruiz et al. 2011).

Reliable, spatially covering and cost-efficient monitoring techniques of lakes and coastal waters are generally growing in importance as a consequence of increasing symptoms of the on-going eutrophication process. Remote sensing offers potentially a significant source of information, and methods are being developed for operational large-scale monitoring of water quality (Härmä et al. 2001). At the same time, additional *in situ* samples and reference field spectra can aid in finding new methods and test not only the accuracy of the final image analysis output, but also the intermediate steps in that process and estimate the accuracy of the remote sensing or image processing technique under development. As a result "ground-truth" or validation data are required, to Support Remote Sensing Research and Development as is used to assist with 1) image analysis and interpretation (e.g. image classification) of remotely sensed imagery, 2) remote sensor calibration, and 3) accuracy assessment of image analysis results (Dekker and S. W. M. 1993; Lillesand et al. 2004; Reif et al. 2012; Yacobi et al. 1995).

Protecting and monitoring lake water quality is a major concern for many local and state agencies (Sawaya et al. 2003). Trophic state is a measure of a lake's productivity and is commonly used to assess water quality. Eutrophication in natural water bodies results from excess growth and reproduction of phytoplankton for absorbing superfluous nutrition salts such as N and P. An increased availability of nutrients results in high levels of biological productivity, which can have harmful effects on water supplies (Krizanich and Finn 2009). This most often results from human caused environmental pollution.

Environmental researchers have been making efforts to monitor, simulate and control eutrophication for more than two decades. Various mathematical models have been developed and applied to rivers, lakes and estuaries (Kuo et al. 1994; Lung 1986; Senay and Shafique 2001b). Satellite and aircraft remote sensing systems have been used to monitor inland water by using the correlation between broadband reflectance and other properties of the water column, including SDD, turbidity, TSS, chl-*a* concentrations, temperature and water quality data analysed in a laboratory (Kloiber et al. 2002; Wang et al. 2004; Zhengjun et al. 2008).

The water quality is known to be affected by SS, phytoplankton biomass (chl-*a* concentration) and dissolved organic carbon. These three components are also the major factors that control the spectral signatures of water bodies (Hudson et al. n.d.; Sváb et al. 2005). Since the 1960–70s, a number of attempts have been made to quantitatively evaluate the trophic state of lakes using single-variable trophic indices or multi-parameter approaches (Xu et al. 2001). The trophic condition of a freshwater lake is linked to densities of algal pigments, or algal biomass, which are indicative of overall productivity, as well as concentrations of certain nutrients, such as nitrogen and phosphorus (Han and Rundquist 1997; Horne and Goldman 1994).

Carlson proposed a TSI (Carlson 1977) that retains the expression of the diverse aspects of the trophic state found in three multi-parameter indices yet also has the simplicity of a single parameter index, for water quality assessment of impounded water bodies. Carlson's trophic state index can be computed from any of the three interrelated water quality parameters: SDD, chl-*a* concentration, and Total Phosphorus (TP) measurement. The index has since then been widely accepted owing to its calculation simplicity and ability to communicate between researchers, government agencies, and local community residents (Carlson 1977).

According to Carlson's theory, a new approach, TSI, was developed in order to define and determine trophic status in lakes. All trophic classification is based on the division of the trophic continuum into a series of classes termed trophic state. Traditional systems divide the continuum into three classes: oligotrophic,

mesotrophic, and eutrophic (Carlson 1977). TSI values based on the SD measurements can be calculated using Carlson's Equation 5.1:

$$TSI_{SD} = 10 * (6 - \frac{\ln SD}{\ln 2}) \quad (5.1)$$

Although, the use of remote sensing for lake trophic index formulation is based on the fact that the consequences of eutrophication and an increase in productivity will be associated with a change in the optical properties of the water mass (Baban 1996). SDT is a standard indicator of water clarity, which is strongly correlated with biomass and annual productivity of suspended algae and is influenced by the abundance of organic and inorganic particulate and dissolved matter (Peckham et al. 2006; Thiemann and Kaufmann 2000). SDT measurements are the most consistently collected data and have been found to correlate well with Landsat data (Kloiber et al. 2000). Turbidity is a unit of measurement quantifying the degree to which light traveling through a water column is scattered by the suspended organic (including algae) and inorganic particles. The light scattering increases with a greater suspended load. Turbidity is commonly measured in Nephelometric Turbidity Units (NTU).

Statistical techniques have been used to investigate the correlation between spectral wavebands or waveband combinations and the desired WQP. Based on these correlations, predictive equations for WQP can be developed (Álvarez-Robles et al. 2007; Malthus and Mumby 2003; Usali and Ismail 2010). However, one of the major difficulties in the development of predictive statistical models or equations is to **define in advance the optimal or suitable spectral region or band ratio in which WQP, such as TSI should be retrieved so as to eliminate any errors.** Undeniably field spectroscopy can overcome those difficulties and, as has been shown by several studies, it is an ideal tool for the development of a reliable regression model prior to the direct use of satellite images (Alparslan et al. 2007, 2010; Hadjimitsis et al. 2006).

5.2 Study Areas

Four study areas were selected for our research field campaigns, representing four different categories of water bodies. The intense modification of their characteristics increases the range of the performed measurements/data, extending the validity of the concluding results, as it will be shown. Special attention was given in choosing sites with ecological interest and/or contains water that is under pressure. Three sampling sites located in Cyprus region and one in Greece, were selected. Specifically as shown in Figure 5. 1, in Cyprus were selected (1) the Asprokremmos Reservoir in Paphos District, (2) the Larnaca main Salt Lake in Larnaca District area, both very close to the coastline of Cyprus. The third area refers to (3) the coastal area of Limassol with three sampling points across the coastline at (3.1) Zugi, (3.2) Vassiliko Cement Works and (3.3) Old Harbour, all facing distinct tensions. The fourth selected area, the (4) Karla Lake, locates in Volos District area in Thessaly, Greece. This area was selected as it shows much higher values of nutrients concentration compared to the respective observations in Cyprus water bodies.

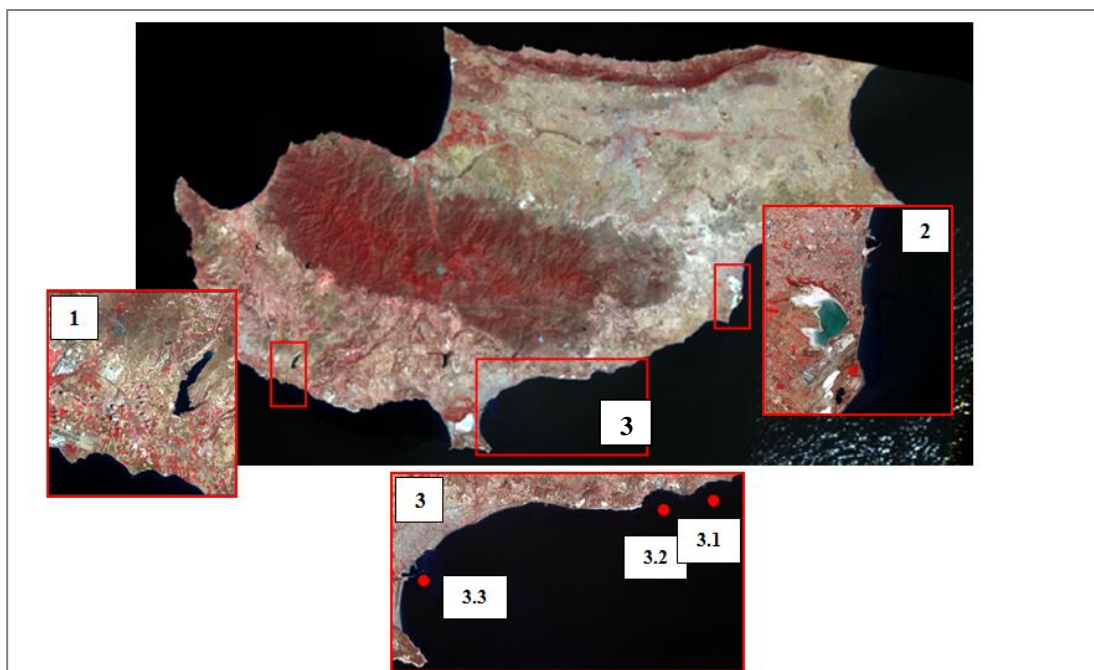


Figure 5. 1: Examined water bodies located in Cyprus, (1) Asprokremmos Reservoir, Paphos District; (2) Larnaca main Salt Lake (Alyki), Larnaca District and (3) Coastal area of Limassol District (3.1 Zugi, 3.2 Vassiliko Cement Works & 3.3 Old Harbour).

During the field campaigns *in situ* spectroradiometric measurements and measurements of the SDD and turbidity were acquired. Samples were collected for laboratory water quality analyses. The main project's objective was the comparison of the water spectral signatures of different water bodies, under various trophic conditions. In this work **characteristic spectral signatures for each water body**, for several turbidity values are presented and discussed. Furthermore, the TSI values based on SD field measurements are calculated and used for the development of a simple algorithm which aims to estimating the TSI_{SD} directly from the Landsat ETM+ spectral bands.

The main objective of this section is to examine the spectral characteristics of several water bodies. The examined water bodies refer to sites with different productivity levels such as oligotrophic (coastal sites), mesotrophic/eutrophic (Asprokremmos Reservoir and Larnaca Salt Lake) and eutrophic/hypertrophic (Karla Lake). The specific coastal sites were selected as potential point sources (harbours and Cement Works are located at those areas) (Papoutsas et al. 2013; Papoutsas, Akyllas, et al. 2014).

5.3 Results

For the aim of this study we used a combination of TSI_{SD} measurements and spectral characteristics of the water bodies to explore the effectiveness of simple algorithms relating directly TSI_{SD} to common spectroradiometric measurements. Specifically, SDD measurements of the Asprokremmos Reservoir were used to calculate the Carlson's TSI_{SD} through the Equation 5.1.

All the spectral measurements were processed in order to calculate the respective mean "in-band" reflectance values using the relative spectral response filters given by the U.S. Geological Survey (USGS) including the spectral characteristics of the Landsat ETM+ sensor as shown in (Hadjimitsis and Clayton 2011). All the TSI_{SD} values were correlated with the corresponding mean "in-band" reflectance values and several tests were done to achieve the best correlation sets. Several regression models between TSI_{SD} and different band combinations were examined in order to

retrieve the most effective relation in order to monitor the TSI_{SD} using Landsat ETM+ sensor data. Results of one- and two-band linear regression were applied, based on the measurements acquired during the extended sampling campaign that took place during 2010 at the main study area of Asprokremmos Reservoir covering the entire reservoir surface. Eighteen field campaigns were performed with a total of 161 measurements. All the results represented the correlation between the TSI measurements and several spectral-related values (single band values or band ratio values) are shown in Figure 5. 2. In most cases a linear relation represents the data reasonably well. In the cases of using spectral data from Band 3 and Band 4 a log linear relation improves the correlation coefficients slightly. In any case the best correlation ($R^2 = 0.87$) was achieved between the TSI_{SD} and the ratio between Bands 2:3 of the Landsat ETM+ mean “in-band” reflectance values (Figure 5. 3), resulting in a clear linear relation of the form

$$TSI_{SD} = 86 - 12 \text{ Band2/Band3} \quad (5.2)$$

As noted, this result was derived during the sampling campaign of Asprokremmos Reservoir indicating that the best correlation was given for the Band ratio 2:3. The result indicates that the maximum TSI value should be around 86, when the ratio 2:3 vanishes. Admitting that the range of the measured data is relatively short, we may try to fit also an exponential curve, which could be approximately linear in the specific short range of the data. As illustrated in Figure 5. 4 it is evident that the approximate linearity in the range of the data is not modified. However, the exponential relation allows for higher TSI values at low 2:3 ratios, estimating a maximum TSI value around 93 as the ratio 2:3 vanishes. Taking into account that the maximum possible TSI value should be 100 [41], we force the intercept to match this limit, obtaining, without any serious distortion to the correlation coefficient, the exponential relation

$$TSI_{SD} = 100 \exp(-0.24 \text{ Band2/Band3}) \quad (5.3)$$

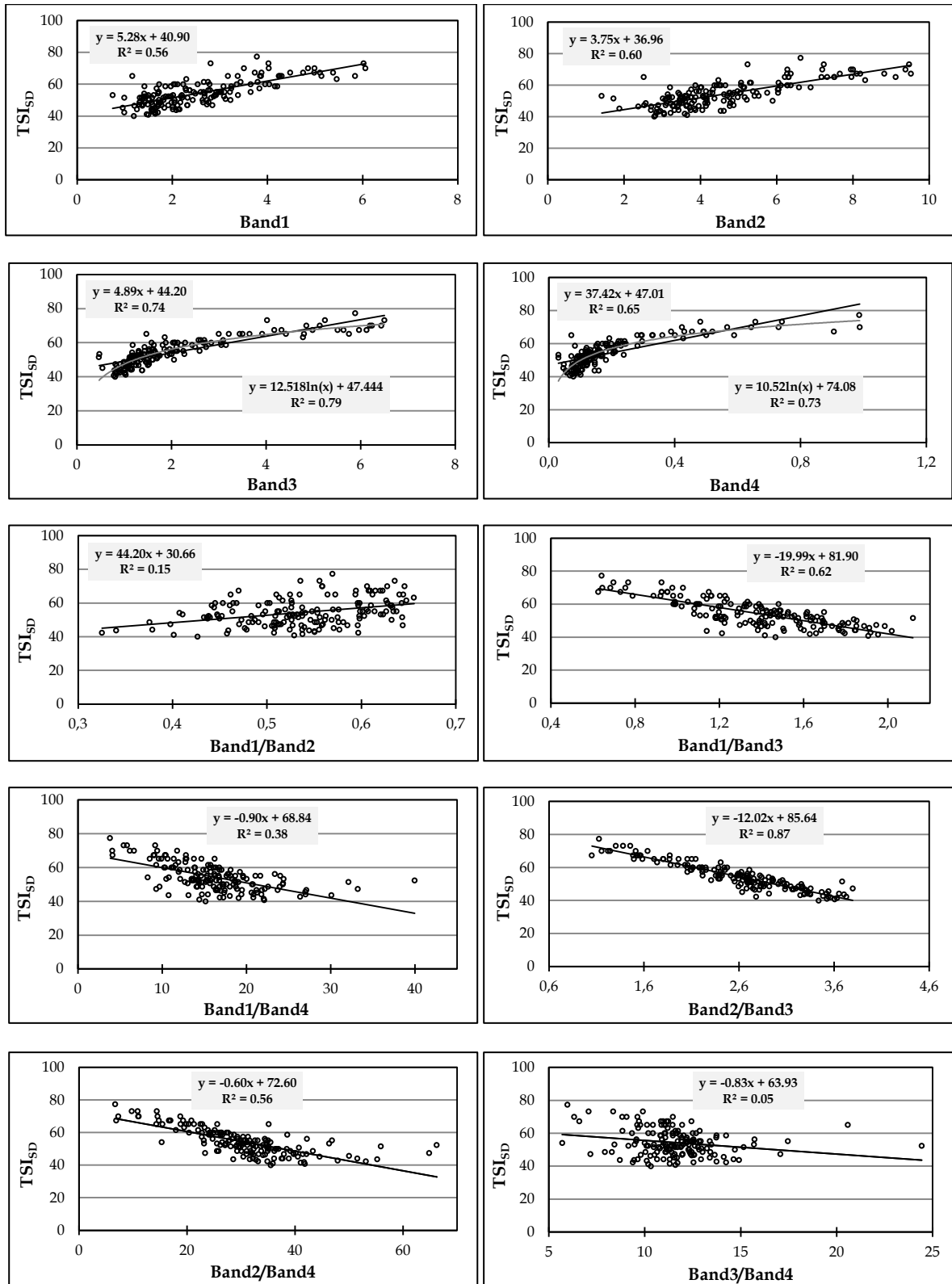


Figure 5. 2: Correlation between TSI_{SD} and several Landsat ETM+ one and two-band combinations derived using the ground truth measurements acquired during the extended field campaigns in Asprokremmos dam, in Paphos District.

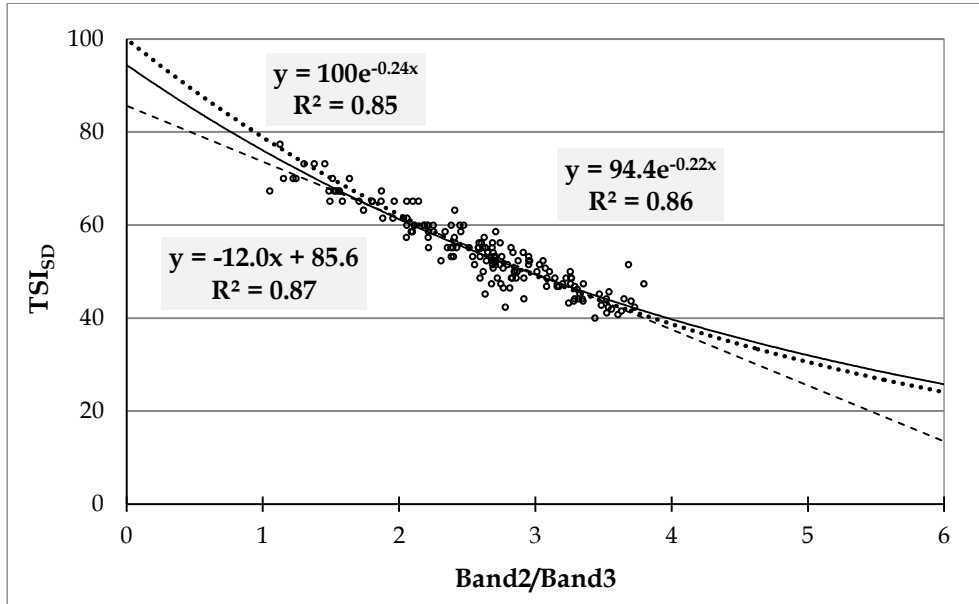


Figure 5. 3: Comparison of a simple linear and two exponential regression models used to describe the relationship between our variables of interest, TSI_{SD} and the ratio Band2/Band3, derived from the ground truth measurements acquired during the extended field campaigns in Asprokremmos dam, in Paphos District. The linear model appears on the diagram as a dashed line, the exponential model is displayed as a continuous line and the exponential model with an intercept of 100 is displayed as a dotted line.

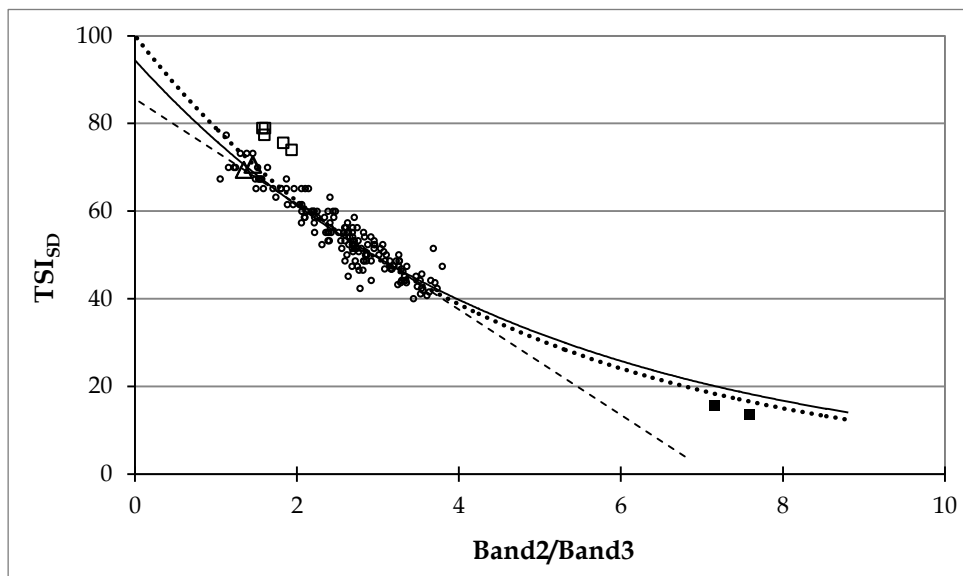


Figure 5. 4: A simple linear and the two exponential regression models used to describe the relationship between our variables of interest, TSI_{SD} and the ratio Band2/Band3, derived from the ground truth measurements acquired during the extended field campaigns in Asprokremmos dam, in Paphos District. The linear model appears on the diagram as a dashed line, the exponential

model is displayed as a continuous line and the exponential model with an intercept of 100 is displayed as a dotted line. Data acquired from four different water bodies, Asprokremmos dam in Paphos District; Larnaca main Salt Lake (Alyki); coastal area of Limassol and Karla Lake in Volos District, Thessaly, Greece are also shown. The empty circles represent measurements taken at the Asprokremmos dam; the empty triangles represent the measurements taken at the Larnaca main Salt Lake (Alyki); the empty squares referred to the measurements taken at the Karla Lake and the filled squares correspond to data acquired at the coastal area of Limassol.

In order to test the generality and the effectiveness of the above Equation 5.3, additional SDD observations acquired in Larnaca's Salt Lake, in Karla Lake and in Limassol coastal survey were examined. Taking into account the results of all the examined water bodies the exponential behaviour becomes evident as it is shown in Figure 5. 4. Both the exponential and the linear model can well describe the results derived from the Asprokremmos sampling campaign as both curves appear similar in that range. The inclusion of the rest of the data however promotes drastically the choice of the exponential fit. Specifically, Asprokremmos dam TSI values range from 40.0 to 77.3 with an average TSI value of 54.4, while for the case of Larnaca's Salt Lake TSI values range from 69.4 to 70.6 with an average TSI value of 70. Both data sets are very accurately described by the acquired Equation 5.3. For the coastal water bodies TSI values range from 13.6 to 15.5 with an average TSI value of 14.5. In that case Equation 5.3 slightly overestimates (about 7%) the measurements. On the other side, for Karla Lake the TSI values range from 73.9 to 90.5 with an average TSI value of 80.3 which is underestimated (about 15%) by Equation 5.3. However, it is evident that the values measurements of Karla Lake reveal a different pattern in comparison to the rest of the data; this is maybe due the fact that Karla Lake is a severely hypertrophic lake with high concentrations of nutrients contrary to the Asprokremmos dam and the rest sites. It is important to mention that the chl-*a* concentration range for the Asprokremmos dam was 4 to 40µg/L (average 14.9µg/L) in contrary to Karla Lake where chl-*a* concentration range from 5 to 311µg/L (average 73.4µg/L). Still, the divergence is considered reasonable.

Aiming to order to secure the validity of Equation 5.3 the fitting procedure of the exponential relation was repeated, including the whole data set from all the measuring sites. As shown in Figure 5. 5, in that case the two parameter exponential fitting reveals an intercept very close to the limit of 100 (102). By fitting constrained least square regression and adjusting the intercept coefficient to 100, once more, we conclude with exactly the same coefficient in the exponential (-0.24) that appears in (3). It is worth noted that in this case, where all the measurements are used, the overall correlation coefficient increases to 0.92. This result indicates that the acquired empirical equation seems trustful, and could be used as a first guide for the estimation of TSI values from spectral characteristics, showing a good overall performance with a smooth behaviour between the limiting values of TSI (0 – 100) (Papoutsas, Akylas, et al. 2014).

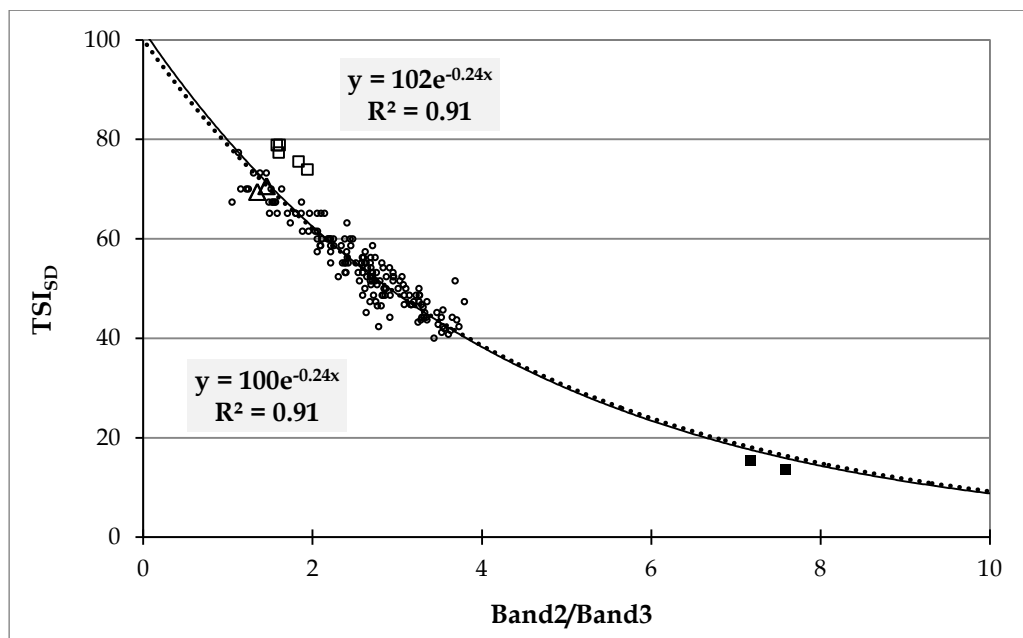


Figure 5. 5: Correlation between TSI_{SD} and ratio Band2/Band3 of the mean “in-band” reflectance of ETM+ derived from the ground truth measurements performed over four different water bodies, Asprokremmos dam in Paphos District; Larnaca main Salt Lake (Alyki); coastal area of Limassol and Karla Lake in Volos District, Thessaly, Greece. The two exponential regression models used to describe the relationship between our variables of interest are shown. The exponential model is displayed as a continuous line and the exponential model with an intercept of 100 is displayed as a dotted line. The empty circles represent measurements taken at the Asprokremmos dam; the empty

triangles represent the measurements taken at the Larnaca main Salt Lake (Alyki); the empty squares referred to the measurements taken at the Karla Lake and the filled squares correspond to data acquired at the coastal area of Limassol.

The resulted equation was further tested using both “dependent” and “independent” datasets. For the aim of the first test the dataset of reflectance values corresponds to Band2 and Band3 which was used for the development of the model was used to calculate the TSI values which resulted using the predictive model and the retrieved correlation coefficient was equal to 0.90 (Figure 5. 6a). On the other hand the model was further tested using an “independent” dataset that was not included in the dataset for the development of the TSI predictive model. This “independent” dataset include field data that was acquired during the field campaigns in Asprokremmos Reservoir during the years 2011 and 2012 for evaluation purposes (Figure 5. 6b). The results of the “independent” data-set between the TSI acquired through the predictive model (using the mean in-band reflectance values of the Landsat’s Bands 2 & 3) and the TSI based on the SDD values has indicated that there is a good correlation between the two methods for retrieving the TSI values; and the correlation coefficient was equal to 0.81.

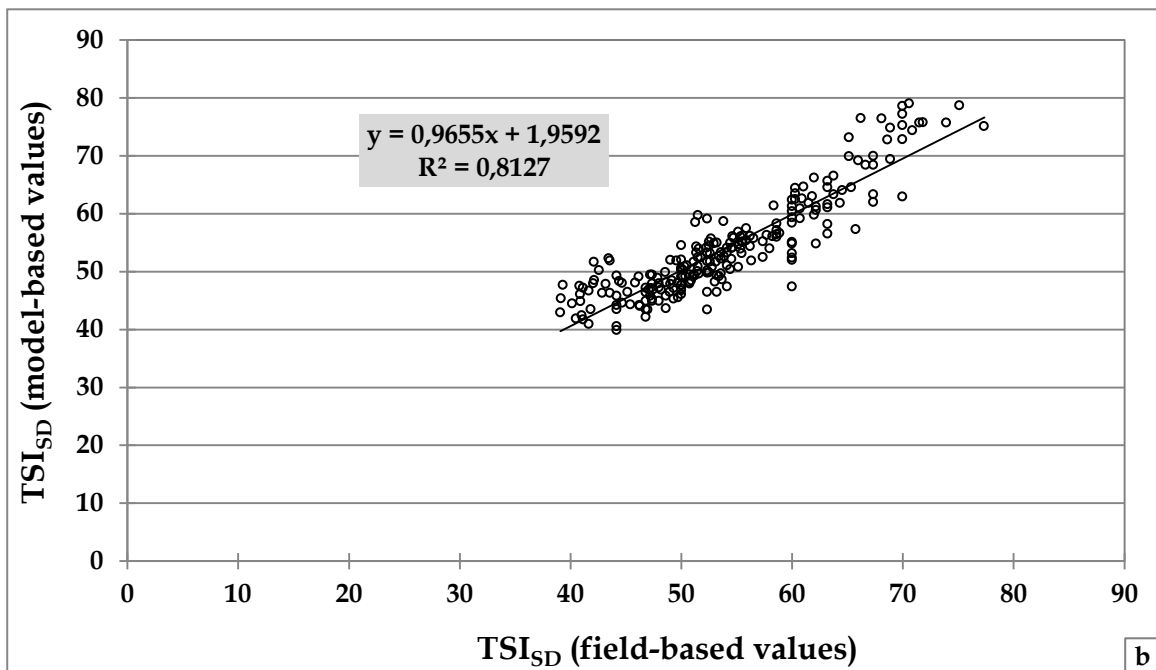
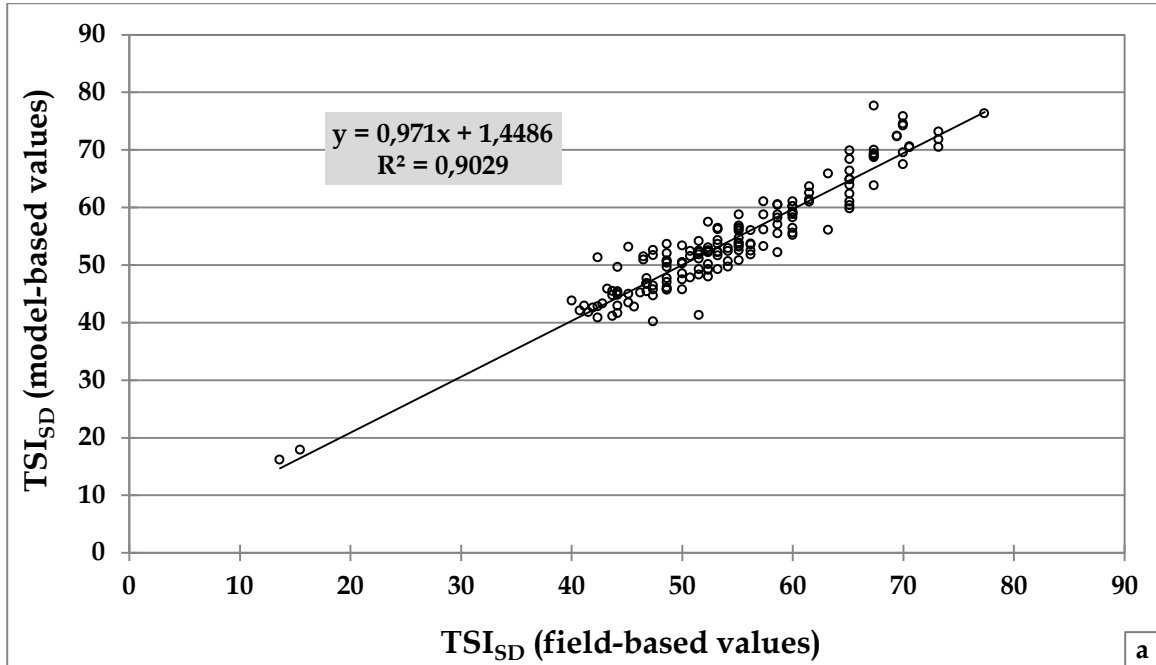


Figure 5. 6: Relation between the model-based and the field-based values of TSI_{SD}. (a) Represent the correlation resulted using only the “dependent” data-set that was used to develop the model and (b) represent the correlation resulted using only the “independent” data-set that was not included in the data-set used to develop the model. These data was acquired during the field campaigns in Asprokremmos Reservoir during 2011 and 2012.

Still further work is needed, in order to strengthen and test the previous result with measurements at the range of relatively low TSI values (less than 40) as well as at the range of high TSI values (more than 70). Also due to the simplicity of the relation the theoretical investigation and the link of the relation to known physical mechanisms that drive this result would be a provoking opportunity. Such possibility is left for future research.

Concluding, further analysis of the measurements acquired during the sampling campaigns in Asprokremmos dam has shown that there is an exponential relation between turbidity (NTU) and SDD. As shown in Figure 5. 7 the relation between the two variables can expressed as $\ln SDD = 1.72 - 0.86 \ln NTU$. This equation can be used in order to convert any available turbidity (NTU) measurement to SDD and further calculate the TSI_{SD} using the extracted Equation 5.3.

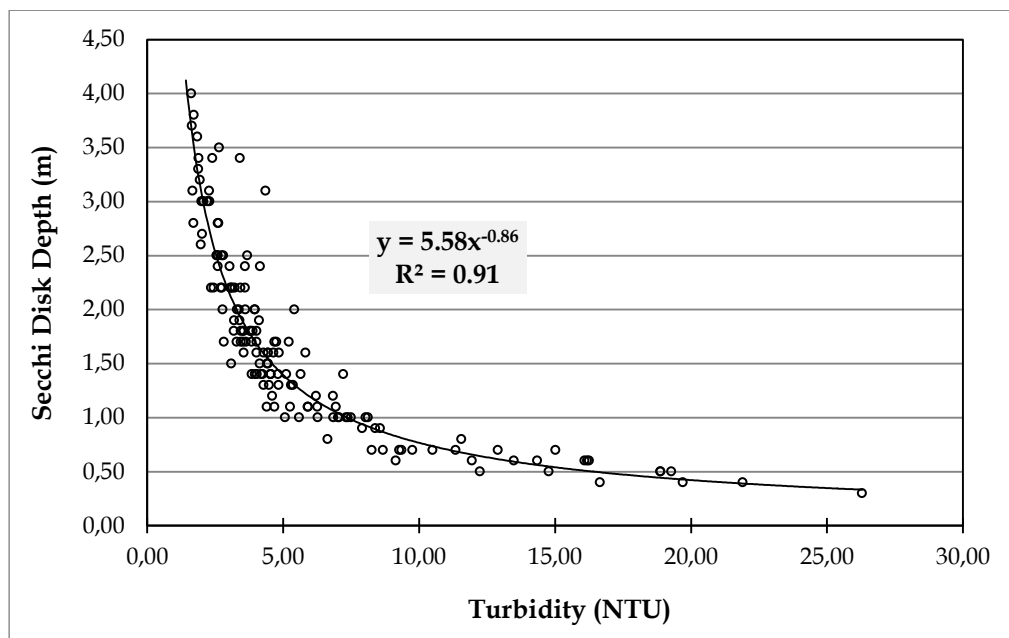


Figure 5. 7: Correlation between SDD and turbidity (NTU) acquired during the field campaigns in Asprokremmos dam, in Paphos District.

Trophic state is an important parameter for the water quality studies and there is a great need for its systematic monitoring in different water bodies such as inland and coastal waters. Above all, TSI can be used as an alert tool from the local water

management authorities. This study fills the gap of developing the suitable regression model between TSI and spectral reflectance values acquired from field spectroscopy with the main aim for future satellite observation. The development of a suitable regression model that utilizes reflectance measurements acquired using field spectroscopy assists the remote sensing users for retrieving accurate statistical results since atmospheric interventions are eliminated. Data from four different field campaigns were presented and utilized. Specifically, *in situ* spectroradiometric measurements and measurements of the SDD and turbidity were analysed and correlated. The TSI values based on SD field measurements were used for the development of a simple algorithm which helps in the direction of estimating TSI_{SD} directly from the Landsat ETM+ spectral bands. As it was shown, an optimal correlation between spectral characteristics and TSI values may be obtained by using an exponential regression model of the form:

$$TSI_{SD} = 100e^{-0.24(Band2/Band3)} \quad (5.4)$$

The formula performs surprisingly well in a wide range of data from very different sources. The acquired empirical equation seems trustful, and could be used as a first guide for the estimation of TSI values from spectral characteristics, showing a good overall performance with a smooth behaviour between the limiting values of TSI (0 – 100) for Case-2 water bodies in the Mediterranean region (Papoutsas, Akylas, et al. 2014).

6 Diffuse Attenuation Coefficient (k_d) over Asprokremmos Reservoir

In this Chapter the outcomes derived by the correlation of diffuse attenuation coefficient (k_d) values and the water quality measurements conducted over Asprokremmos Reservoir are presented. All the ground truth subsurface reflectance values acquired, using the diffuser mode of the spectroradiometer, were processed in order to calculate the diffuse attenuation coefficient values over different bandwidths derived from the downwelling irradiance measurements at different depths (E_d). All the retrieved $k_{d(\lambda_2-\lambda_1)}$ values were then correlated with the water quality values respectively, aiming to detect the optimal spectral region which gives the best correlation between k_d and TSI or SDD, respectively.

6.1 Theoretical Background - Attenuation Coefficient

Information on the attenuation of solar radiation with depth in water is important in a number of areas including primary production, thermal stratification, underwater visibility and the operation of solar ponds (Kirk 1984). The radiance reflectance (R_r) right under a lake surface is an important component of the signal that can be inferred by a remote sensor. On the way through the lake surface and up to the sensor, the reflected signal is modified by reflection from the lake surface and by scattering and absorption in the atmosphere. The radiance reflectance in the water can be described in an approximate way by the Equation 6.1,

$$R_r = 0.083 b_b / (a + b_b) \quad (6.1)$$

Where b_b is the total backscattering and a is the total absorption of the lake water; 0.083 is a constant that has been found to best describe the magnitude of the reflection over different sun angles; and a and b_b are usually called IOPs, since they

are optical properties that only depend on the water and its content and not on the incoming sunlight (Kirk 1983; Strömbeck and Pierson 2001).

The radiance flux measured above and below the water surface consists of four separate components (Figure 6. 1). Ultimately, the most interesting is the emergent flux (component 1), but different measurement strategies, instrumentation, and measurement geometry will measure varying proportions of these fluxes. It is only the emergent flux which is influenced by the IOPs of the underlying water column and which can provide information regarding relevant water quality concentrations. The only way to directly measure this component is to make L_u measurements just below the surface (0^-). The 0^- radiance reflectance measurements are therefore, extremely useful for the purpose of model verification. They allow the performance of the model in predicting water column dynamics to be evaluated separately from the different reflected fluxes which must be added and subtracted from the primary flux in order to predict the reflection just above the surface (0^+) (Lindell et al. 1999).

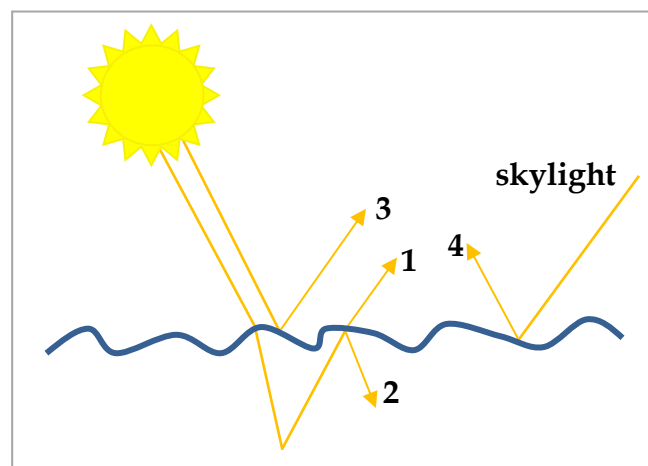


Figure 6. 1: Diagram of various possible radiance fluxes: 1) Emergent flux: affected by the IOPs of the water and contains information relative to water quality; 2) Portion of the emergent flux: reflected back into the water body before passing through the surface; 3) Reflection of the surface of direct solar radiance; 4) Reflection from the surface of diffuse sky radiance (Reproduced from Source: Lindell et al. 1999).

The attenuation characteristics of a given water body, are conveniently summarized in the form of the vertical attenuation coefficient for downward irradiance, defined by Equation 6.2. This parameter describes the spectral attenuation of the sunlight in the water and is most easily estimated by measurements of the downwelling irradiance (E_d) at two known depths; z and z_0 . Where $\Delta \ln E_d$ is the change in the natural logarithm of E_d and Δz is the depth interval.

$$K_d(\lambda) = -\Delta \ln E_d(\lambda, z, z_0) / \Delta z \quad (6.2)$$

The attenuation coefficient is classified as an AOP of the medium (Preisendorfer 1961), to be distinguished from the inherent optical: k_d can be monochromatic light at a particular wavelength or for a broad wave band such as that of Photosynthetically Available Radiation (PAR), which is another derived quantity of interest results from spectral integration over the wavebands active in photosynthesis, generally taken as the interval from 350 or 400 nm to 700 or 750 nm ($k_d(\text{PAR}) \approx 400\text{-}700$ nm, units of W m^{-2} or quanta $\text{s}^{-1} \text{m}^{-2}$; Equation 6.3) (Kirk 1984).

$$k_d(\text{PAR}) = \int_{400}^{700} E_d(z, \lambda) d\lambda \quad (6.3)$$

The vertical attenuation coefficient (k_d) is a composite measure of PAR attenuation by water, suspended particles, chl-*a*, and organic colour (Lorenzen 1980; Megard et al. 1980).

If the measurements are made right under the surface and at the depth where the irradiance has diminished to 1% of the value right under the surface, we get the average vertical attenuation coefficient for downwelling irradiance within the euphotic zone, $k_d(\text{av})$. $k_d(\text{av})$ depends on the IOPs a and b , but also on the volume scattering function of the water, i.e. to what extent and in which directions scattering occurs. When $k_d(\lambda, \text{av})$ is known, the downwelling irradiance $E_d(\lambda)$ can be estimated at any depth within a water body by the Equation 6.4 (Strömbeck 2001).

$$E_d(\lambda, z) = E_d(\lambda, z_0)e^{-k_d(\lambda, \lambda_0)z} \quad (6.4)$$

Remote sensing of freshwaters can be considered to be useful only for estimations of WQP in the upper most part of the water column. 90 % of the light reflected from a water body originates from within the depth that can be calculated as $1 / k_d$ (J. T. O. Kirk 1994).

The value of k_d of the water column is obtained by linear regression of the natural logarithm of the downward irradiance (E_d) measured *in situ* at different depths versus depth z (Equation 6.5).

$$\ln E_d(\lambda, z) = -k_d z + \ln E_d(\lambda, z_0) \quad (6.5)$$

According to J. T. Kirk (1994), the values of k_d range from 0.03 m^{-1} for the clearest ocean water to $>15 \text{ m}^{-1}$ for turbid lakes, rivers and estuaries, corresponding to euphotic depths of 150 m and $<0.3 \text{ m}$, respectively. The study of Gons et al. (1998) included the large, shallow and eutrophic IJssel lagoon in the Netherlands, eighteen Dutch lakes differing in depth and trophic state, and the large, shallow and eutrophic Lake Tai in China and the attenuation coefficient for downward irradiance ranged from 0.7 to 5.4 m^{-1} . Koenings and Edmundson (1991), studied the Alaskan lakes aiming to classify them into clear, stained, and turbid classes based on visually apparent colour and turbidity. According to their findings, unlike SDT, the median value for k_d in stained lakes was equal to that of the turbid lakes and higher than the median for clear lakes. The values ranged for 1) **Clear lakes**: Turbidity=0.2-2.0 NTU, chl-*a*=0.2-5.6 $\mu\text{g/L}$, SDD=2.3-14.7 m, $k_d=0.16-0.63 \text{ m}^{-1}$, 2) **Stained lakes**: Turbidity=0.3-3.0 NTU, chl-*a*=0.4-3.7 $\mu\text{g/L}$, SDD=2.2-7.1 m, $k_d=0.41-1.70 \text{ m}^{-1}$ and 3) **Turbid lakes**: Turbidity=0.8-49.0 NTU, chl-*a*=0.1-1.3 $\mu\text{g/L}$, SDD=0.2-3.9 m, $k_d=0.26-4.27 \text{ m}^{-1}$. According to Strömbeck (2001), the clearest water body Lake Vättern has an average lowest k_d -value of 0.18 m^{-1} at around 555 nm. That means that most reflected light comes from 0 to 5.6 m. Considering that Lake Vättern is a very

clear lake for being in Sweden, this depth interval will in most other lakes be much smaller and consequently there are no practical problems with influences of bottom reflection (Strömbeck 2001).

6.2 Analysis of Attenuation Coefficient

For the current study, all the *in situ* downwelling irradiance measurements (E_d) acquired at several depths within the water column during the field campaigns over Asprokremmos Reservoir were processed in order to retrieve the k_d values correspond to different wavebands based on Equation 6.5 (see Figure 6. 2).

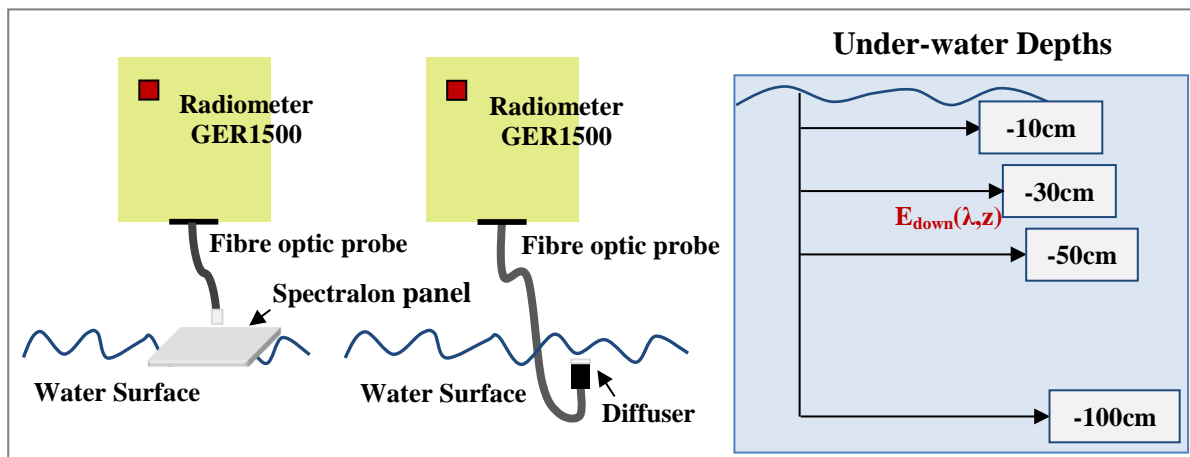
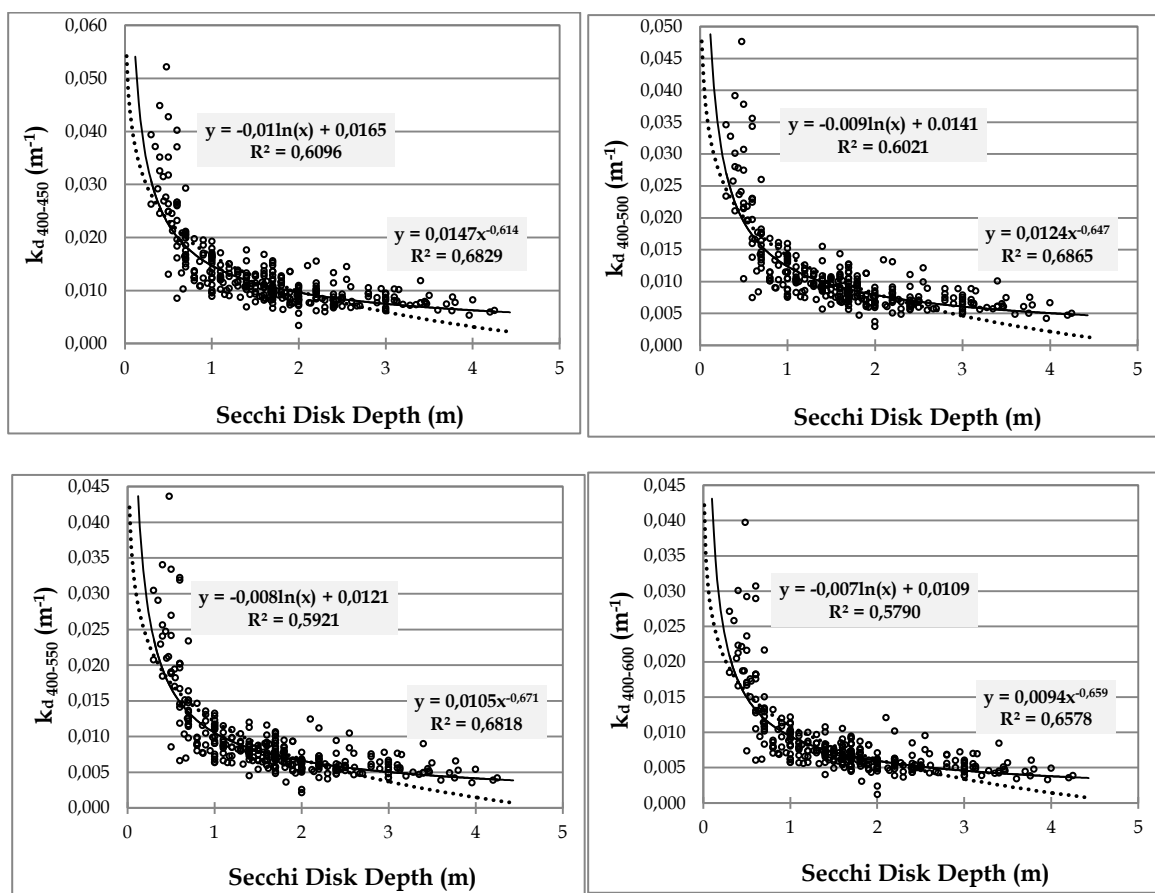
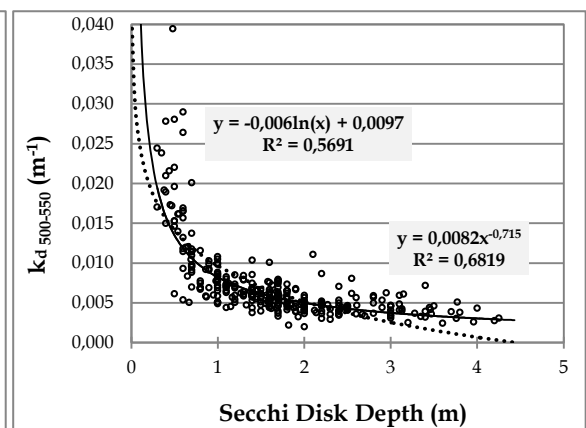
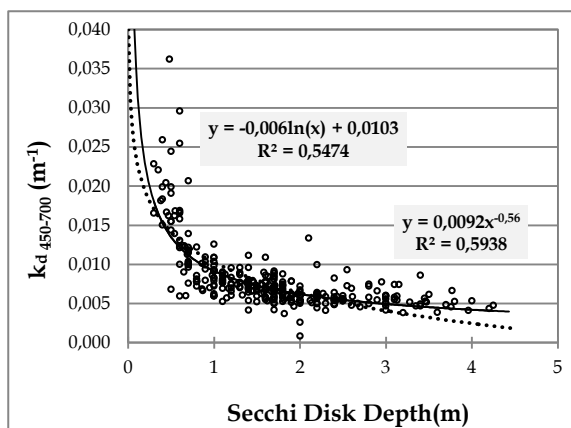
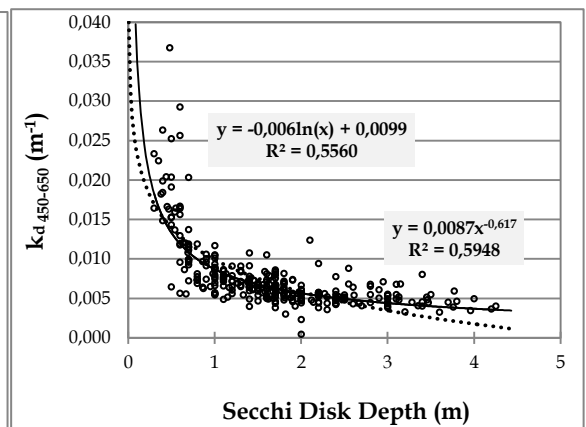
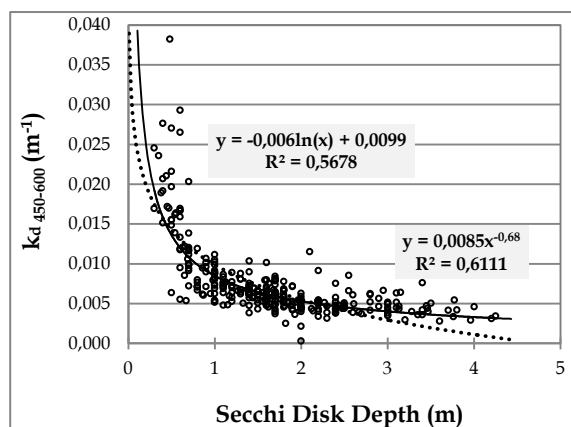
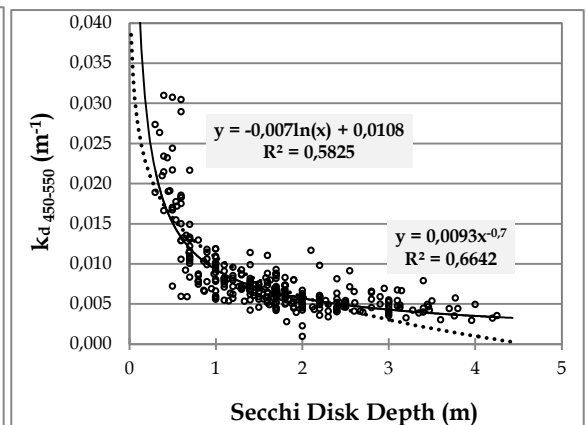
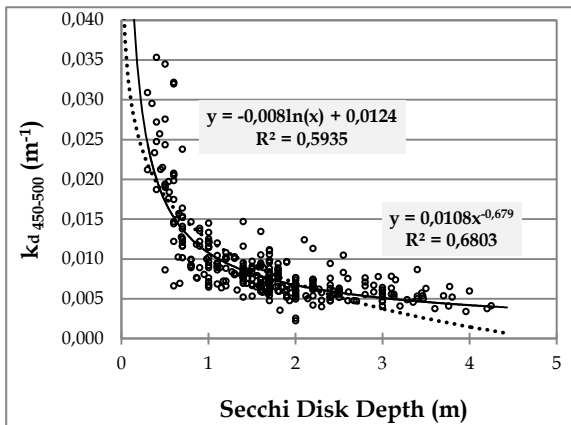
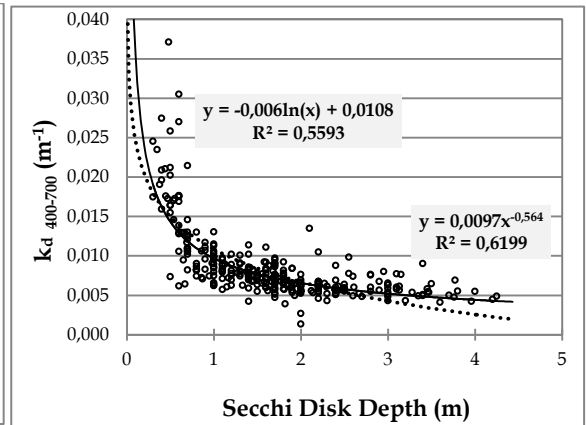
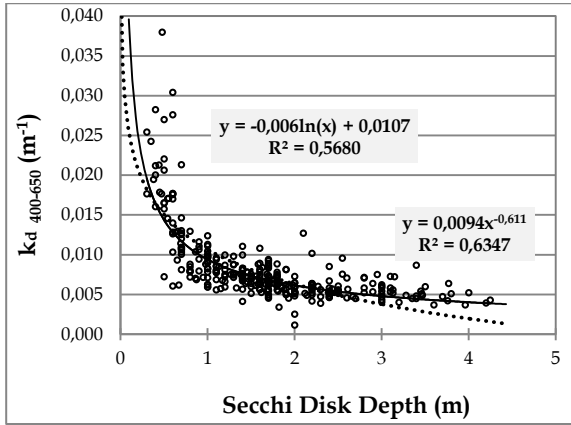


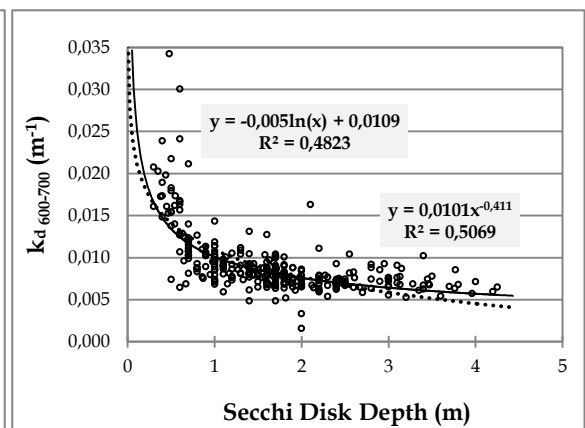
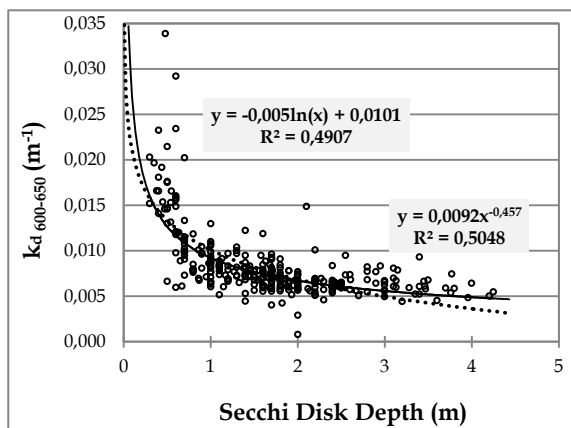
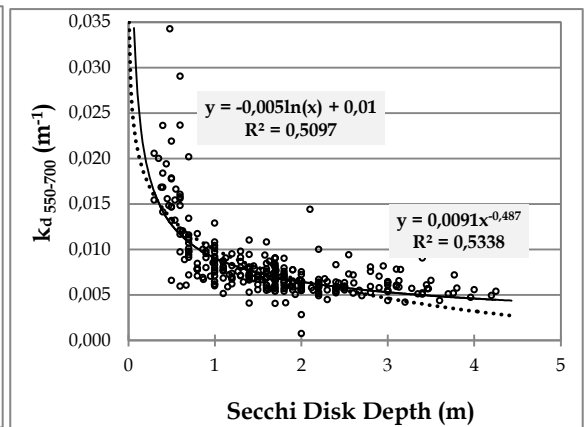
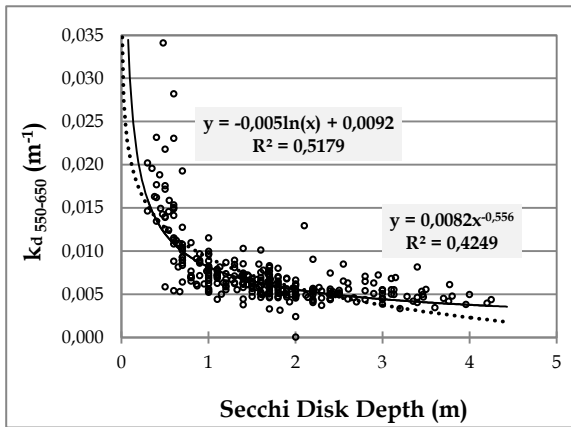
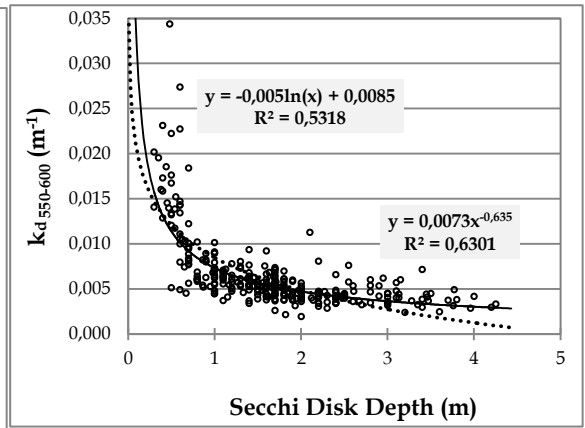
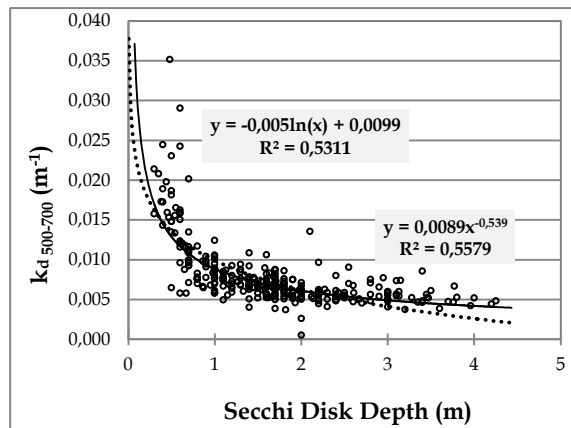
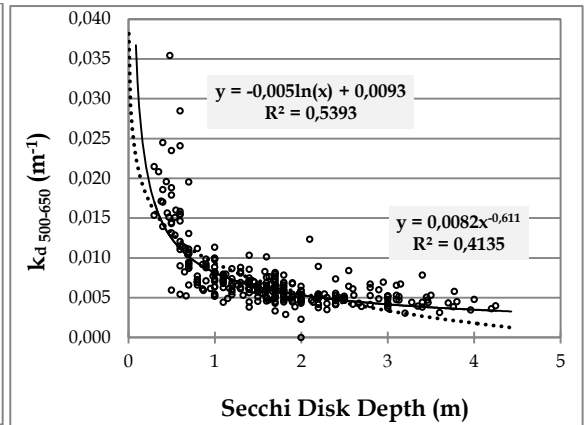
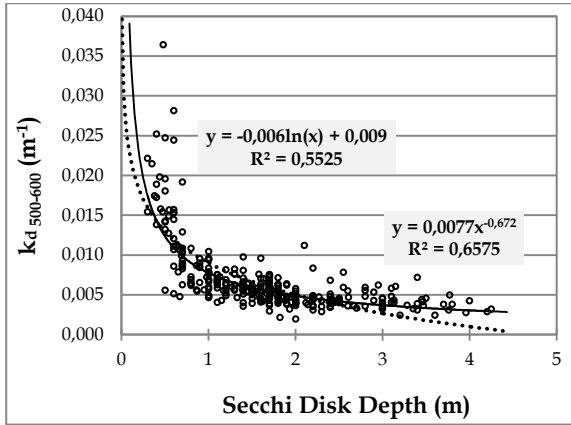
Figure 6. 2. In situ reflectance measurement procedure: (a) Measuring the downwelling radiance $L_d(\lambda)$ at depth 0^+ ; (b) Measuring the downwelling radiance $L_d(\lambda)$ at several depths bellow water surface (0^- , -10, -30, -50 & -100cm).

Plots of $\ln E_d(\lambda, z_i)$ versus z_i were performed for every single sampling station and sampling date where slope corresponds to k_d values and y-intercept to $\ln E_d(\lambda, z_0)$ values. The main goal was to identify the waveband with the best correlation between k_d and TSI or SDD, which would be more suitable to predict the TSI or SDD using remotely sensed data. k_d values were calculated for all the possible combination of wavebands ranged from 400 to 700 nm (with minimum “band-step” of 50 nm) as shown on Table 6. 1. Afterwards, all the k_d -values correspond to the wavebands shown on Table 6. 1, were correlated with the corresponding TSI and

SDD values and several mathematical forms such as linear, exponential, logarithmic and polynomial models were used to infer the best relationship. The best correlations for the parameters SDD and TSI, were identified from the determination factor (R^2). All the possible correlations for the case of SDD, are represented using the power regression curves model which exhibited better performances with high determination factor. The results are analytically illustrated in Figure 6. 3. The same was performed for TSI values using the exponential regression curves model. The derived correlation coefficient values (R^2) are presented on Table 6. 1.







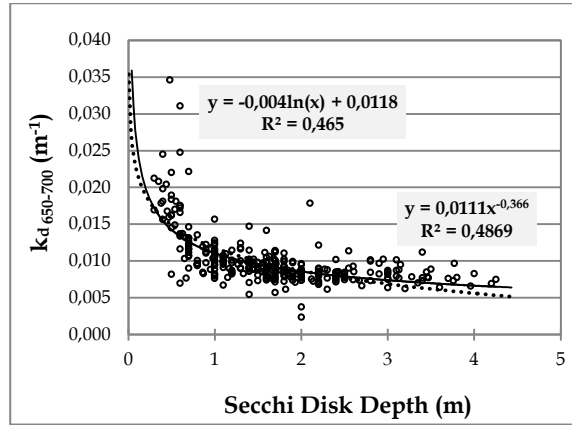


Figure 6. 3: Plots of $k_{d(\lambda_1-\lambda_2)}$ versus Secchi Disk Depth values using all possible wavebands presenting on Table 6. 1.

Table 6. 1: Values of correlation coefficient (R^2) for correlation $k_{d(\lambda_1-\lambda_2)}$ with corresponding Secchi Disk Depth values (power series) as well as $k_{d(\lambda_1-\lambda_2)}$ with corresponding TSI values (exponential series). Table illustrated the waveband range used for calculation of $k_{d(\lambda_1-\lambda_2)}$.

Waveband Range (nm)	450	500	550	600	650	700
400	0.6829	0.6865	0.6818	0.6578	0.6347	0.6199
450	x	0.6803	0.6642	0.6111	0.5948	0.5938
500	x	x	0.6819	0.6575	0.4135	0.5579
550	x	x	x	0.6301	0.4249	0.5338
600	x	x	x	x	0.5048	0.5069
650	x	x	x	x	x	0.4869

The analysis of the derived results indicated that the best correlation was retrieved for the waveband 400 to 500 nm.

(a)	400-550 nm		550-700 nm			
(b)	400-500 nm		500-600 nm		600-700 nm	
(c)	400-450 nm R ² =0.6829	450-500 nm R ² =0.6803	500-550 nm R ² =0.6819	550-600 nm R ² =0.6301	600-650 nm R ² =0.5048	650-700 nm R ² =0.4869

Figure 6. 4: Diagram illustrating the correlation coefficients corresponding to correlation between k_d versus Secchi Disk, for wavebands ranging from 400 to 700 nm with different “band-steps” (a) 150 nm; (b) 100 nm and (c) 50 nm.

In general, it is obvious that better correlation results are observed for the wavebands in the lower area of the spectrum ranged from 400 to 550 nm than for these ranged from 550 to 700 nm (Figure 6. 4 (a)). Further analysis of the spectrum areas exhibiting better results, are presented in Figure 6. 4(b) & (c). Examining the results correspond to Figure 6. 4(b) better performances with higher determination factors were observed for the waveband ranged from 400 to 500 nm than for the range 500 to 600 nm. On the other hand, the results derived using a “band-step” of 50 nm (Figure 6. 4(c)) showed that better performances can be observed for the areas 400 to 450 nm and 500 to 550 nm with the first giving slightly better results. Overall, analysis of the results showed that in general better performances can be observed moving from higher to shorter wavebands for all the examining “band-steps” and that the best results can be retrieved using the bandwidth ranging from 400 to 500 nm.

7 Examining the Spectral Characteristics of Different Water Bodies using Field Spectroscopy

This Chapter deals with the characteristic areas of the spectra that can be used to characterise a water body. Several spectral signatures been acquired over different water bodies, both inland and coastal, are presented and an extensive analysis and comment on the obtained results are provided.

7.1 Theoretical Background - Water Spectrum Characteristics

The colour of natural water is determined by changes in the spectral composition of the underwater light due to the optically active components in the water. The spectral backscattering and absorption coefficients of the major constituents of a particular water body must be known in order to understand the spectra in detail (Gons et al. 1998; Rijkeboer et al. 1998).

Gons et al. (1998) acquired the subsurface irradiance reflectance spectra in different inland water types, including: 1) the large, shallow and eutrophic IJssel lagoon in the Netherlands, 2) eighteen Dutch lakes differing in depth and trophic state, and 3) the large, shallow and eutrophic Lake Tai in China. According to their findings, the subsurface irradiance reflectance spectra varied greatly in peak value and shape and the variation was greatest at near infrared wavelengths. *Evidently, $R(0^-)$ around 750 nm depended mainly on the concentration of TSM.* The explanation for this dependency is a lack of significant absorption by substances other than water in this spectral region. If this is true, this feature of the near infrared reflectance can be used for estimating the backscattering coefficient b_b .

Thiemann et al. (2001) based on *in situ* water sampling and reflectance measurements to develop algorithms for the determination of the trophic parameters SDT and chl-*a* from hyperspectral airborne casi and HyMap data with multi-temporal validity. Their study area located about 70 km northwest of Berlin, Germany and they investigated the Mecklenburg Lake District, which covers about

300 km² with more than 30 lakes. The two lakes 1) Lake Wumm (oligo-mesotrophic) and 2) Lake Bramin (highly eutrophic) revealed extremes values, with all the other lakes vary between these two extremes. According to their findings *chl-a* shows two diagnostic absorption bands centred at 435 and 678 nm. The reflectance peak around 700 nm rises with increasing chlorophyll concentration. This phenomenon is reported in the literature to be caused by (i) fluorescence, (ii) abnormal scattering due to the chlorophyll absorption at 675 nm, or (iii) a combination of the decreasing chlorophyll absorption and the increasing water absorption in this wavelength range. Different semi-empirical and semi-analytical regression approaches using the **chlorophyll absorption band** in the red and the near-infrared **reflectance peak** were tested to determine the chlorophyll concentration from the reflectance spectra (Dekker 1993; Gitelson et al. 1994; Thiemann and Kaufmann 2000, 2002).

Han (1997) performed a controlled experiment conducted outdoors in a 7510-litre water tank using natural sunlight. The objective was to characterize and compare the relationship between SS concentration and reflectance in clear and algae-laden waters. A red loam soil was added and suspended in the tank filled with clear and algae-laden waters, respectively. A total of 20 levels of SS concentration (from 25 to 500 mg l⁻¹) were created for each type of treatment. Reflectance was recorded using an ASD spectroradiometer, and the bi-directional reflectance factor was computed and analysed. The outcomes of this research show that *the same amount of suspended sediment generated higher reflectance between 400 and 700 nm in clear water than in algae-laden water due to the blue and red absorption of chlorophyll*. The effect of chlorophyll on the SS concentration-reflectance relationship was minimum at wavelengths between 700 and 900 nm. For both clear and algae-laden waters, the linearity in the SS concentration -reflectance relationship increased with wavelength between 400 and 900 nm. A near-linear relationship between SS concentration and reflectance was found between 720 and 900 nm.

Relationships between reflectance and WQP have general validity because $R(0^\circ)$ is relatively stable under varying solar angles, atmospheric conditions and states of water surface (Dekker et al. 1996). A condition for successfully applying optical

remote sensing techniques is the availability of adequate models or algorithms relating optical signature to WQP (Rijkeboer et al. 1998).

Menken et al. (2005), obtained detailed reflectance spectra from the water surfaces of 15 lakes in east-central Minnesota and found patterns related to chl-*a*, turbidity and humic matter (CDOM). *CDOM absorbs light and decreases reflectance in the visible portion of the spectrum, especially in the blue region.* This is best demonstrated by comparing the spectra of three humic-rich lakes with the spectrum of the lake with lowest C_{440} . All four lakes had low chl-*a*, but the three humic-rich lakes had considerably lower reflectance from 400 to 600 nm. This results are in accordance to the resemble spectra of humic lakes from studies by Arenz et al. (1996) and Kallio et al. (2001), who reported that humic lakes with low levels of other optically active constituents had very low reflectance and no distinguishable peaks and troughs across the spectrum. *Increasing chl-*a* and turbidity generally resulted in higher reflectance across the visible and near-infrared spectrum. Increasing CDOM led to low reflectance, especially below ~500 nm.* The ratio of reflectance at 700 nm to that at 670 nm was the best predictor of chl-*a* over a wide range of conditions, including high turbidity and CDOM. The ratio of reflectance at 670 nm to 571 nm provided the best estimates of humic colour despite the low absorbance of CDOM at these wavelengths.

7.2 Analysis of Spectral Signatures over Different Water Bodies

In this section the typical spectral signatures acquired during the study-period 2010-2014 over various water bodies in Cyprus and Greece will be presented. An extensive discussion and comment is given regarding the main differences observed considering the qualitative characteristics of the spectrums acquired during the *in situ* campaigns over the four main water body-categories described below:

- ❑ Asprokremmos Reservoir (oligotrophic lake)
- ❑ 'Alyki'- Larnaca's Salt Lake (shallow lake - algal bloom observed)
- ❑ Karla Lake (mesotrophic - eutrophic lake)
- ❑ Coastal areas

7.2.1 Asprokremmos Reservoir (oligotrophic)

Aiming to investigate the spectral characteristics of water bodies with different concentrations of SS several spectral signatures conducted in the study area of Asprokremmos Reservoir will be studied in order to point out the main differences being observed. Spectral signatures acquired during the same sampling campaign along the Reservoir were examined. The spectral signatures correspond to Sampling Station 2, which can be characterised as a 'low-concentration' station and those of Sampling Station 9, which can be characterised as a 'high-concentration' station over the Reservoir are presented as they represent the two extreme water quality cases being observed (Figure 7. 1).

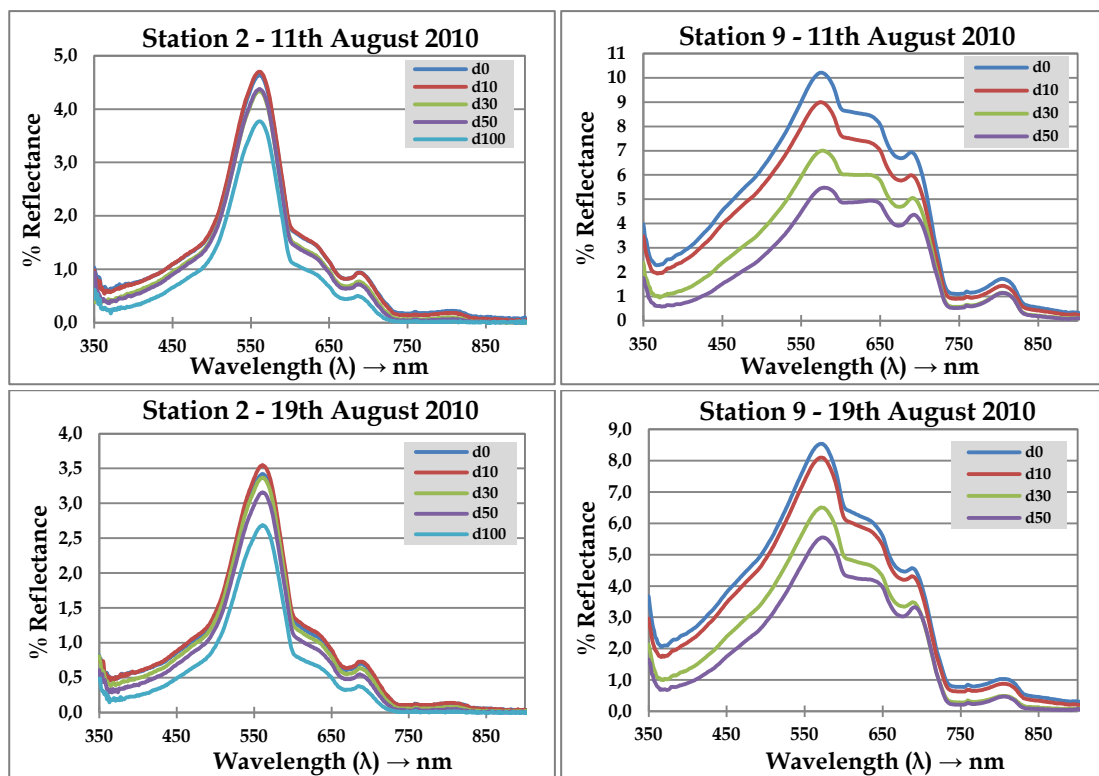


Figure 7. 1: Spectral signatures of Asprokremmos Reservoir correspond to different turbidity values acquired using the field spectroradiometer GER1500.

Measurements of the upwelling energy, first at the surface of the water and then at increasing interval depths, were acquired during the field campaigns; aiming to investigate how spectral signatures changes along the water column. These

measurements were made in an effort to understand the extinction coefficient of the water and the relationship of the optical data as compared to various attenuation functions (k-functions). A typical example of the spectral signatures correspond to different depths below water surface is illustrated in Figure 7. 2. As it is obvious a gradual reduction of reflectance values is observed as the depth increasing.

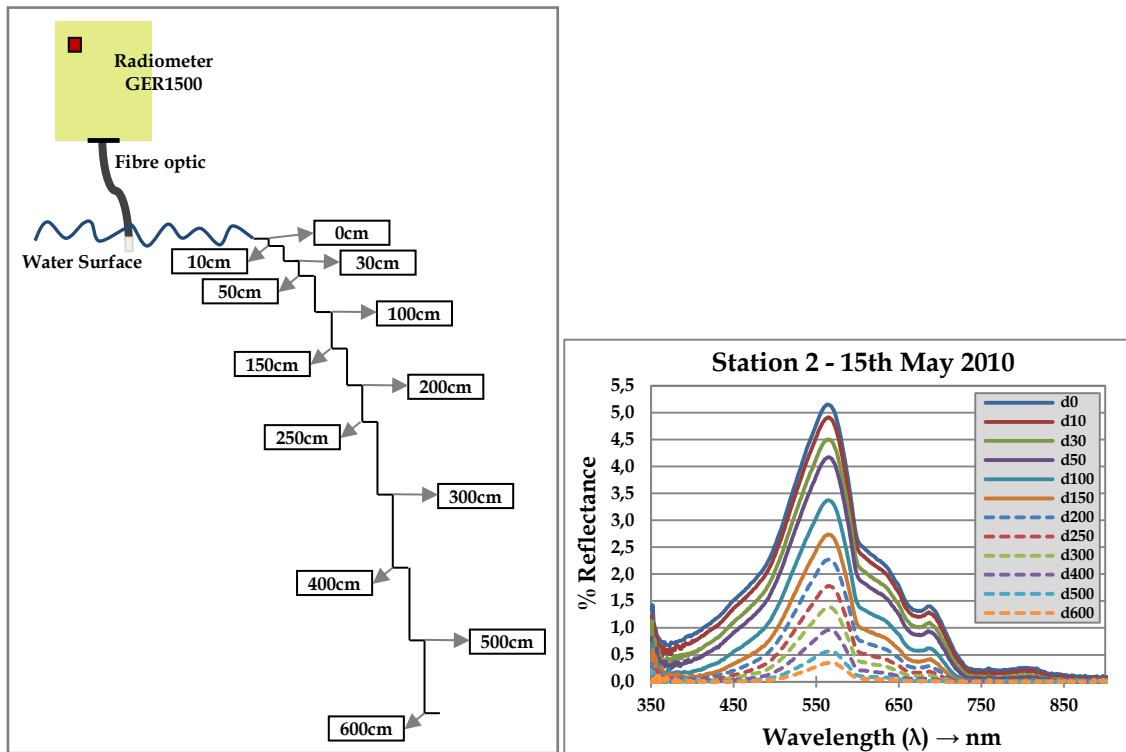


Figure 7. 2: Spectral signatures of Asprokremmos Reservoir correspond to different water depths below water surface acquired using the field spectroradiometer GER1500.

Sampling dates, sky conditions, and data referring to turbidity, SDD, and TSI values for sampling station 2 (low-turbidity values area) and sampling station 9 (high-turbidity values area) are shown in the following Tables. Table 7. 1 referred to 2010 and Table 7. 2 to 2011. TSI values based on the SDD measurements were calculated using Carlson’s Equation (7.1):

$$TSI_{SD} = 10 * \left(6 - \frac{\ln SD}{\ln 2} \right) \quad (7.1)$$

According to Carlson's theory, a new approach, TSI, was developed in order to define and determine trophic status in lakes. All trophic classification is based on the division of the trophic continuum into a series of classes termed trophic state. Traditional systems divide the continuum into three classes: oligotrophic, mesotrophic, and eutrophic (Carlson 1977). Based upon the TSI values deriving from the SDD measurements, Area No. 2 can be characterized as mesotrophic and Area No. 4 as eutrophic. TSI parameter is further discussed in Chapter 5.

Table 7. 1: Field campaign data acquired during 2010 over Asprokremmos Reservoir referring to sampling date: turbidity, SDD, TSI values; and sky conditions for sampling station 2 (low-turbidity values area) and sampling station 9 (high-turbidity values area).

	2010	Sampling Station 2			Sampling Station 9			Sky Condition
No	Sampling Date	SDD (m)	Turbidity (NTU)	TSI	SDD (m)	Turbidity (NTU)	TSI	1-4 *
1	29-April-10	2.55	-	46.51	-	-	-	1
2	07-May-10	2.55	-	46.51	0.70	-	65.14	1
3	15-May-10	-	3.80	-	-	7.94	-	1
4	31-May-10	1.70	3.53	52.35	0.60	11.95	67.36	1
5	10-Jun-10	1.60	4.97	53.23	-	-	-	3
6	16-Jun-10	1.50	4.14	54.16	0.40	19.70	73.20	1
7	24-Jun-10	2.00	3.61	50.01	0.30	26.30	77.35	2
8	02-Jul-10	2.20	2.45	48.64	0.40	21.90	73.20	1
9	18-Jul-10	2.20	3.10	48.64	0.50	18.88	69.99	1
10	03-Aug-10	3.00	2.26	44.17	0.50	19.28	69.99	1
11	11-Aug-10	3.70	1.65	41.15	0.50	18.88	69.99	1
12	19-Aug-10	4.00	1.62	40.02	0.70	10.50	65.14	1
13	27-Aug-10	2.40	2.60	47.38	0.60	16.25	67.36	1
14	20-Sep-10	2.40	3.04	47.38	-	-	-	1
15	28-Sep-10	3.10	1.67	43.70	0.60	16.18	67.36	1
16	06-Oct-10	2.80	2.62	45.16	0.50	15.02	69.99	1
17	14-Oct-10	1.40	4.04	55.15	0.60	14.35	67.36	1
18	22-Oct-10	1.10	5.92	58.63	0.40	16.66	73.20	1
	Average	2.36	3.19	48.40	0.52	16.70	69.76	
	Min	1.10	1.62	40.02	0.30	7.94	65.14	

Max	4.00	5.92	58.63	0.70	26.30	77.35
		*1: clear	*2: thin clouds	*3: partly cloudy	*4: cloudy	

Table 7. 2: Field campaign data acquired during 2011 over Asprokremmos Reservoir referring to sampling date: turbidity, SDD, trophic state index (TSI) values; and sky conditions for sampling station 2 (low-turbidity values area) and sampling station 12 (high-turbidity values area).

No	2011	Sampling Station 2			Sampling Station 12			Sky Condition
	Sampling Date	SDD (m)	Turbidity (NTU)	TSI	SDD (m)	Turbidity (NTU)	TSI	1-4 *
1	31-Mar-11	2.00	2.93	50.01	-	-	-	1
2	02-May-11	1.20	3.29	57.37	0.65	5.29	66.21	1, 5
3	10-May-11	1.62	2.72	53.05	0.57	12.42	68.10	1
4	10-Jun-11	1.00	3.87	60.00	0.35	27.20	75.13	1
5	27-Jun-11	1.85	3.83	51.14	0.50	13.34	69.99	1
6	05-Jul-11	2.90	2.90	44.66	0.70	11.59	65.14	1
7	13-Jul-11	3.00	2.73	44.17	0.50	20.67	69.99	1, 6
8	29-Jul-11	2.40	2.93	47.38	0.50	32.60	69.99	1
9	22-Aug-11	2.20	3.77	48.64	0.30	24.48	77.35	1, 6
10	30-Aug-11	2.10	2.45	49.31	-	-	-	3 to 4
11	15-Sep-11	2.42	1.90	47.26	0.48	20.29	70.58	1
12	23-Sep-11	2.90	1.82	44.66	-	-	-	1
13	30-Sep-11	3.45	2.14	42.16	0.38	20.29	73.94	1
14	10-Oct-11	4.25	1.53	39.15	0.44	19.89	71.83	1
15	17-Oct-11	3.46	2.16	42.11	0.60	12.15	67.36	1
16	10-Nov-11	1.82	3.78	51.37	-	-	-	1
	Average	2.41	2.80	48.28	0.50	18.35	70.47	
	Min	1.00	1.53	39.15	0.30	5.29	65.14	
	Max	4.25	3.87	60.00	0.70	32.60	77.35	
		*1: clear	*2: thin clouds	*3: partly cloudy	*4: cloudy	*5: dusty	*6: yellow particles	

Analyses of both the *in situ* field spectroradiometric and water quality data have indicated that four areas can be distinguished over the Asprokremmos Reservoir: **Area No. 1:** Outlet area (sampling stations 1, 2, 3, 4); **Area No. 2:** located in the central area of the Reservoir (sampling stations 5, 11, 6); **Area No. 3:** located near the Inlet area (sampling stations 10, 7); and **Area No. 4:** Inlet area (sampling stations 8, 9, 12 - the latter was used only during 2011/2012) (see Figure 7. 3). In total, 198 spectroradiometric measurements were acquired during 2010 (18 sampling campaigns including measurements at each of the 11 sampling stations) and 192 during 2011 (16 sampling campaigns including measurements at each of the 12 sampling stations). *In situ* turbidity and SDD data were determined for all the water samples.

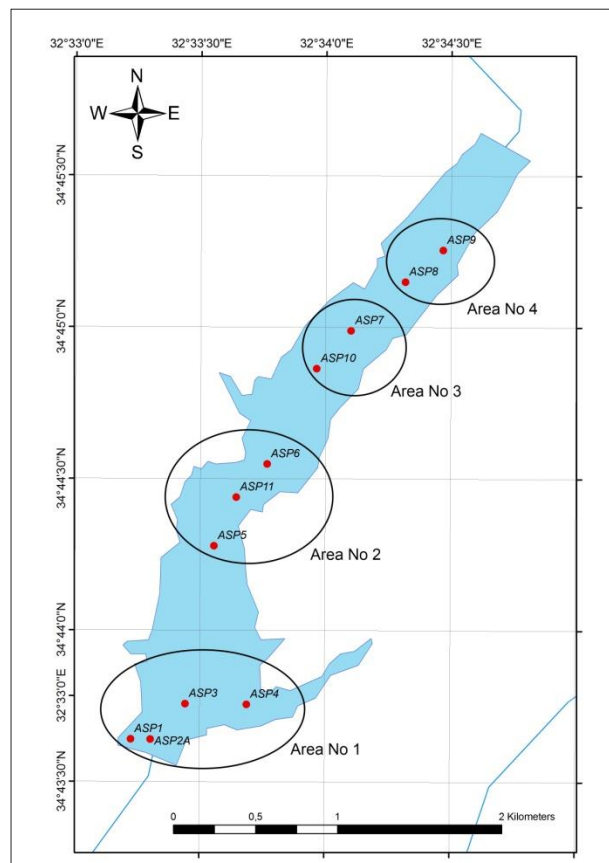


Figure 7. 3: Map of the sampling station network used during the field campaigns over Asprokremmos Reservoir - Distinguish areas referred to turbidity variations are indicated.

Comparing the turbidity values measured at the sampling points closer to the area where the Xeros River flows into the reservoir (Areas No. 4 to 3) to those distant to the inlet of the Xeros River (Areas No. 1 to 2), higher variations can be observed as the distance to the river inlet decreases. In Figure 7. 4 the two characteristic areas appearing extremely different water quality conditions are illustrated. The Outlet area is the area where water from Asprokremmos Reservoir is pumped to the treatment works through a 2.7 km long 600 mm diameter pipe which treats and delivers the water to the city of Paphos. The inlet area is the area where the Xeros River flows into the Reservoir resulting into higher turbidity values along the Reservoir since an amount of solid particles that are suspended in the water are carried into the Reservoir.

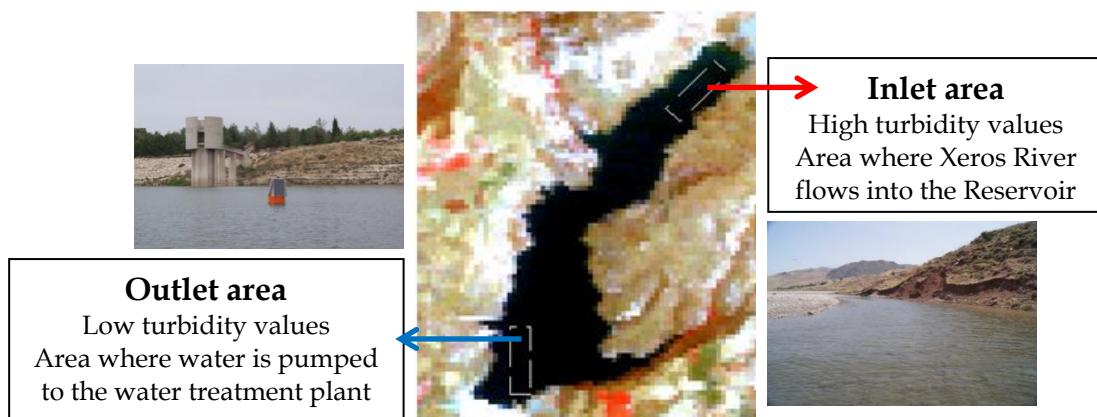
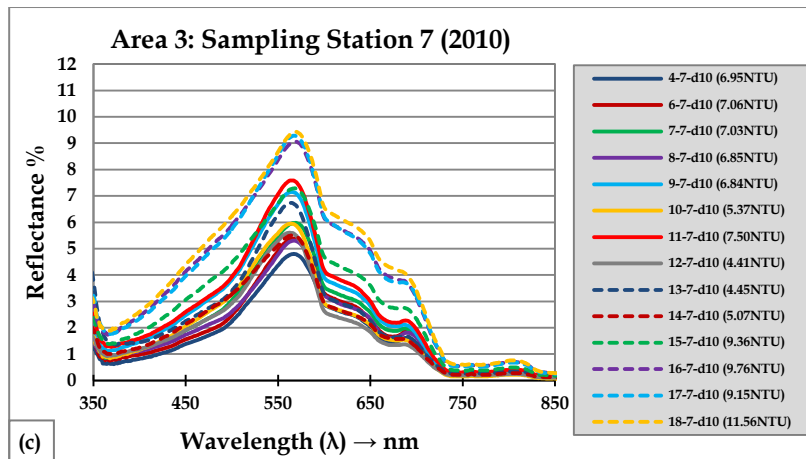
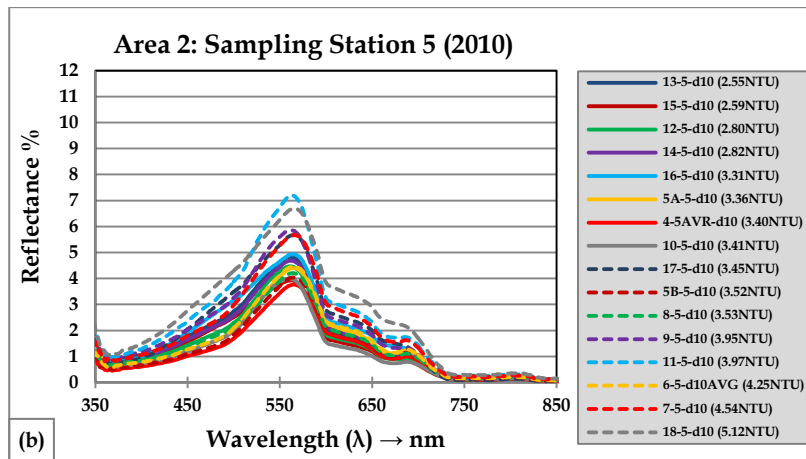
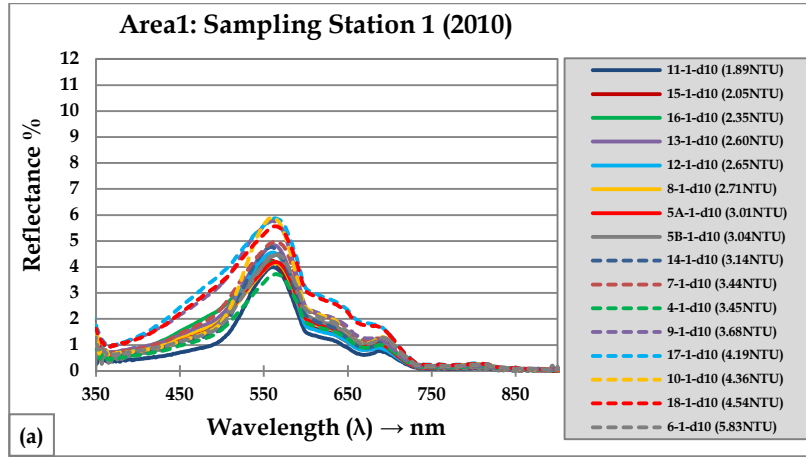


Figure 7. 4: Landsat TM Image focused in the area of Asprokremmos Reservoir pointed out the two study areas of the Reservoir; Inlet & Outlet.

Typical spectral signatures acquired from the two Areas appearing extreme turbidity values (Area 1 & Area 4) and Areas of mid-turbidity values (Area 2 & 3) are illustrated in Figure 7. 5(a-d). Examining the spectral signatures acquired over the Reservoir it has been indicated that sampling stations located in the same area appear similar patterns (12-9-8, 7-10, 6-5, and 1-2-3-4).



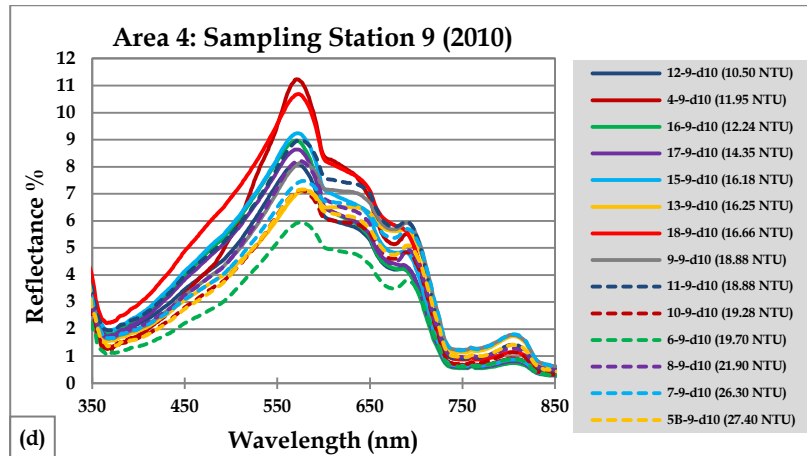


Figure 7. 5: Comparison of the spectral signatures corresponds to the Areas 1 to 4 of the Asprokremmos Reservoir.

The spectral signatures were processed in order to investigate the overall turbidity increasing trend over the Reservoir. The results of the spectral signatures analysis proved that for all the samplings campaigns:

- ❑ the highest reflectance values were observed for the areas appear the highest turbidity values which are referred to the sampling stations of the Area 4
- ❑ the lowest reflectance values were observed for the areas appear the lowest turbidity values which are referred to the sampling stations of the Area 1 and
- ❑ sampling stations located into the Areas 2 & 3 appear mid-values comparing to the extreme values of Areas 1 & 4 (see Figure 7. 6).

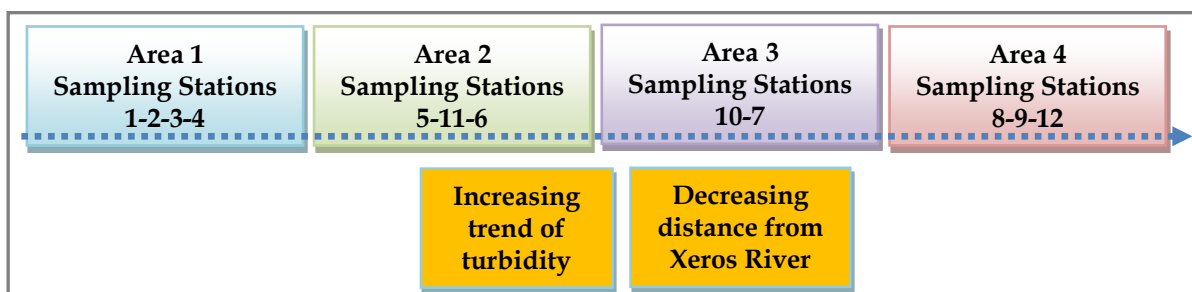


Figure 7. 6: Turbidity increasing trend across the Reservoir Areas.

Analysis of the reflectance curves been acquired over the Asprokremmos Reservoir have shown that two characteristic peaks are observed over all the examined sampling stations. A third peak is observed only for the sampling stations close to Xeros River.

1st peak: The analysis of the spectral signatures correspond to Sampling Station 2 appear a sharp peak at 540-560nm. In contrast, the spectral signatures of the Sampling Station 9 indicated that the peak corresponds to the same area of the spectrum tend to be broader and less specific. A slightly shifting to higher wavelengths is being observed (560-580nm) for this case, as well.

2nd peak: A second peak is observed for Sampling Station 2 at 660-680 nm and for Sampling Station 9 at 675-695nm (slight shifting in higher wavelength). Further, comparison of the reflectance values correspond to the two Sampling Stations have showed that reflectance values are about 7 times higher for Sampling Station 9 comparing to those of Sampling Station 2.

3rd peak: A third peak is observed at 790-810 nm only for the case of Sampling Station 9. This peak does not exist examining the spectral signatures referred to Sampling Station 2.

7.2.2 'Alyki'- Larnaca's Salt Lake (shallow lake - algal bloom observed)

Several interesting findings were extracted by the processing of the spectral signatures retrieved during the *in situ* campaigns in the Alyki Salt Lake, located in the city of Larnaca. This is mainly based on the different -weather conditions and -water status, observed over the study area during the field campaigns. The first campaign was performed when the Salt Lake was almost dry giving us the opportunity to study the water spectral characteristics over sampling points of different "dryness-level". At the first sampling station which is located near Tekkes Mosque, water level was very low and not adequate for collecting the spectral signature of the water; however, several spectroradiometric measurements were conducted over points with different dryness level. A characteristic example is illustrated in Figure 7. 7 where three different dryness-level can be recognized: (a)

points of high dryness - covered with a layer of salt; (b) points of lower dryness where the salt is not so visible and (c) deepest areas where water level exceeds 10cm.

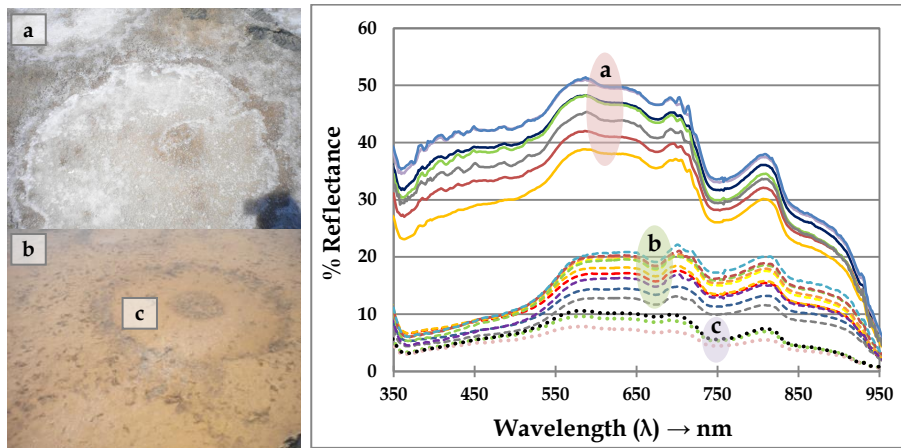


Figure 7. 7: Spectral signatures of Salt Lake (1st Sampling Campaign) where sampling points correspond to different dryness level were studied.

Moreover, additional field campaigns over the Salt Lake resulted in similar spectral signatures to those conducted over the ‘high-concentration’ of SS Sampling Station of the Reservoir (see Figure 7. 8). Referring to the 1st peak observed, the analysis of the spectral signatures revealed that as the concentration of the SS increases the peak in this area tend to be broader. Further, we can see that the same trend observed examining the spectral signatures of Asprokremmos Reservoir can be noticed for the Salt Lake as well; reflectance values increases with the increasing of the turbidity values. These results can validate our previous findings since for Sampling Station 2 we have a sharp peak at 540-560nm with relatively low reflectance values (up to 5%); for Sampling Station 9 the peak is broader and appears at 560-580nm with higher reflectance values (up to 11%) comparing to Station 2; and for the Salt Lake is tend to be broader covering a range from 550 to 570nm and having higher reflectance values (up to 17%) comparing to Station 9. The 2nd peak for Salt Lake is observed in the same area as the second peak for Sampling Station 9 at 675-695nm but is less sharp and less specific comparing to that of Sampling Station 9. Finally, the 3rd peak is observed at 780-810 nm and comparing to the one observed for the case of Sampling

Station 9 the reflectance values are higher, ranging from 0.5-1% for Sampling Station 9 and from 1-3% for the case of Salt Lake.

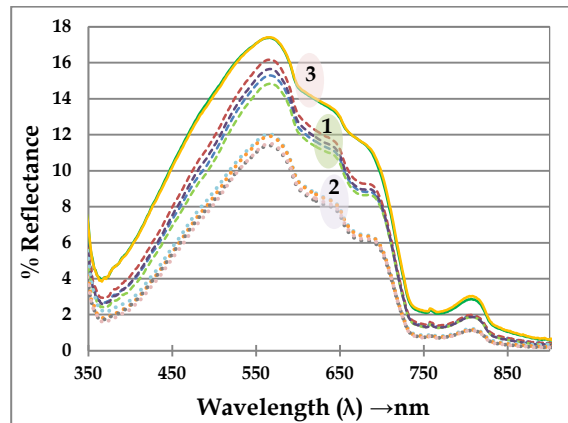


Figure 7. 8: Water’s spectral signatures acquired during 3 different sampling campaigns over the Salt Lake correspond to different turbidity levels (3: 29.30 NTU; 1: 18.42 NTU and 2: 11.90 NTU).

Moreover, during the 3rd sampling campaign an unusual algal bloom was observed at the sampling station located near Tekkes Mosque. The algal bloom has long been recognized as the result of importing nutrients, mainly as nitrogen and phosphorus. In Figure 7. 9 the ideal bloom conditions are shown. The most important factors controlling the growth and composition of algae are availability of nutrients, light and mixing conditions, the water residence time and temperature (Lawrence et al. 2000). Warm and calm weather coupled with an inflow of low salinity water and relatively high nutrient loads provide ideal conditions for blue-green algae to develop. Phytoplankton blooms are a natural occurrence in spring. Blooms can also occur in summer and fall when there is an increase in nutrients from natural sources such as wind-driven mixing of surface waters with deeper waters, or human sources, such as wastewater treatment plants.

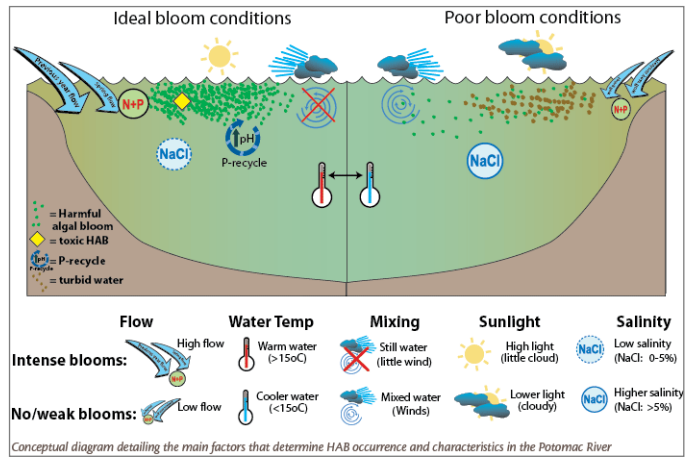


Figure 7. 9: Diagram of the ideal bloom conditions (Source: Ian.umces.edu 2005).

In Figure 7. 10(a), the spectral signatures collected during the 2nd and 3rd sampling campaigns regarding both the water body of the Salt Lake and the unusual algal bloom are presenting. Figure 7. 10(b) is focused on the spectral signatures retrieved at different depths below the water surface during the algal bloom.

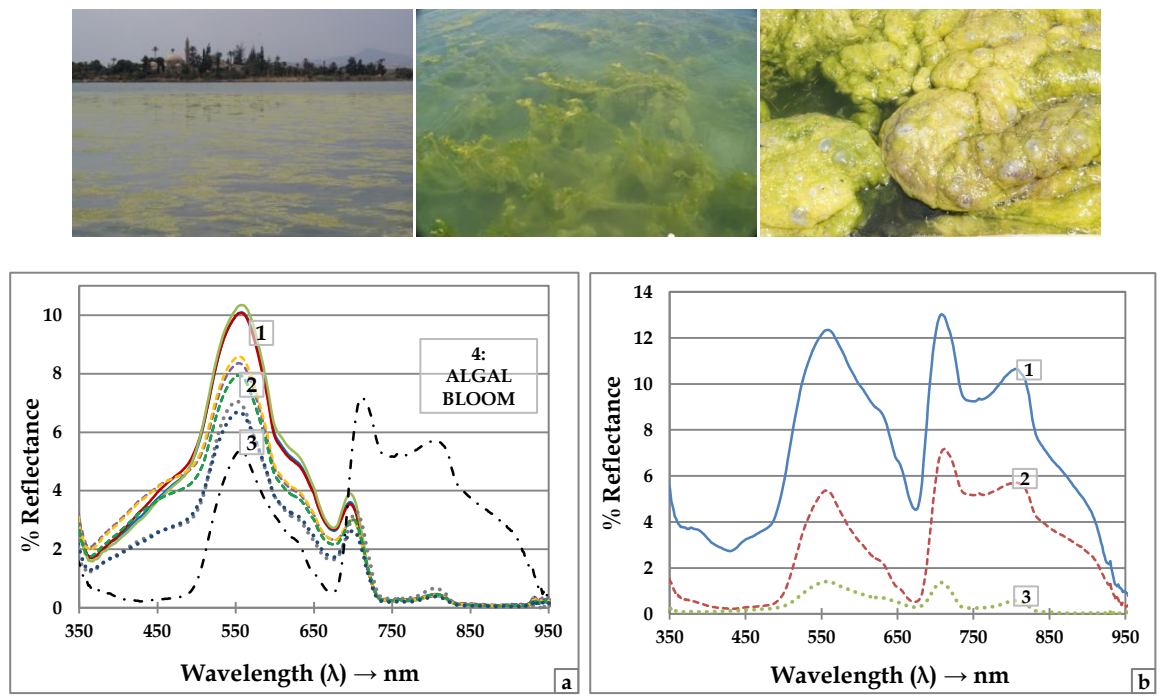


Figure 7. 10: Water's spectral signatures acquired during the 3rd Sampling campaign over the Salt Lake (a) correspond to different turbidity levels and to an algal bloom (1: 9.30 NTU;

2: 6.50 NTU, 3: 4.85 NTU and 4: Algal Bloom) and (b) representing the spectral signatures retrieved at different depths below the water surface during the algal bloom.

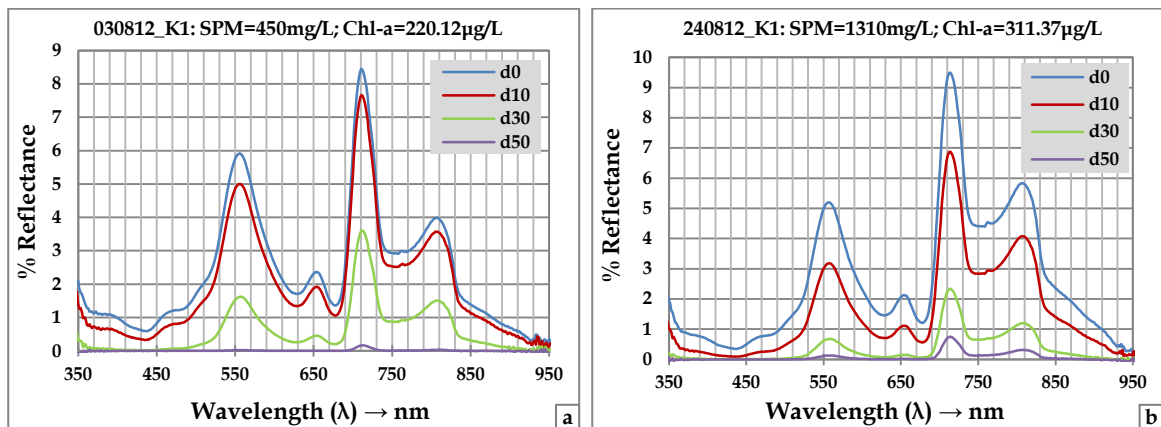
As shown in Figure 7. 10 the spectral signatures correspond to an algal bloom are very characteristic and differed in several areas of the spectrum comparing to those of waters. It is easy to notice that for wavelength up to 665nm, the patterns of the spectral signatures correspond to the algal bloom are similar to those of the water bodies; however, for longer wavelengths they differ significantly. A characteristic sharp peak centred at 710nm is observed due to the presence of chl-*a* in high concentration levels in the water column, appearing a high reflectance value. The peak near 700 nm in water reflectance spectra is most often used as a proxy for phytoplankton biomass in productive waters. Moreover, a variety of different algorithms aiming to quantify chl-*a*, have been developed and all are based on the properties of the peak near 700 nm. This peak is in the spectral range of minimal combined absorption of algae, inorganic suspended matter, DOM and water, and is shifted toward longer wavelengths as chl-*a* concentration increases (Gitelson 1992, 1993; Matthews and Boxall 1994; Vos et al. 1986; Zimba and Gitelson 2006). Absorption by water and its constituents (phytoplankton, CDOM) has minima in the wavelength range 700-720 nm that causes the peak in reflectance spectra of phytoplankton-rich waters (Kutser 2009). An additional broader peak is appeared ranged from 790-820nm as it was observed for the water bodies but this has significantly higher values of reflectance (6-10%) comparing to the water (1-3%).

7.2.3 Karla Lake (mesotrophic - eutrophic lake)

Some typical examples of the spectral signatures conducted over the mesotrophic - eutrophic Lake Karla located in Thessaly will be presented. Two typical examples acquired from the sampling station K1 during the summer (3rd & 24th of August 2012) when the highest temperatures are observed and which are characterised by the high concentration levels of chl-*a*, exceeding 200µg/L are given on the Figure 7. 11(a-b). Further, in Figure 7. 11(c) examples of spectral signatures correspond to

lower chl-*a* concentration (lower than 55 $\mu\text{g/L}$) are given as well aiming to compare the two cases. It is important to focused on the 3rd peak which is depended mainly on the concentration of chl-*a*.

It is apparent that four peaks appear to the spectral signatures of Lake Karla. The 1st peak is located at 550-570nm, the 2nd at 640-660nm, the 3rd at 690-720nm and the 4th at 790-820nm. As it is obvious looking at the examples of Figure 7. 11a-b the 3rd peak which is mainly influenced by the presence of chl-*a* is sharp and centred at 710nm for chl-*a*=220 $\mu\text{g/L}$ and at 715nm for chl-*a*=311 $\mu\text{g/L}$ and is becoming broader and slightly shifted to shorter wavelengths as the chl-*a* concentration decreases such as the example illustrated in Figure 7. 11c for chl-*a*≈40 $\mu\text{g/L}$ then the peak is centred at 700nm. Moreover, it is important to comment at the reflectance values being observed for the two cases examined since the first category appears reflectance values more than 8% in contrary to the second which appears reflectance values less than ≈6.5%.



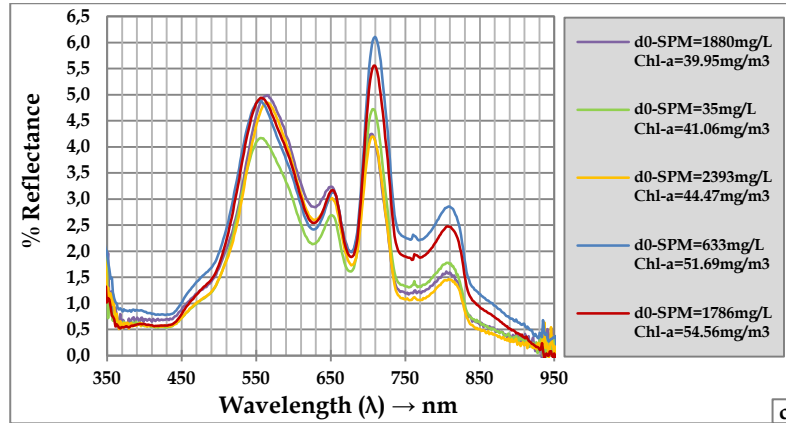


Figure 7. 11: Water's spectral signatures acquired during the Sampling campaigns over Lake Karla in Thessaly; (a-b) corresponds to high chl-*a* concentration - more than 200µg/L and (c) to lower chl-*a* concentration - less than 60µg/L.

7.2.4 Coastal Areas

Several spectral signatures obtained during the field campaign in coastal areas of Paphos and Limassol District areas in Cyprus are presented in Figure 7. 12. All the spectral signatures presented below refer to underwater spectroradiometric data acquired just below the water surface using a fibre optic probe. Examining these spectral characteristics it is obvious that some similarities can be recognised between (a) water bodies of different clarity such as SDD=3.2m and SDD=2.0m; (b) shallow coastal water bodies whose seabed consists of rocky or sandy materials; and (c) coastal water bodies whose seabed consists of rocks covered with seaweed or seaweed/algae. Referring to the first example (see Figure 7. 12a), the overall rule is that the reflectance increases as the clarity values increases, this phenomenon it is observed as well for the case of inland water bodies. The second example (see Figure 7. 12b) showed that rocky seabed coastal areas appear lower reflectance values comparing to sandy seabed areas since, in general, rocky materials are darkest than sandy surfaces resulting in higher absorbance values and as a result in lower reflectance values. Finally, the third example (see Figure 7. 12c) illustrates the spectral signatures obtained over areas covered with algae or seaweed. Both of the spectral signatures appear a characteristic peak centred at 690 to 720 nm which is

mainly influenced by the presence of chl-*a* concentration. The spectral signature corresponds to the rocky surface covered with seaweed appear lower reflectance values comparing to that of the sea grass meadows (seaweed/algae) in the characteristic area of determining chl-*a*. This can be attributed / explained to its lower chl-*a* concentration comparing to the areas fully covered by sea grass meadows.

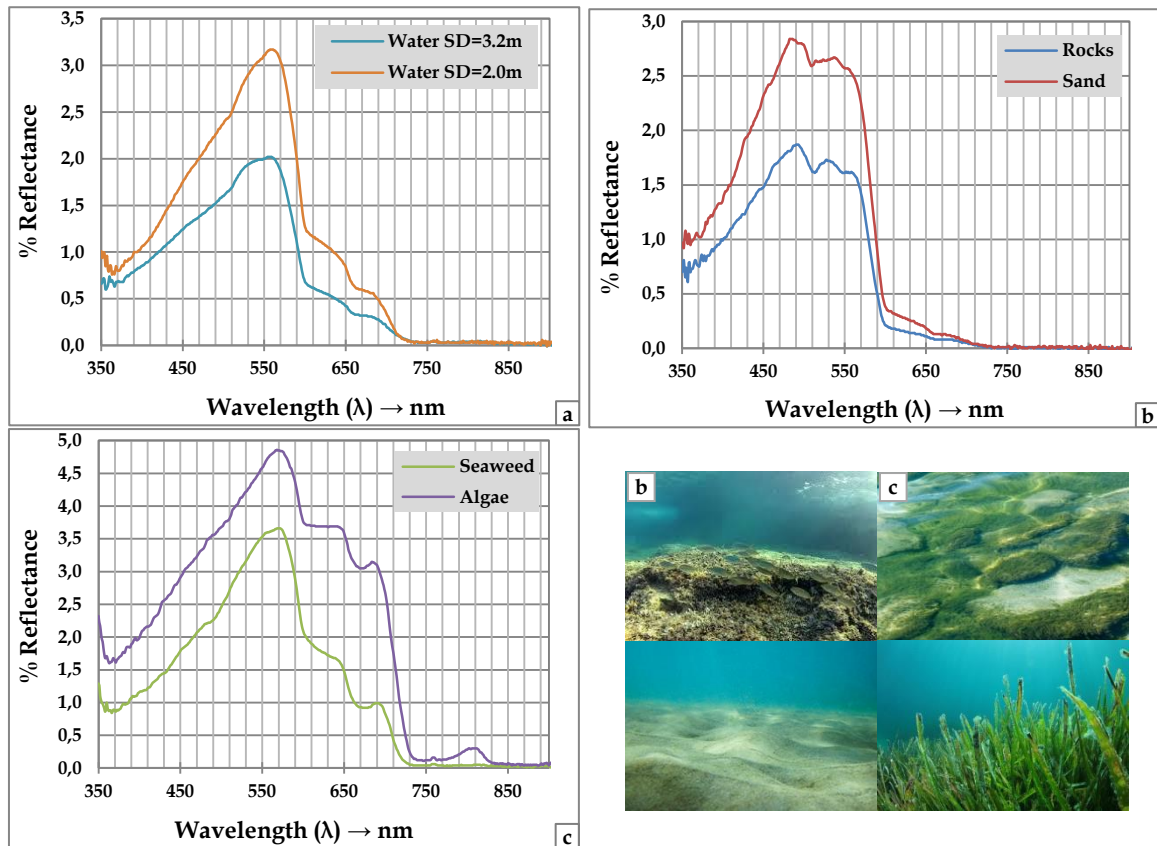


Figure 7.12: Water spectral signatures acquired during the Sampling campaigns over several coastal areas in Paphos and Limassol; (a) represents two examples of waters differ on suspended solids concentration; (b) corresponds to coastal water having different bottom reflections - rocks & sand; and (c) illustrates the spectral signatures correspond to rocky surfaces covered with seaweed and surfaces covered with seaweed / algae plants.

8 DISCUSSION AND CONCLUSIONS

In this chapter, the most important conclusions which have resulted from the PhD research of monitoring water quality over several Case-2 water bodies in Cyprus and Greece are described. For this implementation ground truth data (spectroradiometric and water quality) combined with remotely sensed data were used. The results have shown that remote sensing can be used as a supportive method for monitoring large surface Case-2 water bodies and improving significantly the availability of water quality data. A discussion regarding the results and their future application follows.

8.1 Conclusions

The review of similar studies presented in Chapter 2 showed that the use of remotely sensed data can significantly enhance the process of obtaining WQP of water bodies. Nowadays, a plethora of remote sensing sensors are available while a rapid development of space technology is observed. A trend to design new satellites aiming to improve existing applications or to develop new applications is observed.

This work is focused on the implementation of new water quality monitoring tools aiming to observe large water bodies on a systematic basis using a series of existing multispectral and hyperspectral satellite sensors. In this study, a novel approach to estimate turbidity, SDD and TSI has been applied and tested. Remotely sensed data along with field spectroradiometric and water quality measurements, statistical analysis and modelling techniques were analysed. All these procedures were combined in order to provide the basis for constructing the models that will be used to determine the values of WQP from satellite images. This has resulted in a large volume of satellite data that are currently available for free and can serve to stakeholders and decision makers of Water Authorities for improving water management in a national level.

Field spectroscopy is a very important step prior to the development and use of any satellite-based algorithm. It can provide useful information supporting both the pre-

processing of satellite images, in which ground truth data are used to evaluate the effectiveness of the applied atmospheric correction methods and the post-processing where ground measurements are used for the development of models aiming to estimate several WQP.

A three-year campaign for collecting in situ data was conducted. A field spectroradiometer equipped with a FO probe and a diffuser was used for acquiring the spectral signatures of several water bodies. A standard procedure for collecting these measurements which is analytically described in Chapter 3 was followed. Using fine resolution instruments – spectroradiometers – combining with field water quality observations can provide a valuable data set in order to identify the optimal spectral region for determining each of the parameter of interest. The mean “in-band” reflectance values correspond to each band of a sensor can be calculated by processing the available ground truth spectroradiometric data.

For the aim of this work spectroradiometric data were transformed into Landsat’s, MERIS’s and Chris-Proba’s bands ranging from the Visible to the Near-Infrared spectrum. These data were finally used in the modelling procedure aiming to retrieve the best predicting model for each sensor. Moreover, the effectiveness of several sensors to predict the water parameter of interest was compared. Based on our findings we can take a decision regarding the suitability of the available satellite images and further to propose the development of a new band covering a particular wavelength-range. The methodology applied for the three pre-mentioned satellite sensors can easily be adapted for other satellites. The use of field spectroradiometer can facilitate the procedure since it provides a ‘high-density’ spectrum providing reflectance data with a bandwidth of 1,5nm. This information can be utilized to calculate the reflectance values of different satellites’ bands by simple transformation, using the RSR filters given for each satellite.

Finally emphasis was given on the analysis of spectral signatures, and particularly in interpreting how certain optical properties of water such as the upwelling reflectance and the downwelling attenuation coefficient (k_d) can be correlated to the

corresponding WQP. Furthermore, the obtained spectral signatures can be used as reference spectral data-base in order to classify water bodies and determine their water quality characteristics.

8.2 Thesis Original Research Contribution

The thesis is providing an extensive reference spectral library covering a wide range of Case-2 water bodies including oligotrophic and eutrophic inland water bodies; a shallow salt-lake (algal-bloom) and several coastal areas. This is the first time that an extensive field campaign including a variety of Case-2 water bodies is conducted in the Mediterranean region. This innovative addition can assist to the scientific community to characterize and classify any water body based on its spectral information which can be retrieved from the single use of the available satellite data (see Chapter 7).

In addition, the thesis has provided an innovative algorithm which can be used on a systematic basis for estimating the TSI over large surface Case-2 water bodies in the Mediterranean region using remotely sensed data. For the development of this algorithm both spectroradiometric and SDD field data acquired during the field campaigns over different water bodies inland and coastal were processed in order to examine and retrieve the 'best-fit' algorithm. This algorithm is of great importance since it can be applied for a wide range of water bodies with different TSI values based on the Landsat's Band ratio 2:3. Correlation coefficient was found to be very high illustrating the strength of this model (see Chapter 5).

Through this PhD the best spectral regions for monitoring turbidity and SDD based on field data (extensive 3-years field campaign over the main study area of the Asprokremmos Reservoir) were identified. *In situ* data were processed and empirical models for both the turbidity and the SDD values have been developed using regression analysis, which had shown high coefficient of determination (R^2). Further, the field spectroradiometric data were processed aiming to predict the suitable

bands for monitoring turbidity and SDD using different satellite sensors such as Landsat, Envisat MERIS and Chris-Proba.

Aiming to test the derived algorithm, eight available Landsat-5 TM and Landsat-7 ETM+ satellite images which acquired at the same time with the field campaigns were processed and the correlation of the satellite derived comparing to the ground truth data was significant (see Chapter 4).

Finally, the downwelling diffuse attenuation coefficient (k_d) was calculated using the field spectroradiometric measurements obtained over the Reservoir in various depths below the water surface. k_d values were then correlated to the corresponding SDD and TSI and the waveband giving the best correlation was selected as the most suitable for this estimation (Chapter 6).

8.3 Discussion & Recommendations

The concentration of TSS in water bodies can be determined either by measuring the turbidity or the SDD. The values of these WQP are of vital importance for the WDD given that high values of TSS may cause damages to the filters of the pumping station sending the water from the Reservoir to the water treatment plant. Furthermore, these parameters are essential since they can become an indicator predicting either an unusual disposal of wastewater or any point pollution source flows into the reservoir area. Since Cyprus suffers from serious droughts, maintaining the reservoir water bodies in good condition is one of the highest priority national tasks and a key component in water resources management.

However, this is a demanding task to achieve by the Cyprus WDD since the island has more than 100 dams, 56 of which are included in the Register of the International Committee on Large Dams (ICOLD). The traditional way of water sampling and laboratory analysis is very time and labour consuming while also having the disadvantage of not being able to provide spatial monitoring since water samples collected during the field campaigns refers only to specific sampling stations over the large surface of the reservoirs. On the other hand, remote sensing, in addition to

reducing the high costs of sampling and laboratory analysis can also improve dramatically the temporal resolution of the obtainable data. It has the ability to provide information for a large number of reservoirs once or twice a month, depending on the availability of satellite images and the weather condition (cloud coverage). However, due to the good weather conditions in Cyprus the latter cannot be considered as a limitation for satellite images availability. Overall, remote sensing can provide a valuable tool for supporting the management of large inland water bodies providing the technology which will push towards sustainable water resources management.

All the above applications can become a very valuable water quality monitoring tool for the stakeholders, such as the Cyprus WDD for the continuous monitoring of the large number of reservoirs existing in Cyprus. All the field data can be further used to develop new algorithms based on the spectral resolution of any other satellite providing the opportunity to select satellites with different temporal and spatial resolution depending on the aim of the application and the availability of the satellite images.

Satellite data can provide spatially distributed estimates of SDD, TSI and turbidity enabling the stakeholders to act immediately in the case that an unexpected “threat” is detected. Furthermore additional field spectroradiometric data can be collected over several reservoirs in order to apply any necessary modification to the tested model. Finally, additional data regarding the WQP can be selected in a systematic basis through the development of a smart monitoring buoy system deployed with various sensors to support the calibration of the developed algorithms in ‘key point-stations’.

REFERENCES

- Agapiou, A., Hadjimitsis, D. G., Papoutsas, C., Alexakis, D. D., and Papadavid, G. (2011). "The Importance of accounting for atmospheric effects in the application of NDVI and interpretation of satellite imagery supporting archaeological research: The case studies of Palaepaphos and Nea Paphos sites in Cyprus." *Remote Sensing*, 3, 2605–2629.
- Alikas, K., and Reinart, A. (2008). "Validation of the MERIS products on large European lakes: Peipsi, Vanern and Vattern." *Hydrobiologia*, 599, 161–168.
- Alparslan, E., Aydoner, C., Tufekci, V., and Tufekci, H. (2007). "Water quality assessment at Omerli Dam using remote sensing techniques." *Environmental Monitoring and Assessment*, 135(1), 391–398.
- Alparslan, E., Coskun, H. G., and Alganci, U. (2010). "An Investigation on Water Quality of Darlik Dam Drinking Water using Satellite Images." *The Scientific World Journal*, 10, 1293–1306.
- Althuis, I. A., and Shimwell, S. (1995). "Modelling of Remote Sensing Reflectance Spectra for Suspended Matter Concentration Detection in Coastal Waters." *EARSel Advances in Remote Sensing*, 4((1 -IX)), 53–59.
- Álvarez-Robles, J. A., Zarazaga-Soria, F. J., Latre, M. Á., Béjar, R., and Muro-Medrano, P. R. (2007). "Water Quality Monitoring to Support the European Commission's Water Framework Directive Reporting Requirements." *Transactions in GIS*, 11(6), 835–847.
- Ammenber, P., Flink, P., Lindell, T., Pierson, D., and Strombeck, N. (2002). "Bio-optical Modelling Combined with Remote Sensing to Assess Water Quality." *International Journal of Remote Sensing*, 23, 1621–1638.
- Anderson, K., and Milton, E. J. (2006). "On a temporal stability of ground calibration targets: Implications for the reproducibility of remote sensing methodologies." *International Journal of Remote Sensing*, 27(16), 3365–3374.
- Anderson, K., Milton, E. J., and Rollin, E. M. (2006). "Calibration of dual-beam spectroradiometric data." *International Journal of Remote Sensing*, 27(5), 975–986.
- Araus, J. L. (2004). "The problems of sustainable water use in the Mediterranean and research requirements for agriculture." *Annals of Applied Biology*, 144(3), 259–272.
- Arenz, R. F., Lewis, W. M., and Saunders, J. F. (1996). "Determination of chlorophyll and dissolved organic carbon from reflectance data for Colorado reservoirs." *International Journal of Remote Sensing*, 17(8), 1547–1566.
- Attila, J., Koponen, S., Kallio, K., Lindfors, A., Kaitala, S., and Ylostalo, P. (2013). "MERIS Case II Water Processor Comparison on Coastal Sites of the Northern Baltic Sea." *Remote Sensing of Environment*, 128, 138–149.
- Baban, S. M. J. (1996). "Trophic classification and ecosystem checking of lakes using remotely sensed information." *Hydrological Sciences Journal*, 41(6), 939–957.
- Baban, S. M. J. (1999). "Use of remote sensing and geographical information systems in developing lake management strategies." *Hydrobiologia*, 395/396, 211–226.
- Beisl, U. (2001). *Correction of bidirectional effects in imaging spectrometer data. Remote Sensing Series*, Remote Sensing Laboratories, University of Zurich, Zurich, Switzerland.
- Bhatti, A., Suttinon, P., and Nasu, S. (2011). "Monitoring Spatial and Temporal Variability of Suspended Sediment in Indus River by Means of Remotely Sensed Data." *Annals of GIS*, 17(2), 125–134.

- Binding, C. E., Bowers, D. G., and Mitchelson-Jacob, E. G. (2003). "An algorithm for the retrieval of suspended sediment concentrations in the Irish Sea from SeaWiFS ocean colour satellite imagery." *International Journal of Remote Sensing*, 24(19), 3791–3806.
- Binding, C. E., Bowers, D. G., and Mitchelson-Jacob, E. G. (2005). "Estimating suspended sediment concentrations from ocean colour measurements in moderately turbid waters; the impact of variable particle scattering properties." *Remote Sensing of Environment*, 94, 373–383.
- Birk, S., and Hering, D. (2006). "Direct comparison of assessment methods using benthic macroinvertebrates: a contribution to the EU Water Framework Directive intercalibration exercise." *Hydrobiologia*, 566, 401–415.
- Borja, Á., Galparsoro, I., Solaun, O., Muxika, I., Tello, E. M., Uriarte, A., and Valencia, V. (2006). "The European Water Framework Directive and the DPSIR, a methodological approach to assess the risk of failing to achieve good ecological status." *Estuarine, Coastal and Shelf Science*, 66(1-2), 84–96.
- Bresciani, M., Adamo, M., De Carolis, G., Matta, E., Pasquariello, G., Vaiciute, D., and Giardino, C. (2014). "Monitoring blooms and surface accumulation of cyanobacteria in the Curonian Lagoon by combining MERIS and ASAR data." *Remote Sensing of Environment*, 146, 124–135.
- Bricaud, A., Morel, A., and Prieur, L. (1981). "Absorption by dissolved organic matter of the sea (yellow substance) in the UV and visible domains." *Limnology and Oceanography*, 26(1), 43–53.
- Bruegge, C., Chrien, N., and Haner, D. (2001). "A Spectralon BRF data base for MISR calibration applications." *Remote Sensing of Environment*, 76, 354–366.
- Buiteveld, H., Hakvoort, J. H. M., and M. Donze. (1994). "The optical properties of pure water." *Proc. SPIE 2258, Ocean Optics XII*, J. S. Jaffe, ed., 174–183.
- Büttner, G., Korándi, M., Gyömörei, A., Köte, Z., and Szabó, G. (1987). "Satellite remote sensing of inland waters." *Acta Astronautica*, 15(6/7), 305–311.
- Carbo, P., Krom, M., Homoky, W., Benning, L., and Herut, B. (2005). "Impact of atmospheric deposition on N and P geochemistry in the southeastern Levantine basin." *DEEP-SEA RES PT II*, 52, 3041–3053.
- Carlson, R. E. (1977). "A trophic state index for lakes." *Limnology and Oceanography*, 22(2), 361–369.
- Carr, G. M., and Neary, J. P. (2008). *Water Quality for Ecosystem and Human Health*.
- Carrick, H. J., Worth, D., and Marshall, M. L. (1994). "The Influence of Water Circulation on Chlorophyll-turbidity Relationships in Lake Okeechobee as Determined by Remote Sensing." *Journal of Plankton Research*, 16, pp. 1117–1135.
- Chavez, P. S. (1996). "Image-based Atmospheric Corrections—Revisited and Improved." *Photogrammetric Engineering and Remote Sensing*, 62, 1025–1036.
- Chen, Q., Zhang, Y., Ekroos, A., and Hallikainen, M. (2004a). "The role of remote sensing technology in the EU water framework directive (WFD)." *Environmental Science & Policy*, 7(4), 267–276.
- Chen, Q., Zhang, Y., Ekroos, A., and Hallikainen, M. (2004b). "The role of remote sensing technology in the EU water framework directive (WFD)." *Environmental Science & Policy*, 7(4), 267–276.
- Chen, X., Vierling, L., and Deering, D. (2005). "A Simple and Effective Radiometric Correction Method to Improve Landscape Change Detection Across Sensors and Across Time." *Remote Sensing of Environment*, 98, 63–79.
- Chen, Z., Hu, C., Muller-Karger, F. E., and Luther, M. E. (2010). "Short-term Variability of Suspended Sediment and Phytoplankton in Tampa Bay, Florida: Observations from a Coastal Oceanographic Tower and Ocean Color Satellites." *Estuarine, Coastal and Shelf Science*, 89(1), 62–72.

- Coble, P., Hu, C., Gould, R. W. J., Chang, G., and Wood, A. M. (2004). "Colored Dissolved Organic Matter in the Coastal Ocean: An Optical Tool for Coastal Zone Environmental Assessment and Management." *Oceanography*, 17(2), 50–59.
- Dall'Olmo, G., and Gitelson, A. A. (2005). "Effect of bio-optical parameter variability and uncertainties in reflectance measurements on the remote estimation of chlorophyll-a concentration in turbid productive waters: modeling results." *Applied optics*, 44(3), 412–422.
- Dekker, A. G. (1993). *Detection of optical water quality parameters for eutrophic waters by high resolution remote sensing*.
- Dekker, A. G., Malthus, T. J. M., and Hoogenboom, H. J. (1994). "Quantitative Determination of Chlorophyll-a, Cyanophycocyanin, Seston Dry Weight, Secchi Depth Transparency and Vertical Attenuation Coefficient in Eutrophic Surface Waters by Airborne Imaging Spectrometry." *Proceedings of the First International Airborne Remote Sensing Conference I*, Strasbourg, France, pp.141–152.
- Dekker, A. G., Malthus, T. J. M., and Hoogenboom, H. J. (1995). "The remote sensing of inland water quality." *Advances in Environmental Remote Sensing* (Danson, F.M. and Plummer, E.S., Eds.), Chichester, U.K., John Wiley & Sons, 123–142.
- Dekker, A. G., Malthus, T. J., and Seyhan, E. (1991). "Quantitative modeling of inland water quality for high-resolution MSS systems." *IEEE Transactions on Geoscience and Remote Sensing*, 29, 89–95.
- Dekker, A. G., and S. W. M., P. (1993). "The use of the Thematic Mapper for the analysis of eutrophic lakes: A case study in the Netherlands." *International Journal of Remote Sensing*, 14, 799–821.
- Dekker, A. G., Vos, R. J., and Peters, S. W. M. (2002). "Analytical Algorithms for Lake Water TSM Estimation for Retrospective Analyses of TM and SPOT Sensor Data." *International Journal of Remote Sensing*, 23, 15–35.
- Dekker, A. G., Zamurović-Nenad, Ž., Hoogenboom, H. J., and Peters, S. W. M. (1996). "Remote sensing, ecological water quality modelling and in situ measurements: a case study in shallow lakes." *Hydrological Sciences Journal*, 41(4), 531–547.
- Delipetrou, P., Makhzoumi, J., Dimopoulos, P., and Georghiou, K. (2008). "Cyprus." *Mediterranean Island Landscapes*, I. N. et al. Vogiatzakis, ed., Springer Science + Business Media B. V., 170–203.
- Demetropoulos, A. (2006). *Sustainability and Protection of Freshwater Ecosystems in Cyprus*. Nicosia, Cyprus.
- Demetropoulos, A. (2002). *Cyprus National Report for the Strategic Action Plan for the Conservation of Marine and Coastal Biological Diversity in the Mediterranean (SAP BIO)*. RAC/SPA.
- Department of Environment. (2010). *Cyprus*. Nicosia, Cyprus.
- Dewider, K., and Khedr, A. (2001). "Water quality assessment with simultaneous Landsat-5 TM at Manzala Lagoon, Egypt." *Hydrobiologia*, 457, 49–58.
- Doron, M., Belanger, S., Doxaran, D., and Babin, M. (2011). "Spectral Variations in the Near-infrared Ocean Reflectance." *Remote Sensing of Environment*.
- Doxaran, D., Froidefond, J.-M., Lavender, S., and Castaing, P. (2002). "Spectral signature of highly turbid waters. Application with SPOT data to quantify suspended particulate matter concentrations." *Remote Sensing of Environment*, 81, 149–161.
- Doxaran, D., Ruddick, K., McKee, D., Gentili, B., Tailliez, D., Chami, M., and Babin, M. (2009). "2009_Doxaran et al." *Limnology and Oceanography*, 54, pp.1257–1271.
- Duggin, M. J. (1980). "The field measurement of reflectance factors." *Photogrammetric Engineering & Remote Sensing*, 46, 643–647.

- Duggin, M. J. (1981). "Simultaneous measurement of irradiance and reflected radiance in field determination and reflected radiance in field determination of spectral reflectance." *Applied optics*, 20(38), 16–38.
- Duggin, M. J., and Philipson, W. R. (1982). "1982_Duggin and Philipson." *Applied optics*, 21(15), pp. 2833–2840.
- Dworak, T., Gonzalez, C., Laaser, C., and Interwies, E. (2005). "The need for new monitoring tools to implement the WFD." *Environmental Science & Policy*, 8, 301–306.
- Econews.gr. (2009). "Dead fish were found in the drainage ditch near Lake Karla."
- EEA. (2009a). *Water resources across Europe - confronting water scarcity and drought*. Copenhagen.
- EEA. (2009b). *Water resources across Europe – confronting water scarcity and drought. EEA Report 2/2009*. (R. Collins, P. Kristensen, and N. Thyssen, eds.), Copenhagen.
- EEA. (2010). "Use of freshwater resources." <http://www.eea.europa.eu/data-and-maps/indicators/use-of-freshwater-resources/use-of-freshwater-resources-assessment-2>.
- EEA. (2012). *Towards efficient use of water resources in Europe*. EEA Report/ No 1/2012.
- Ekericin, S. (2007). "Water Quality Retrievals from High Resolution Ikonos Multispectral Imagery: A case Study in Istanbul, Turkey." *Water, Air and Soil Pollution*, 183((1-4)), 239–251.
- Eurostat. (2010). "Eurostat_2010." <http://appsso.eurostat.ec.europa.eu/nui/show.do>.
- Eurostat European Commission. (2010). *Environmental statistics and accounts in Europe*.
- Flink, P., Lindell, T., and Ostlund, C. (2001). "Statistical analysis of hyperspectral data from two Swedish lakes." *The Science of the total environment*, 268, 155–169.
- Froidefond, J.-M., Gardel, L., Guiral, D., Parra, M., and Ternon, J.-F. (2002). "Spectral remote sensing reflectances of coastal waters in French Guiana under the Amazon influence." *Remote Sensing of Environment*, 80(2), 225–232.
- Fuller, L. M., Aichele, S. S., and Minnerick, R. J. (2002). *Predicting Water Quality by Relating Secchi-Disk Transparency and Chlorophyll a Measurements to Satellite Imagery for Michigan Inland Lakes, August 2002*.
- Fuller, L. M., Jodoin, R. S., and Minnerick, R. J. (2011). "Predicting lake trophic state by relating Secchi-disk transparency measurements to Landsat-satellite imagery for Michigan inland lakes, 2003–05 and 2007–08: U.S." 36.
- García-Ruiz, J. M., López-Moreno, J. I., Vicente-Serrano, S. M., Lasanta-Martínez, T., and Beguería, S. (2011). "Mediterranean water resources in a global change scenario." *Earth-Science Reviews*, Elsevier B.V., 105(3-4), 121–139.
- GEO. (2007). *GEO Final Report. Inland and Nearshore Coastal Water Quality Remote Sensing Workshop*. Geneva, Switzerland.
- Giardino, C., Brando, V. E., Dekker, A. G., Strömbeck, N., and Candiani, G. (2007). "Assessment of water quality in Lake Garda (Italy) using Hyperion." *Remote Sensing of Environment*, 109(2), 183–195.
- Gitelson, A. (1992). "The peak near 700 nm on reflectance spectra of algae and water: relationships of its magnitude and position with chlorophyll concentration." *International Journal of Remote Sensing*, 13(17), 3367–3373.
- Gitelson, A. (1993). "Algorithms for remote sensing of phytoplankton pigments in inland waters." *Advances in Space Research*, 13(5), (5)197–(5)201.
- Gitelson, A. A., Dall’Olmo, G., Moses, W., Rundquist, D. C., Barrow, T., Fisher, T. R., Gurlin, D., and Holz, J. (2008). "A simple semi-analytical model for remote estimation of chlorophyll-a in turbid waters: Validation." *Remote Sensing of Environment*, 112(9), 3582–3593.

- Gitelson, A. A., Schalles, J. F., and Hladik, C. M. (2007). "Remote Chlorophyll-a Retrieval in Turbid, Productive Estuaries: Chesapeake Bay Case Study." *Remote Sensing of Environment*, 109, 464–472.
- Gitelson, A. A., Stark, R., Grits, U., Rundquist, D., Kaufman, Y., and Derry, D. (2002). "Vegetation and soil lines in visible spectral space: a concept and technique for remote estimation of vegetation fraction." *International Journal of Remote Sensing*, 23(13), 2537–2562.
- Gitelson, A., Mayo, M., Yacobi, Y. Z., Parparov, A., and Berman, T. (1994). "The use of high-spectral-resolution radiometer data for detection of low chlorophyll concentrations in Lake Kinneret." *Journal of Plankton Research*, 16(8), 993–1002.
- Gitelson, A., Szilagyi, F., and Mittenzwey, K.-H. (1993). "Improving quantitative remote sensing for monitoring of inland water quality." *Water Research*, 27(7), 1185–1194.
- Gons, H. J., Ebert, J., and Kromkamp, J. (1998). "Optical teledetection of the vertical attenuation coefficient for downward quantum irradiance of photosynthetically available radiation in turbid inland waters." *Aquatic Ecology*, 31, 299–311.
- Gordon, H. R., and Morel, A. (1983). *Remote Assessment of Ocean Color for Interpretation of Satellite Visible Imagery: A Review*. Springer-Verlag, New York.
- Gordon, R., Brown, O. B., Evans, H., Brown, W., Smith, C., Baker, K., and Clark, D. K. (1988). "A semianalytical radiance model of ocean color." *Journal of Geophysical Research*, 93(D9), 10909–10924.
- Hadjichristophorou, M. (2004). "The Larnaca Salt Lakes. Information leaflet of the Department of Fisheries and Marine Research." Ministry of Agriculture Natural Resources and Environment., Nicosia, Cyprus.
- Hadjichristophorou, M. (2008). *Lead shot at Larnaca Salt Lake - Assessment and Restoration Activities*. Department of Fisheries and Marine Research (DFMR), Nicosia, Cyprus.
- Hadjimitsis, D., and Clayton, C. (2011). "Field Spectroscopy for Assisting Water Quality Monitoring and Assessment in Water Treatment Reservoirs Using Atmospheric Corrected Satellite Remotely Sensed Imagery." *Remote Sensing*, 3(12), 362–377.
- Hadjimitsis, D. G. (2008). "Description of a new method for retrieving the aerosol optical thickness from satellite remotely sensed imagery using the maximum contrast value and darkest pixel approach." *Transactions in GIS*, 12(5), 633–644.
- Hadjimitsis, D. G., Clayton, C. R. I., and Hope, V. S. (2004). "An assessment of the effectiveness of atmospheric correction algorithms through the remote sensing of some reservoirs." *International Journal of Remote Sensing*, 25(18), 3651–3674.
- Hadjimitsis, D. G., Clayton, C. R. I., and Retalis, A. (2003). "Darkest pixel atmospheric correction algorithm: a revised procedure for environmental applications of satellite remotely sensed imagery." *Proceedings 10th International Symposium on Remote Sensing*, NASA, SPIE Conference, Barcelona, Spain, 414.
- Hadjimitsis, D. G., Clayton, C., and Toullos, L. (2010). "Retrieving visibility values using satellite remote sensing data." *Physics and Chemistry of the Earth, Parts A/B/C*, Elsevier Ltd, 35(1-2), 121–124.
- Hadjimitsis, D. G., Hadjimitsis, M. G., Clayton, C. R. I., and Clarke, B. (2006). "Determination of Turbidity in Kourris Dam in Cyprus Utilizing Landsat TM Remotely Sensed Data." *Water Resources Management: An International Journal*, 20(3), 449–465.
- Hadjimitsis, D. G., Hadjimitsis, M. G., Toullos, L., and Clayton, C. (2010). "Use of space technology for assisting water quality assessment and monitoring of inland water bodies." *Physics and Chemistry of the Earth, Parts A/B/C*, 35(1-2), 115–120.
- Hakvoort, H., de Haan, J., Jordans, R., Vos, R., Peters, S., and Rijkeboer, M. (2002). "Towards airborne remote sensing of water quality in The Netherlands – validation and error analysis." *ISPRS Journal of Photogrammetry and Remote Sensing*, 57(3), 171–183.

- Hall, D. O., and Rao, K. K. (1987). *Photosynthesis. New studies in biology.* (M. Baltimore and E. Arnold, eds.), London.
- Hamdy, A., Abu-Zeid, M., and Lacirignola, C. (1995). "Water Crisis in the Mediterranean: Agricultural Water Demand Management." *Water International*, 20(4), 176–187.
- Han, L. (1997). "Spectral reflectance with varying suspended sediment concentrations in clear and algae-laden waters." *Photogrammetric Engineering and Remote Sensing*, 63(6), 701–705.
- Han, L., and Rundquist, D. C. (1997). "Comparison of NIR/RED ratio and first derivative of reflectance in estimating algal-chlorophyll concentration: A case study in a turbid reservoir." *Remote Sensing of Environment*, 62(3), 253–261.
- Härmä, P., Vepsäläinen, J., Hannonen, T., Pyhälähti, T., Kämäri, J., Kallio, K., Eloheimo, K., and Koponen, S. (2001). "Detection of water quality using simulated satellite data and semi-empirical algorithms in Finland." *Science of The Total Environment*, 268(1-3), 107–121.
- Harrington, J. a, Schiebe, F. R., and Nix, J. F. (1992). "Remote sensing of Lake Chicot, Arkansas: Monitoring suspended sediments, turbidity, and Secchi depth with Landsat MSS data." *Remote Sensing of Environment*, 39(1), 15–27.
- Heim, B. (2005). "Qualitative and Quantitative Analyses of Lake Baikal ' s Surface-Waters Using Ocean Colour Satellite Data (SeaWiFS)." University of Potsdam.
- Hellweger, F. L., Schlosser, P., Lall, U., and Weissel, J. K. (2004). "Use of satellite imagery for water quality studies in New York Harbor." *Estuarine, Coastal and Shelf Science*, 61(3), 437–448.
- Herut, B., Tibor, G., Yacobi, Y. Z., and Kress, N. (1999). "Synoptic measurements of chlorophyll-a and suspended particulate matter in a transitional zone from polluted to clean seawater utilizing airborne remote sensing and ground measurements, Haifa Bay (SE Mediterranean)." *Marine Pollution Bulletin*, 38(9), 762–772.
- Horne, A. J., and Goldman, C. R. (1994). *Limnology.* McGraw Hill, New York.
- Howarth, R., Anderson, D., Cloern, J., Elfring, C., Hopkinson, C., Lapointe, B., Malone, T., Marcus, N., McGlathery, K., Sharpley, A., and Walker, D. (2000). *Nutrient Pollution of Coastal Rivers, Bays, and Seas. Issues in Ecology.*
- Hu, C., Muller-Karger, F. E., Taylor, C. J., Carder, K. L., Kelble, C., Johns, E., and Heil, C. A. (2005). "Red Tide Detection and Tracing using MODIS Fluorescence Data: A Regional Example in SW Florida Coastal Waters." *Remote Sensing of Environment*, 97, 311 – 321.
- Huang, G. H., and Xia, J. (2001). "Barriers to sustainable water-quality management." *Journal of Environmental Management*, 61(1), 1–23.
- Hudson, S. J., Moore, G. F., Bale, A. J., Dyer, K. R., and Aitken, J. (n.d.). "An operational approach to determining suspended sediment distributions in the Humber estuary by airborne multi-spectral imagery." *Proceedings of the First Airborne Remote Sensing Conference and Exhibition*, Strasbourg, France.
- Hueni, a., Nieke, J., Schopfer, J., Kneubühler, M., and Itten, K. I. (2009). "The spectral database SPECCHIO for improved long-term usability and data sharing." *Computers and Geosciences*, 35(3), 557–565.
- Iacovides, I. (2011). "Water Resources in Cyprus: Endowments and Water Management Practices." *Water Resources Allocation Policy and Socioeconomic Issues in Cyprus*, P. Koundouri, ed., Springer, 11–22.
- Ian.umces.edu. (2005). "Environmental conditions that lead to harmful algal blooms (HABs)." *Integration & Application Network. University of Matyland. Center for Envoronmental Science*, <<http://ian.umces.edu/imagelibrary/displayimage-7038.html>>.
- Iglesias, A., Garrote, L., Flores, F., and Moneo, M. (2007). "Challenges to manage the risk of water scarcity and climate change in the Mediterranean." *Water Resources Management*, 21(5), 775–788.

- Iglesias, A., Rosenzweig, C., and Pereira, D. (2000). "Agricultural impacts of climate change in Spain: developing tools for a spatial analysis." *Global Environmental Change*, 10(1), 69–80.
- IGOS. (2006). *IGOS A Coastal Theme for the IGOS Partnership – for the Monitoring of our Environment from Space and from Earth 2006*. Paris.
- IOCCG. (2000). *Remote Sensing of Ocean Colour in Coastal, and Other Optically-Complex, Waters. Reports of the International Ocean-Colour Coordinating Group*, Dartmouth, Canada.
- IPCC. (2001). "Intergovernmental Panel on Climate Change. Climate change 2001: impacts, adaptation and vulnerability." Cambridge University Press, Cambridge.
- Irvine, K. (2004). "Classifying ecological status under the European Water Framework Directive: The need for monitoring to account for natural variability." *Aquatic Conservation: Marine and Freshwater Ecosystems*, 14(2), 107–112.
- Jackson, R. D., Clarke, T. R., and Moran, M. S. (1992). "Bi-directional calibration results for 11 Spectralon and 16 BASO4 reference reflectance panels." *Remote Sensing of Environment*, 40, 231–239.
- Jerlov, N. G. (1968). *Optical Oceanography*. American Elsevier Oceanography Series 5, New York.
- Jerlov, N. G. (1976). *Marine Optics*. Elsevier, Amsterdam, The Netherlands.
- Jupp, D. L. B., Kirk, J. T. ., and Harris, G. P. (1994). "Detection, identification and mapping of cyanobacteria: Using remote sensing to measure the optical water quality of turbid inland waters." *Australian Journal of Marine Freshwater Research*, 45, 801–828.
- Kaiser, M. F., Aboulela, H., Serehy, H. E., and Edin, H. E. (2010). "Spectral Enhancement of SPOT Imagery Data to Assess Marine Pollution Near Port Said, Egypt." *International Journal of Remote Sensing*, 31(7), 1753–1764.
- Kallio, K., Kutser, T., Hannonen, T., Koponen, S., Pulliainen, J., Vepsäläinen, J., and Pyhälä, T. (2001). "Retrieval of water quality variables from airborne spectrometry of various lakes types in different seasons." *The Science of the total environment*, 268(1-3), 59–77.
- Khorram, S., Cheshire, H., Geraci, A. L., and Rosa, G. L. (1991). "Water Quality Mapping of Augusta Bay, Italy from Landsat-TM Data." *International Journal of Remote Sensing*, 12(4), 803–808.
- Kirk, J. T. (1994). "Estimation of the absorption and the scattering coefficients of natural waters by use of underwater irradiance measurements." *Applied optics*, 33(15), 3276–3278.
- Kirk, J. T. O. (1983). "Light and photosynthesis in aquatic ecosystems." (1), 1–5.
- Kirk, J. T. O. (1984). "Attenuation of solar radiation in scattering-absorbing waters: a simplified procedure for its calculation." *Applied optics*, 23(21), 3737–3739.
- Kirk, J. T. O. (1994). "Characteristics of the light field in highly turbid waters: A Monte Carlo study." *Limnology and Oceanography*, 39(3), 702–706.
- Kishino, M., Tanaka, A., and Ishizaka, J. (2005). "Retrieval of Chlorophyll a, suspended solids, and colored dissolved organic matter in Tokyo Bay using ASTER data." *Remote Sensing of Environment*, 99(1-2), 66–74.
- Kloiber, S. M., Anderle, T., Brezonik, P. L., Olmanson, L. G., Bauer, M. E., and Brown, D. A. (2000). "Trophic state assessment of lakes in the Twin Cities (Minnesota, USA) region by satellite imagery." *Arch. Hydrobiol. Spec. Issues. Advanc. Limnol.*, 55, 137–151.
- Kloiber, S. M., Brezonik, P. L., Olmanson, L. G., and Bauer, M. E. (2002). "A procedure for regional lake water clarity assessment using Landsat multispectral data." *Remote Sensing of Environment*, 82(1), 38–47.
- Knight, J. F., and Voth, M. L. (2012). "Application of MODIS Imagery for Intra-Annual Water Clarity Assessment of Minnesota Lakes." *Remote Sensing*, 4, 2181–2198.

- Koenings, J. P., and Edmundson, J. a. (1991). "Secchi disk and photometer estimates of light regimes in Alaskan lakes: Effects of yellow color and turbidity." *Limnology and Oceanography*, 36(1), 91-105.
- Kokkinos, K., and Mylopoulos, N. (2007). "The Lake Karla Basin in Thessaly, Greece." *2nd OpenMI-LIFE Workshop*, CEH, Wallingford, UK.
- Koponen, S. (2006). *Remote sensing of water quality for Finnish lakes and coastal areas. Development.*
- Koponen, S., Pulliainen, J., Kallio, K., and Hallikainen, M. (2002). "Lake water quality classification with airborne hyperspectral spectrometer and simulated MERIS data." *Remote sensing of Environment*, 79(1), 51-59.
- Kratzer, S., Brockmann, C., and Moore, G. (2008). "Using MERIS full resolution data to monitor coastal waters - A case study from Himmerfjarden, a fjord-like bay in the northwestern Baltic Sea." *Remote Sensing of Environment*, 112(5), pp.2284-2300.
- Kratzer, S., Harvey, E. T., and Philipson, P. (2014). "The use of ocean color remote sensing in integrated coastal zone management-A case study from Himmerfjarden, Sweden." *Marine Policy*, 43, 29-39.
- Krizanich, G. W., and Finn, M. P. (2009). *Table Rock Lake Water-Clarity Assessment Using Landsat Thematic Mapper Satellite Data. U.S. Geological Survey Scientific Investigations Report 2009-5162.*
- Krom, M. D., Emeis, K. C., and Cappellen, P. Van. (2010). "Why is the Eastern Mediterranean phosphorus limited?," *Progress in Oceanography*, 85, 236-244.
- Kuo, J. T., Wu, J. H., and Chu, W. S. (1994). "Water quality simulation of Te-Chi Reservoir using two-dimensional models." *water science technology*, 30(2), 63-72.
- Kutser, T. (2009). "Passive optical remote sensing of cyanobacteria and other intense phytoplankton blooms in coastal and inland waters." *International Journal of Remote Sensing*, 30(17), 4401-4425.
- Kutser, T., Arst, H., Miller, T., Kaarmann, L., and Milius, A. (1995). "Telespectrometrical Estimation of Water Transparency, Chlorophyll-a and Total Phosphorus Concentration of Lake Peipsi." *International Journal of Remote Sensing*, 16, pp.3069-3085.
- Kutser, T., Metsamaa, L., Strömbeck, N., and Vahtmäe, E. (2006). "Monitoring cyanobacterial blooms by satellite remote sensing." *Estuarine, Coastal and Shelf Science*, 67(1-2), 303-312.
- Kutser, T., Pierson, D. C., Kallio, K. Y., Reinart, A., and Sobek, S. (2005). "Mapping lake CDOM by satellite remote sensing." *Remote Sensing of Environment*, 94(4), 535-540.
- Lavender, S., Nunny, R., and Tillett, D. (2002). *A Pilot Study of the Use of Satellite Ocean Colour Imagery for Water Quality Monitoring in Optically Shallow Tropical Coastal Environments.*
- Lavery, P., Pattiaratchi, C., Wyllie, A., and Hick, P. (1993). "Water Quality Monitoring in Estuarine Waters Using the Landsat Thematic Mapper." 280(March), 268-280.
- Lillesand, T. M., and Kiefer, R. W. (1994). *Remote sensing and image interpretation.* Wiley, Chichester.
- Lillesand, T. M., R.W., K., and J. W., C. (2004). "Remote sensing and image interpretation." 5th ed. Hoboken, NJ: John Wiley & Sons.
- Lindell, T., Pierson, D., and Premazzi, G. (1999). *Manual for Monitoring European Lakes using Remote Sensing Techniques.*
- Liu, Y., Islam, M. A., and Gao, J. (2003). "Quantification of shallow water quality parameters by means of remote sensing." *Progress in Physical Geography*, 27(1), 24-43.
- Lorenzen, M. W. (1980). "Use of chlorophyll-Secchi disk relationships." *Limnology Oceanography*, 25, 371-372.
- Loukas, a, Mylopoulos, N., Vasiliades, L., Tarnanas, H., Polykretis, J., and Dimitriou, A. (2005). "Sustainable Water Resources Management in Pinios River and Lake." *EWRA2005.*

- Lung, W. S. (1986). "Assessing phosphorus control in the James River Basin." *Journal of Environmental Engineering*, 112(1), 44–60.
- Ma, W., Xing, Q., Chen, C., Zhang, Y., Yu, D., and Shi, P. (2011). "Using the normalized peak area of remote sensing reflectance in the near-infrared region to estimate total suspended matter." *International Journal of Remote Sensing*, 32(22), 7479–7486.
- Mahtab, A. L., Rundquist, D. C., Han, L., and Kuzila, M. S. (1998). "Estimation of suspended sediment concentration in water using integrated surface reflectance." *Geocarto International*, 13(2), 11–15.
- Malthus, T. J., and Dekker, A. G. (1995). "First derivative indices for the remote sensing of inland water quality using high spectral resolution reflectance." *Environment International*, 21(2), 221–232.
- Malthus, T. J., and Mumby, P. J. (2003). "Remote sensing of the coastal zone: An overview and priorities for future research." *International Journal of Remote Sensing*, 24(13), 2805–2815.
- Mannion, A. M. (1995). *Agriculture and Environmental Change. Temporal and Spatial Dimensions*. John Wiley & Sons, Chichester, UK.
- Manolaki, P. (n.d.). "The Salt Lake at Larnaka Cyprus: A complex ecosystem." *Biodiversity East*, <<http://bio-e.org/lib/larnaka-salt-lake>>.
- Mather, P. (2004). "Computer Processing of Remotely-sensed Images: An Introduction." Wiley, Chichester, UK.
- Matthews, A. M., and Boxall, S. R. (1994). "Novel algorithms for the determination of phytoplankton concentration and maturity." *Proceedings of the Second Thematic Conference on Remote Sensing for Marine and Coastal Environments*, 173–180.
- McLoy, K. R. (1995). "Resource Management Information Systems." Taylor and Francis, London, UK, 244–281.
- Megard, R. O., Settles, J. C., Boyer, H. A., and Combs, W. S. (1980). "Light, Secchi disks, and trophic states." *Limnology Oceanography*, 25, 373–377.
- Menken, K., Brezonik, P. L., and Bauer, M. E. (2005). *Influence of Chlorophyll and Colored Dissolved Organic Matter (CDOM) on Lake Reflectance Spectra: Implications for Measuring Lake Properties by Remote Sensing. Developments in water science*,.
- Miller, R. L., and McKee, B. a. (2004). "Using MODIS Terra 250 m imagery to map concentrations of total suspended matter in coastal waters." *Remote Sensing of Environment*, 93(1-2), 259–266.
- Milton, E. J. (1987). "Review Article Principles of field spectroscopy." *International Journal of Remote Sensing*, 8(12), 1807–1827.
- Milton, E. J., and Rollin, E. M. (2006). "Estimating the irradiance spectrum from measurements in a limited number of spectral bands." *Remote Sensing of Environment*, 100(3), 348–355.
- Mitchelson-Jacob, E. G. (1999). *Utilisation of satellite ocean colour data for military applications: retrieval of suspended particulate matter concentrations from ocean colour imagery*.
- Morel, A. (1974). "Chapter I: Optical Properties of Pure Water and Pure Sea Water." *Optical aspects of oceanography. Academic*, N. G. J. and E. S. Nielsen, ed., France, 1–24.
- Morel, A., and Prieur, L. (1977). "Analysis of variations in ocean color." *Limnology and Oceanography*, 22(4), 709–722.
- Moustaka, E., Mylopoulos, N., and Loukas, A. (2002). "Assessment of the restored lake Karla operation under different hydrological and water demand scenarios." *Proceedings of the 6th International Conference of Protection and Restoration of the Environment*, Skiathos, Greece, 207–215.
- Nas, B., Karabork, H., Ekercin, S., and Berktaş, A. (2009). "Mapping chlorophyll-a through in-situ measurements and Terra ASTER satellite data." *Environmental Monitoring and Assessment*, 157(1-4), 375–382.

- Newman, H. R. (2013). "The Mineral Industry of Cyprus." *2011 Minerals Yearbook*, U.S. Department of the Interior U.S. Geological Survey, Cyprus.
- Newman, H. R. (2014). "The Mineral Industry of Cyprus." *2012 Minerals Yearbook*, Interior, U.S. Department of the Survey, U.S. Geological, Cyprus.
- Nicodemus, F. F., Richmond, J. C., Hsia, J. J., Ginsberg, I. W., and Limperis, T. L. (1977). "Geometrical considerations and nomenclature for reflectance." *National Bureau of Standards Monograph, Washington D.C U.S. Govt. Printing Office.*, 160, pp. 20402.
- Novo, E. M. M., Hansom, J. D., and Curran, P. J. (1989). "The effect of sediment type on the relationship between reflectance and suspended sediment concentration." *International Journal of Remote Sensing*, 10(7), 1283–1289.
- O'Reilly, J., Maritorena, S., Mitchell, B. G., Siegel, D. A., Carder, K. L., Kahru, M., Garver, S. A., and McClain, C. R. (1998). "Ocean color algorithms for SeaWiFS." *Journal of Geophysical Research*, 103, 24,937–24,953.
- Oikonomou, A., Katsiapi, M., Karayanni, H., Moustaka-Gouni, M., and Kormas, K. A. (2012). "Plankton Microorganisms Coinciding with Two Consecutive Mass Fish Kills in a Newly Reconstructed Lake." *The Scientific World Journal*, 2012, 1–14.
- Östlund, C., Flink, P., Strömbeck, N., Pierson, D., and Lindell, T. (2001). "Mapping of the water quality of Lake Erken, Sweden, from Imaging Spectrometry and Landsat Thematic Mapper." *Science of The Total Environment*, 268(1-3), 139–154.
- Ouillon, S., Forget, P., Froidefond, J. M., and Naudin, J. J. (1997). "Estimating Suspended Matter Concentrations from SPOT Data and from Field Measurements in the Rhone River Plume." *Marine Technology Society Journal*, 31, 15–20.
- Oyama, Y., Matsushita, B., Fukushima, T., Matsushige, K., and Imai, A. (2009). "Application of spectral decomposition algorithm for mapping water quality in a turbid lake (Lake Kasumigaura, Japan) from Landsat TM data." *ISPRS Journal of Photogrammetry and Remote Sensing*, International Society for Photogrammetry and Remote Sensing, Inc. ISPRS, 64(1), 73–85.
- Palintest. (2003). "MICRO 950 TURBIDITY METER Operating Instructions for using the Palintest Portable Turbidity Meter." PALINTEST LTD, Palintest House, Team Valley, Gateshead, Tyne & Wear England NE11 0NS.
- Papadimitriou, T., Stampouli, Z., and Kagalou, I. (2011). "Preliminary Results on the cyanotoxicity in the 'new' Lake Karla (Thessaly – Greece)." *Proceedings of the 12th International Conference on Environmental Science and Technology*, Rhodes, Greece.
- Papoutsas, C., Akylas, E., and Hadjimitsis, D. (2013). "The spectral signature analysis of inland and coastal water bodies acquired from field spectroradiometric measurements." *Proceedings of SPIE - The International Society for Optical Engineering*, 1–8.
- Papoutsas, C., Akylas, E., and Hadjimitsis, D. (2014). "Trophic State Index derivation through the remote sensing of Case-2 water bodies in the Mediterranean region." *Central European Journal of Geosciences*, 6(1), 67–78.
- Papoutsas, C., and Hadjimitsis, D. G. (2012). "Field Spectroscopy Measurements over Asprokremmos Dam in Cyprus Intended for Water Quality Monitoring." *Remote Sensing and Environment letters*, 2(2), 5–9.
- Papoutsas, C., and Hadjimitsis, D. G. (2013). "Remote Sensing for Water Quality Surveillance in Inland Waters: The Case Study of Asprokremmos Dam in Cyprus." *Remote Sensing of Environment - Integrated Approaches*, 131–153.
- Papoutsas, C., Hadjimitsis, D. G., and Alexakis, D. (2010). "Characterizing the spectral signatures and optical properties of dams in Cyprus using field spectroradiometric measurements." *SPIE Proceedings Vol. 8174: Remote Sensing for Agriculture, Ecosystems, and Hydrology XIII*, 817419, 10.

- Papoutsas, C., Hadjimitsis, D. G., Themistocleous, K., Perdikou, P., Retalis, A., and Toullos, L. (2010). "Smart monitoring of water quality in Asprokremmos Dam in Paphos, Cyprus using satellite remote sensing and wireless sensor platform." *Proc. SPIE 7831*, 7831Q.
- Papoutsas, C., Retalis, A., Toullos, L., and Hadjimitsis, D. G. (2014). "Defining the Landsat TM/ETM+ and CHRIS/PROBA spectral regions in which turbidity can be retrieved in inland waterbodies using field spectroscopy." *International Journal of Remote Sensing*, Taylor & Francis, 35(5), 1674-1692.
- Peckham, S. D., Chipman, J. W., Lillesand, T. M., and Dodson, S. I. (2006). "Alternate Stable States and the Shape of the Lake Trophic Distribution." *Hydrobiologia*, 571(1), 401-407.
- Peddle, D. R., White, H. P., Soffer, R. J., Miller, J. R., and LeDrew, E. F. (2001). "Reflectance processing of remote sensing spectroradiometer data." *Computers and Geosciences*, 27(2), 203-213.
- Petrou, A., Kallianiotis, A., Hannides, A. K., Charalambidou, I., Hadjichristoforou, Myroula Hayes, D. R., Lambridis, C., Lambridi, V., Loizidou, X. I., Orfanidis, S., Scarcella, G., Stamatis, N., Triantafillidis, G., and Vidoris, P. (2012). *Initial Assessment of the Marine Environment of Cyprus Part I - Characteristics*. Nicosia, Cyprus.
- Pfitzer, K., Bartolo, R. E., Ryan, B., and Bollhofer, A. (2005). "Issues to consider when designing a spectral library database." *Proceedings of the SSC 2005 Spatial Intelligence, Innovation and Praxis: The national biennial Conference of the Spatial Sciences Institute*, Melbourne, Australia, pp. 416-425.
- Pfitzer, K., Bollhofer, A., and Carr, G. (2006). "A standard design for collecting vegetation reference spectra: Implementation and implications for data sharing." *Journal of Spatial Science*, 51(2), pp.79-92.
- Pope, R. M., and Fry, E. S. (1997). "Absorption Spectrum (380-700 nm) of Pure Water. II. Integrating Cavity Measurements." *Applied optics*, 36, 8710-8723.
- Postel, S. (1999). "Pillar of Sand. Can the Irrigation Miracle Last?" New York: WW Norton & Company.
- Pozdnyakov, D., Shuchman, R., Korosov, a, and Hatt, C. (2005). "Operational algorithm for the retrieval of water quality in the Great Lakes." *Remote Sensing of Environment*, 97(3), 352-370.
- Prangma, G. J., and Roozkrans, J. N. (1989). "Using NOAA AVHRR Imagery in Assessing Water Quality Parameters." *International Journal of Remote Sensing*, 10(4-5), 811-818.
- Preisendorfer, R. W. (1961). "Application of radiative transfer theory to light measurements in the sea." *Monogr. Int. Union Geod. Geophys.*, Paris, France, 10, 11-30.
- Prieur, L., and Sathyendranath, S. (1981). "An optical classification of coastal and oceanic waters based on the specific spectral absorption curves of phytoplankton pigments, dissolved organic matter, and other particulate materials." *Limnology And Oceanography*, 26(4), 671-689.
- Pulliainen, J., Kallio, K., Eloheimo, K., Koponen, S., Servomaa, H., Hannonen, T., Tauriainen, S., and Hallikainen, M. (2001). "A semi-operative approach to lake water quality retrieval from remote sensing data." *Science of the Total Environment*, 268(1-3), 79-93.
- Quibell, G. (1991). "The effect of suspended sediment in reflectance from freshwater algae." *International Journal of Remote Sensing*, 12, 177-182.
- Van Raaphorst, W., Philippart, C. J. M., Smit, J. P. C., Dijkstra, F. J., and Malschaert, J. F. P. (1998). "Distribution of suspended particulate matter in the North Sea as inferred from NOAA/AVHRR reflectance images and in situ observations." *Journal of Sea Research*, 39, pp. 197-215.
- Radif, A. A. (1999). "Integrated water resources management (IWRM): an approach to face the challenges of the next century and to avert future crises." *Desalination*, 124(1-3), 145-153.
- Reif, M., Piercy, C., Jarvis, J., Sabol, B., Macon, C., Loyd, R., Colarusso, P., Dierssen, H., and Aitken, J. (2012). *Ground Truth Sampling to Support Remote Sensing Research and Development: Submersed Aquatic Vegetation Species Discrimination Using an Airborne Hyperspectral / Lidar System*.

- Rijkeboer, M., Dekker, A. G., and Gons, H. J. (1998). "Subsurface irradiance reflectance spectra of inland waters differing in morphometry and hydrology." *Aquatic Ecology*, 31, 313-323.
- Ritchie, J. C., and Charles, M. C. (1996). "Comparison of Measured Suspended Sediment Concentration Estimated from Landsat MSS data." *International Journal of Remote Sensing*, 9(3), 379-387.
- Ritchie, J. C., Cooper, C. M., and Schiebe, F. R. (1990). "The relationship of MSS and TM digital data with suspended sediments, chlorophyll, and temperature in Moon Lake, Mississippi." *Remote Sensing of Environment*, 33(2), 137-148.
- Ritchie, J. C., McHenry, J. R., Schiebe, F. R., and Wilson, R. B. (1974). "The relationship of reflected solar radiation and the concentration of sediment in the surface water of reservoirs." *Remote Sensing of Earth Resources Vol.III*, F. Shahrokhi, ed., Tullahoma, Tennessee, 57-72.
- Ritchie, J. C., Zimba, P. V, and Everitt, J. H. (2003). "Remote sensing techniques to assess water quality." *...& Remote Sensing*, 69(6), 695-704.
- Robertson, A. H. F., and Woodcock, N. H. (1979). "Mamonia Complex, Southwest Cyprus: Evolution and Emplacement of a Mesozoic Continental Margin." *Geological Society of America Bulletin*, 90(7), 651-665.
- Robinson, B. F., and Biehl, L. L. (1979). "Calibration Procedures For Measurement Of Reflectance Factor In Remote Sensing Field Research." *Proc. SPIE 0196, Measurements of Optical Radiations*, H. P. Field, E. F. Zalewski, and F. M. Zweibaum, eds., San Diego.
- Rollin, E. M., and Milton, E. J. (1998). "Processing of High Spectral Resolution Reflectance Data for the Retrieval of Canopy Water Content Information." *Remote Sensing of Environment*, 65(1), 86-92.
- Rosenqvist, A., Milne, A., Lucas, R., Imhoff, M., and Dobson, C. (2003). "A Review of Remote Sensing Technology in Support of the Kyoto Protocol." *Environmental Science & Policy*, 6(5), 441-455.
- Roson, R., and Sartori, M. (2010). "Water Scarcity and Virtual Water Trade in the Mediterranean." *SSRN Electronic Journal*, 1-19.
- Rossel, F. (2001). "Reassessment of the island's water resources and demand - assessment of groundwater resources of Cyprus." WDD/FAO TCP/CYP/8921, Nicosia, Cyprus.
- Ruddick, K. G., De Cauwer, V., Park, Y.-J., and Moore, G. (2006). "Seaborne measurements of near infrared water-leaving reflectance: The similarity spectrum for turbid waters." *Limnology and Oceanography*, 51(2), 1167-1179.
- Ruddick, K. G., Ovidio, F., and Rijkeboer, M. (2000). "Atmospheric correction of SeaWiFS imagery for turbid coastal and inland waters." *Applied optics*, 39, 897-912.
- Ruhl, C. A., Schoellhamer, D. H., Stumpf, R. P., and Lindsay, C. L. (2001). "Combined Use of Remote Sensing and Continuous Monitoring to Analyse the Variability of Suspended-Sediment Concentrations in San Francisco Bay, California." *Estuarine, Coastal and Shelf Science*, 53, 801-812.
- Ruiz-Verdú, A., Simis, S. G. H., de Hoyos, C., Gons, H. J., and Peña-Martínez, R. (2008). "An evaluation of algorithms for the remote sensing of cyanobacterial biomass." *Remote Sensing of Environment*, 112(11), 3996-4008.
- Sathyendranath, S., Longhurst, A., Caverhill, C. M., and Platt, T. (1995). "Regionally and seasonally differentiated primary production in the North Atlantic." *Deep-Sea Res*, 42, 1773-1802.
- Sathyendranath, S., and Morel, A. (1983). "Light Emerging from the Sea-interpretation and Uses in Remote Sensing." *Remote Sensing Applications in Marine Science and Technology*, 106, 323-357.
- Sathyendranath, S., Prieur, L., and Morel, a. (1989). "A three-component model of ocean colour and its application to remote sensing of phytoplankton pigments in coastal waters." *International Journal of Remote Sensing*, 10(8), 1373-1394.

- Sathyendranath, S., Stuart, V., Cota, G., Maas, H., and Platt, T. (2001). "Remote sensing of phytoplankton pigments: a comparison of empirical and theoretical approaches." *International Journal of Remote Sensing*, 22, 249–273.
- Sawaya, K. E., Olmanson, L. G., Heinert, N. J., Brezonik, P. L., and Bauer, M. E. (2003). "Extending satellite remote sensing to local scales: land and water resource monitoring using high-resolution imagery." *Remote Sensing of Environment*, 88, 144–156.
- Schaepman, M. E. (2007). "Spectrodirectional remote sensing: From pixels to processes." *International Journal of Applied Earth Observation and Geoinformation*, 9(2), 204–223.
- Schalles, J. F., Gitelson, A. A., Yacobi, Y. Z., and Kroenke, A. E. (1998). "Estimation of Chlorophyll a from Time Series Measurements of High Spectral Resolution Reflectance in an Eutrophic Lake." *Journal of Physiology*, 34, 383–390.
- Schwarz, J. N., Kowalczyk, P., Kaczmarek, S., Cota, G. F., Mitchell, B. G., Kahru, M., Chavez, F. P., Cunningham, A., McKee, D., Gege, P., Kishino, M., Phinney, D., and Raine, R. (2002). "Two models for absorption by coloured dissolved organic matter (CDOM)." *Oceanologia*, 44, 209–241.
- Seckler, D., Amarasinghe, U., Molden, D., Silva, R. de, And, and Barker, R. (1998). *World water demand and supply, 1990 to 2025: Scenarios and issues*.
- Senay, G., and Shafique, N. (2001a). "The selection of narrow wavebands for optimizing water quality monitoring on the Great Miami River, Ohio using hyperspectral remote sensor data." *Journal of Spatial Hydrology*, 1(1), 1–22.
- Senay, G., and Shafique, N. (2001b). "The selection of narrow wavebands for optimizing water quality monitoring on the Great Miami River, Ohio using hyperspectral remote sensor data." *Journal of Spatial Hydrology*, 1, 1–22.
- Sheela, A. M., Letha, J., Joseph, S., Ramachandran, K. K., and Sanalkumar, S. P. (2011). "Trophic State Index of a Lake System Using IRS (P6-LISS III) Satellite Imagery." *Environmental Monitoring Assessment*, 177, pp. 575–592.
- Smith, R. C., and Baker, K. S. (1981). "Optical properties of the clearest natural waters (200–800 nm)." *Applied optics*, 20(2), 177–184.
- Sofroniou, A., and Bishop, S. (2014). "Water Scarcity in Cyprus: A Review and Call for Integrated Policy." *Water*, 6, 2898–2928.
- Sogandares, F. M., and Fry, E. S. (1997). "Absorption spectrum (340 - 640 nm) of pure water. I. photothermal measurements." *Applied optics*, 36, 8699 - 8709.
- Song, C., Woodcock, C. E., Seto, K. C., Lenney, M. P., and Macomber, S. A. (2001). "Classification and Change Detection using Landsat TM Data: When and How to Correct Atmospheric Effects?" *Remote Sensing of Environment*, 75, 230–244.
- Strömbeck, N. (2001). "Water quality and optical properties of Swedish lakes and coastal waters in relation to remote sensing." *Comprehensive Summaries of Uppsala Dissertations from the Faculty of Science and Technology* 633. 27 pp. Uppsala. ISBN 91-554-5037-7.
- Strömbeck, N., and Pierson, D. C. (2001). "The effects of variability in the inherent optical properties on estimations of chlorophyll a by remotesensing in Swedish freshwaters." *The Science of the Total Environment*, 268, 123–137.
- Su, Y.-F., Liou, J.-J., Hou, J.-C., Hung, W.-C., Hsu, S.-M., Lien, Y.-T., Su, M.-D., Cheng, K.-S., and Wang, Y.-F. (2008). "A Multivariate Model for Coastal Water Quality Mapping Using Satellite Remote Sensing Images." *Sensors*, 8(10), 6321–6339.
- Sváb, E., Tyler, a. N., Preston, T., Présing, M., and Balogh, K. V. (2005). "Characterizing the spectral reflectance of algae in lake waters with high suspended sediment concentrations." *International Journal of Remote Sensing*, 26(5), 919–928.

- SVC. (2002). "Spectra Vista Corporation: GER1500." <<http://www.spectravista.com/ground.html>>.
- Tanaka, A., Kishino, M., Doerffer, R., Schiller, H., Oishi, T., and Kubota, T. (2004). "Development of a neural network algorithm for retrieving concentrations of chlorophyll, suspended matter and yellow substance from radiance data of the ocean color and temperature scanner." *Journal of Oceanography*, 60, 519–530.
- Teillet, P. M. (1986). "Image Correction for Radiometric Effects in Remote Sensing." *International Journal of Remote Sensing*, 7(12), 1637–1651.
- Teillet, P. M. (1995). "The role of surface observations in support of remote sensing." *The Canadian Remote Sensing Contribution to Understanding Global Change. Department of Geography Publication Series*, University of Waterloo, Waterloo, ON, Canada, 333–352.
- Teodoro, A. C., Marcal, A. R. S., and Veloso-Gomes, F. (2007). "Correlation analysis of water wave reflectance and local TSM concentrations in the breaking zone, using remote sensing techniques." *Journal of Coastal Research*, 23(6), 1491–1497.
- Themistocleous, K., Hadjimitsis, D. G., Retalis, A., Chrysoulakis, N., and Michaelides, S. (2013). "Precipitation effects on the selection of suitable non-variant targets intended for atmospheric correction of satellite remotely sensed imagery." *Atmospheric Research*, Elsevier B.V., 131, 73–80.
- Theng, B. K. G. (1987). "Clay-humic interactions and soil aggregate stability." *Soil Structure and Aggregate Stability*, 32–73.
- Thiemann, S., and Kaufmann, H. (2000). "Determination of chlorophyll content and trophic state of lakes using field spectrometer and IRS-1C satellite data in the Mecklenburg Lake District, Germany." *Remote Sensing of Environment*, 73(2), 227–235.
- Thiemann, S., and Kaufmann, H. (2002). "Lake water quality monitoring using hyperspectral airborne data – a semiempirical multisensor and multitemporal approach for the Mecklenburg Lake District." *Remote sensing of Environment*, 81(2), 228–237.
- Thiemann, S., Wieneke, F., and Kaufmann, H. (2001). "Water quality and trophic state analysis based on hyperspectral remote sensing data in the Mecklenburg Lake District, Germany." *Photogrammetrie-Fernerkundung-Geoinformation*, 5, 331–344.
- Thomas, M. L., Ralph, W. K., and Jonathan, W. C. (2004). *Remote Sensing and Image Interpretation*. United States of America.
- UNEP-MAP. (2007). *Integrated coastal area management in Cyprus: biodiversity concerns on the Coastal Area Management Programme of Cyprus*. Tunis, Tunisia.
- UNEP-MAP. (2010). *The Mediterranean Sea Biodiversity: state of the ecosystems, pressures, impacts and future priorities*. Tunis.
- United Nations Environment Programme (UNEP). (2010). *Clearing the Waters. A focus on water quality solutions*. Nairobi, Kenya.
- United Nations, Dept. of Economic & Social Affairs, P. D. (2013). *World Population Prospects: The 2012 Revision, Highlights and Advance Tables*.
- Usali, N., and Ismail, M. H. (2010). "Use of Remote Sensing and GIS in Monitoring Water Quality." *Journal of Sustainable Development*, 3(3), 228 – 238.
- Vos, W. L., Donze, M., and Bueteveld, H. (1986). *On the reflectance spectrum of algae in water: the nature of the peak at 700 nm and its shift with varying concentration. Technical Report*. Delft, The Netherlands.
- Walter-Shea, E. A., and Biehl, L. L. (1990). "Measuring vegetation spectral properties." *Remote Sensing Reviews. Special Issue: Instrumentation for studying vegetation canopies for remote sensing in optical and thermal infrared regions*, 5(1), pp. 179–205.

- Wang, S., Yan, F., Zhou, Y., Zhu, L., Wang, L., and Jiao, Y. (2005). "Water Quality Monitoring Using Hyperspectral Remote Sensing Data in Taihu Lake China." *Geoscience and Remote Sensing Symposium, 2005. IGARSS'05. Proceedings. 2005 IEEE International*, 4553–4556.
- Wang, Y., Xia, H., Fu, J., and Sheng, G. (2004). "Water quality change in reservoirs of Shenzhen, China: detection using LANDSAT/TM data." *Science of The Total Environment*, 328(1-3), 195–206.
- WDD. (n.d.). "Dams of Cyprus (GR)."
- WDD. (2009). *Annual-Report*.
- WDD. (2010). *Annual-Report*.
- WDD. (2011). *Annual-Report*.
- WDD. (2012). *Annual-Report*.
- Wdd, C. (2012). "Inflow of water to the dams 1987/88 - 2012/13." 2012.
- WFD_L164/19. (2008). "DIRECTIVE 2008/56/EC OF THE EUROPEAN PARLIAMENT AND OF THE COUNCIL of 17 June 2008 establishing a framework for community action in the field of marine environmental policy (Marine Strategy Framework Directive)." *Official Journal of the European Union*.
- WFD_L232/14. (2010). "COMMISSION DECISION of 1 September 2010 on criteria and methodological standards on good environmental status of marine waters (notified under document C(2010) 5956) (Text with EEA relevance) (2010/477/EU)." *Official Journal of the European Union*.
- Wharton, D. A. (2002). *Life at the limits. Organisms in extreme Environments*. Cambridge University Press, Cambridge, UK.
- Williams, W. D. (2002). "Environmental threats to salt lakes and the likely status of inland saline ecosystems in 2025." *Journal of the Environmental Conservation*, 29(2), 154–167.
- Woodruff, D. L., Stumpf, R. P., Scope, J. A., and Paerl, H. W. (1999). "Remote Estimation of Water Clarity in Optically Complex Estuarine Waters." *Remote Sensing of Environment*, 68(1), 41–52.
- Wu, M., Zhang, W., Wang, X., and Luo, D. (2009). "Application of MODIS satellite data in monitoring water quality parameters of Chaohu Lake in China." *Environmental Monitoring and Assessment*, 148, pp.255–264.
- Xu, F. L., Tao, S., Dawson, R. W., and Li, B. G. (2001). "A GIS-based method of lake eutrophication assessment." *Ecological Modelling*, 144(2-3), 231–244.
- Xu, J. P., Li, F., Zhang, B., Gu, X. F., and Yu, T. (2010). "Remote Chlorophyll-a Retrieval in Case-II Waters Using an Improved Model and IRS-P6 Satellite Data." *International Journal of the Remote Sensing*, 31(17-18), pp. 4609–4623.
- Yacobi, Y. Z., A., G., and M., M. (1995). "Remote sensing of chlorophyll in Lake Kinneret using high-spectral-resolution radiometer and Landsat TM: Spectral features of reflectance and algorithm development." *Journal of Plankton Research*, 17, 2155–2173.
- Yacobi, Y. Z., Moses, W. J., Kaganovsky, S., Sulimani, B., Leavitt, B. C., and Gitelson, A. A. (2011). "NIR-red reflectance-based algorithms for chlorophyll-a estimation in mesotrophic inland and coastal waters: Lake Kinneret case study." *Water Research*, 45(7), 2428–2436.
- Yogev, T., Rahav, E., Bar-Zeev, E., Man-Aharonovich, D., Stambler, N., Kress, N., Beja, O., Mulholland, M. R., Herut, B., and Berman-Frank, I. (2011). "Is dinitrogen fixation significant in the Levantine Basin, East Mediterranean Sea?" *Environmental Microbiology*, 13(4), 854–871.
- Zhang, B., Li, J., Shen, Q., and Chen, D. (2008). "A bio-optical model based method of estimating total suspended matter of Lake Taihu from near-infrared remote sensing reflectance." *Environmental Monitoring and Assessment*, 145(1-3), 339–347.

Zhengjun, W., Jianming, H., and Guisen, D. (2008). "Use of satellite imagery to assess the trophic state of Miyun Reservoir, Beijing, China." *Environmental Pollution*, 155(1), 13-19.

Zimba, P. V., and Gitelson, A. (2006). "Remote estimation of chlorophyll concentration in hyper-eutrophic aquatic systems: Model tuning and accuracy optimization." *Aquaculture*, 256(1-4), 272-286.